THE STRUCTURE OF LIQUID ARGON AS DETERMINED BY X-RAY DIFFRACTION

Thesis by

Bruce Edward Kirstein

In Partial Fulfillment of the Requirements

For the Degree of

Doctor of Philosophy

California Institute of Technology

Pasadena, California

1972

(Submitted May 25, 1972)

to John W. Kirstein

ACKNOWLEDGMENTS

I wish to thank Dr. C. J. Pings for his support and the opportunity to study at the California Institute of Technology.

During my graduate studies, I have been the recipient of financial support from the California Institute of Technology and the National Science Foundation. The funds for this investigation were contributed by the Air Force Office of Scientific Research, Directorate of Chemical Sciences.

This investigation would not have been possible without the help of the people in the Chemical Engineering shop, George Griffith, Chic Nakawatase, Bill Schuelke, John Yehle, Ray Reed, and also Hollis Reamer who supplied invaluable aid in the laboratory.

The data handling and subsequent numerical studies using the computing facilities were made possible with the help of Kikuko Matsumoto, Martha Lamson, Edith Huang, Joe Dailey and the entire operating crew, in particular the night crew, Jorge Gonzalez and Mike Martinov.

Numerous conversations with Paul Morrison, Joe Karnicky, Tony Collings, Ray Schmidt and Ron Brown were helpful in this work. Dr. Sten Samson was especially helpful in obtaining a high quality x-ray detection system.

I wish to thank my parents, Mr. and Mrs. H. V. Hansen, for their numerous grants in aid; and also my wife and daughter, Barbara and Shelli, for their continuous encouragement and support.

ABSTRACT

X-ray diffraction measurements and subsequent data analyses have been carried out on liquid argon at five states in the density range of 0.91 to 1.135 gm/cc and temperature range of 127 to 143°K. Duplicate measurements were made on all states. These data yielded radial distribution and direct correlation functions which were then used to compute the pair potential using the Percus-Yevick equation. The potential minima are in the range of -105 to -120°K and appear to substantiate current theoretical estimates of the effective pair potential in the presence of a weak three-body force.

The data analysis procedure used was new and does not distinguish between the coherent and incoherent absorption factors for the cell scattering which were essentially equal. With this simplification, the argon scattering estimate was compared to the gas scattering estimate on the laboratory frame of reference and the two estimates coincided, indicating the data normalized. The argon scattering on the laboratory frame of reference was examined for the existence of the peaks in the structure factor and the existence of an observable third peak was considered doubtful.

Numerical studies of the effect of truncation, normalization, the subsidiary peak phenomenon in the

radial distribution function, uncertainties in the low angle data relative to errors in the direct correlation function and the distortion phenomenon are presented.

The distortion phenomenon for this experiment explains why the Mikolaj-Pings argon data yielded pair potential well depths from the Percus-Yevick equation that were too shallow and an apparent slope with respect to density that was too steep compared to theoretical estimates.

The data presented for each measurement are: empty cell and cell plus argon intensity, absorption factors, argon intensity, smoothed argon intensity, smoothed argon intensity corrected for distortion, structure factor, radial distribution function, direct correlation function and the pair potential from the Percus-Yevick equation.

TABLE OF CONTENTS

TABLE OF CONTENTS

INDEX FOR FIGURES

INDEX FOR FIGURES

INDEX FOR TABLES

INDEX FOR TABLES

I. INTRODUCTION

Information about the structure of an ensemble of spherically symmetric atoms is needed to test statistical mechanical theories of fluids. These theories attempt to describe the physical properties of such systems based on the configurational energy of its particles. Efforts have been made in the past to determine the structure of argon[1,2] and other fluids[3-8] using x-ray or neutron diffraction data. A summarization of the most recent results may be found in Simple Dense Fluids, edited by Frisch and Salsburg.[9]

Since the computations required in statistical mechanics are not simple exercises, and since the diffraction experiments to determine the structure present many problems in technique and numerical analysis which drastically affect the final result, it is then indeed difficult to ascertain if differences in theory and experiment are due to technique, poor theory or both. Reasonable agreement between experiment and theory in the past has not been obtained.

The general subject of experimental technique relative to the structure determination of simple fluids by x-ray diffraction has been reviewed recently by Pings.[10]

The scattering of radiation by matter will involve the distribution of atomic positions if the wavelength

of radiation is of the order of the interatomic distance. The scattering from each atom will constructively or destructively interfere with the scattering from other atoms depending upon their relative locations. The distribution of positions of interest in fluid argon or for an ensemble of spherically symmetric scatterers is called the radial distribution function, written henceforth as g(r). This function is also called the pair distribution function and is the relative probability of finding an atom at a distance r in a differential volume element if there is an atom at the origin, normalized to unity at large r. Written in equation form, $g(r) = \rho(r)/\rho$, where ρ is the bulk density.

The coherently scattered radiation, I(s), in an x-ray experiment for such a system of atoms is related to g(r) by:[11-13]

$$i(s) = \frac{I(s)}{f^2(s)} - 1 = \frac{4\pi\rho}{s}\int_0^\infty r\left[g(r)-1\right]\sin(sr)dr \qquad (1)$$

and

$$s = 4\pi\lambda^{-1}\sin(\theta) \qquad (2)$$

where s is termed the scattering parameter, uniquely determined by one-half the scattering angle, θ, and

the wavelength of the radiation, λ, i(s) is the structure factor and $f^2(s)$ is the atomic scattering factor. Coherently scattered radiation means there is no wavelength change in the scattering process as there is in Compton scattering.[14]

The integral equation for i(s) and hence I(s) may be formally inverted to yield g(r) as a function of i(s):

$$g(r)-1 = (2\pi^2\rho r)^{-1}\int_0^\infty si(s)\sin(sr)ds \qquad (3)$$

Another quantity of interest in statistical mechanics is the direct correlation function, c(r), introduced by Ornstein and Zernike[15] in 1914:

$$c(\vec{r}_{12}) = h(\vec{r}_{12})-\rho\int_0^\infty c(\vec{r}_{13})h(\vec{r}_{23})d\vec{r}_3 \qquad (4)$$

where h(r) is g(r)-1. The definition of c(r) is basically mathematical and the function lacks an obvious physical interpretation such as that assigned to g(r). Goldstein[16] has subsequently shown that c(r) can be rigorously computed from diffraction data by the following expression:

$$c(r) = (2\pi^2\rho r)^{-1}\int_0^\infty si(s)\left[1+i(s)\right]^{-1}\sin(sr)ds \qquad (5)$$

The Percus-Yevick theory,[17] henceforth referred to

as PY theory, is of current interest and relates the pair potential, u(r), to the two quantities g(r) and c(r) by the following approximation:

$$u(r) = kT*\ln\left[1-c(r)/g(r)\right] \qquad (6)$$

where T is the absolute temperature and k is the Boltzmann constant. The above approximation may be obtained by examining the density expansion of g(r) and c(r) in terms of graph theory[18] assuming that the configurational energy of the system may be obtained by considering only pairwise interactions. Essentially, terms greater than order two in density are neglected and two graphs in the second order term of c(r) which lack a Mayer f_{12} bond are neglected. However, in the limit of zero density the approximation becomes exact.

It is anticipated that the pair potential would be state independent as predicted by PY theory. However, if the theory predicts a state dependence of the potential, then the conclusion could be drawn that the components of the system do not interact strictly pairwise, the theory is incorrect in neglecting some terms, or the experiment itself including the numerical analysis is not correct.

It has, therefore, been the attempt of this thesis to improve both experimental technique and the numerical

analysis relative to an x-ray diffraction experiment to determine g(r) and c(r) for a simple fluid. The net result has been better control of the experiment. Also a relatively new approach to the numerical analysis involving calculation of absorption corrections, smoothing of data, distortion corrections and Fourier transforming has been developed.

There is now substantial evidence that the configurational energy of a dense fluid will have to include more than just two-body interactions.[19-32] Then the PY theory as previously stated and other theories are not expected to predict a state independent pair potential for this reason, and the interest now is how the potential varies as a function of density.

Recent efforts by some investigators[33-36] have involved computing an effective pair potential in the presence of a weak three-body force. There is more than one such effective potential since the examination of different properties leads to different effective potentials.[34] The relevant effective potential then is the one that yields the correct radial distribution and correlation functions when substituted into the two-body density expansion since these two quantities are obtainable from experiment. Hence, the PY theory may not actually be tested as stated when Eq. (6) is evaluated,

but the result obtained will then be an estimate of the effective pair potential. A comparison between experiment and an assumed configurational energy which includes a weak three-body force may then be made through this computational trick involving an effective pair potential.

The work of Rowlinson,[35,36] et al, computes the effective pair potential for argon that yields the correct radial distribution function from the configurational energy through the ρ^2 term of a system that includes a weak three-body force. These results also provide the non-additive contributions to the fourth virial coefficient for the same force. The calculation requires that a zero density value for the pair potential be introduced since the form of the equation yields the result $(u^*-u)/kT$ where u^* is the effective pair potential and u is the zero density pair potential. Rowlinson uses the zero density pair potential of Barker and Pompe[19] which has a minimum of $-148^{\circ}K$ to plot the actual minimum of u^*/k. There are other estimates of the zero density potential and the more recent estimates have minimum values ranging from that of Barker and Pompe's up to approximately $-140^{\circ}K$.[37]

The results of computing the minimum of u^*/k for an argon-like potential with a weak three-body force as a function of density yields an almost straight line with

an effective minimum of -125°K at one gm/cc for argon. There is a slight upward curvature of u*/k with increasing density reflecting the ρ^2 contribution.

The data of Mikolaj and Pings[38] are compared to this effective potential and it is observed that there is a large discrepancy, the experimental minimum of the potential being much too shallow and having a positive slope with respect to density tentatively observed as being slightly too large. These differences to this date have not been explained and it is difficult to believe that the difference is due to non-additive effects. Other investigators have made the same observations.[19,39,40]

The result of this thesis, which describes diffraction measurements and subsequent data analysis on five thermodynamic states of argon in the liquid region, as indicated in Figure 1. and Table 1., essentially confirms the stated work of Rowlinson and also explains why the Mikolaj-Pings data behave as they do.

The most important experimental phenomenon which was neglected in the past is that of a distortion effect resulting from an x-ray detector accepting a finite angular spread of scattered radiation. The effect of not correcting for this phenomenon is a marked decrease in the computed Percus-Yevick well depth. The error is density dependent, increasing with increasing density

and always being nonzero for finite densities.

Error bands for the data in this thesis were not calculated because of the uncertainty of the validity of such a calculation. Each thermodynamic state was measured at least twice to give some measure of reproducibility. Information in the form of numerical experiments is now presented that indicates that error bands previously estimated do not take into account the observed reproducibility.[1,2] The major effect observed is uncertainty in the low angle data and hence affects c(r) for thermodynamic states with relatively small isothermal compressibilities.

The phenomenon of the subsidiary peak[2,4,41-45] in g(r) was observed, but only sometimes. Data are presented which show that a perturbation in the smoothing of the raw data within reasonable error bands may cause such subsidiary peak to appear or disappear.

The data analysis to be presented makes use of the behavior of g(r) in the region of $0 \leq r \leq 3$ Å. Data are sometimes presented in the form $r\left[g(r)-1\right]$ and this behavior is then masked. The desired result now appears to have g(0)-1 be close to -1. This involves evaluating the sine transform of si(s) for r=0 which is:

$$-2\pi^2\rho = \int_0^\infty s^2 i(s)\,ds \qquad (7)$$

This is essentially the normalization suggested by Krogh-Moe.[46] If positive g(0)-1 values are allowed, the Percus-Yevick well depths will decrease about 5°K for every +3 units of g(0)-1 as indicated by transforming actual experimental results.

The truncation of the structure factor in this work involved estimating what could be observed from the data on the laboratory frame of reference. Essentially no third peak in i(s) was observed at pressures of 19 to 37 atmospheres at 127°K. However, a third peak could barely be inferred at 54 atmospheres and 127°K. As the pressure decreases, the peaks in i(s) are expected to decrease due to a reduction in packing and hence the third peak at lower pressures was not included. It was anticipated that any attempt to include the third peak would result in an incorrect period of oscillation[40] and peak height, and since i(s) must be multiplied by s for the Fourier transform, the resulting error would be unpredictable. The data at 54 atmospheres were transformed for both g(r) and c(r) with and without the third peak in i(s) and the differences indicated a 2°K change in the PY well depth. Three valleys in i(s) were always observed and i(s) was truncated at its zero in the region of $s \approx 5$ Å^{-1}.

Numerical experiments are presented in table and plotted form to indicate the reasoning for the various decisions that were made.

II. APPARATUS

The equipment used to confine a sample of fluid argon (99.996% pure) was essentially the same as that of Mikolaj[1] and Smelser.[2] Changes were made only to the peripheral support equipment. The temperature measuring and control system used was a modification of a method described by Daneman[47] and also previously used by Wu[48] in this laboratory. The pressure measurement and control were obtained by an oil-piston system also used by Wu. Both the temperature control and pressure measuring techniques mentioned above were new to the x-ray experiment and were primarily intended for use in the study of the index of refraction of argon in the critical region.[48] For the data obtained in this thesis, temperature was controlled to within ± 0.002 degrees Kelvin and pressure was controlled to within ± 0.2 psia.

The cryostat vacuum system consisted of a rough pump and a four inch diffusion pump of the E04 series from Edwards High Vacuum, Ltd. Vacuum measurements were obtained with an Edwards Ionization-Pirani Vacuum Gauge Model I and a Model IG.3A gauge head. Vacuums on the order of 10^{-5} torr were obtained with no cold traps on the system. Upon cooling the system for an experiment and filling the cold traps with liquid nitrogen, the vacuums obtained were on the order of 10^{-7} to 10^{-6} torr.

These improved vacuums were the result of using SARAN WRAP® to cover the x-ray slot in the cryostat. Previously Mylar® had been used.[1,2]

The sample cell was constructed of sintered beryllium and described by Smelser.[2] Cell dimensions of importance for calculating absorption corrections are the inside and outside diameter previously quoted at 0.035 and 0.070 inch respectively. These dimensions were reasonably verified by observing the apparent size of the cell with x-rays and knowing the distance of the detector and cell from the x-ray source.

The goniometer and cell were aligned essentially as described by Smelser.[2] The only modification that occurred was the alignment of the 0.005 inch receiving sollers. The actual alignment of the detector required the use of a LiF single crystal, incident slit and a very narrow receiving slit. Once alignment was obtained, the receiving slit was removed and the receiving sollers were mounted. The entire receiving assembly was then "rocked" while looking at a strong Bragg peak to maximize the intensity. This operation set the receiving assembly platform parallel to the scattered rays coming from the goniometer axis. Upon removing the receiving sollers and mounting the receiving slit again, the alignment was destroyed because the actual position of the slit was

changed by the "rocking" of the receiving assembly. Therefore the receiving slit had to be realigned. After this second alignment, the receiving sollers still required a further fine adjustment to insure that they were looking at the goniometer axis. It should be noted that the sollers were 0.005 by 1.25 inches and an error involving the front or rear being 0.001 inch too high or low would foreshorten the view of the region of the goniometer axis. The receiving sollers were then adjusted by inserting a metal shim under the front or rear as was needed. This final adjustment did not upset the alignment as determined by the receiving slit.

The pertinent dimensions of the x-ray path were as follows. The beryllium cell was 18 cm from the x-ray tube target. The incident slit was a 1/6 degree divergence slit, 0.006 inch, located 8 cm from the x-ray tube target. Vertical incident sollers, 0.01 by 1.25 inches, were mounted between the x-ray tube and incident slit. The take-off angle from the x-ray tube target was $5\frac{1}{2}$ degrees. The sample-detector distance, with the rear of the receiving sollers defining the detector face, was 17.1 cm.

The x-ray source was a Norelco® full wave generator and a Standard Focus X-ray Tube, molybdenum target, model number 140 005 00, operated at 48 KV and 35 ma. Solid

state high voltage rectifiers were used instead of the vacuum tube type and this appeared to improve stability.

The x-ray detection and recording system was completely changed from past experiments.[1,2] An Amperex® XP1010 photomultiplier with a Horiba® 4HG2 sodium iodide crystal formed the x-ray detector. The dynode chain was constructed with 150,000 ohm resistors instead of the normal 470,000 ohm. This decreased resistance drew approximately ½ ma from a Hewlett Packard Model 5551A high voltage power supply operated at +1200 volts. Detector resolutions on the order of 28% were consistently obtained with this improved system.

The increased dynode current greatly decreased the gain shift phenomenon. The gain shift in a photomultiplier is caused by the current due to the electron transfer between dynodes becoming an appreciable fraction of the total current through the entire dynode chain and upsetting the voltages between the dynodes. This effect will cause a decrease in the gain of a system.

Data recording and goniometer positioning was obtained through the use of a Canberra Industries DATANIM® system and a Cipher Data Products Model 70H magnetic tape recorder. This system was a ten instruction programmable computer which allowed complete automation of the goniometer positioning, x-ray counting and recording, and dual filter selection.

III. DATA ANALYSIS

A. Introduction to Data Analysis

The objective of this x-ray diffraction experiment on argon was to determine the quantity called the structure factor, i(s), as defined in Eq. (1). The structure factor had to be determined over the range where it was nonzero so that it could be Fourier transformed for the radial distribution and direct correlation functions as defined in Eqs. (3) and (5). The data analysis procedure used here has produced some insight as to the sensitivity of the above quantities to the various techniques used or decisions that had to be made.

Invariably, the procedure to determine the structure factor in this type of experiment, and hence g(r) and c(r), is a technique. A technique in this context is defined to be a procedure that requires the user to make a decision or decisions that may be somewhat subjective. The numerical techniques used in this thesis differ from those used previously.[1,2] The previous techniques, though quite correct on paper, did not lend themselves to clearly defined procedures.

The data analysis to be described is based on a monochromatic x-ray source obtained through the use of dual filters which are described in Appendix A.

Where possible numerical experiments have been

performed using actual data to render justification of the decisions made. These numerical experiments are described in Section V. and are referred to where necessary. The numerical experiments are the following:

A. Effect of Distortion on g(r) and c(r).

B. The Subsidiary Peak Phenomenon.

C. Effect of Uncertainties in Smoothing the Low Angle Data on g(r) and c(r).

D. Truncation, The Existence of a Third Peak in i(s) at Various Pressures and the Effect of Neglecting It.

E. Effect on g(r) and c(r) when g(0) is Significantly Different from Zero.

F. Effect on g(r) and c(r) of Using Post- vs. Pre-cell Alignment for Computation of Absorption Factors.

Because of the interference of the main beam, the quantity I(s) could only be determined with the equipment used in this thesis down to an s value of about 0.4 Å^{-1}, which was about $2\frac{1}{2}$ degrees in 2θ space. The s = 0 value of i(s) is known to be:[49]

$$i(0) = \rho kT\kappa - 1 \qquad (8)$$

where κ is the isothermal compressibility. The usual practice, and used here, is to interpolate over the unobserved low s region using:[38]

$$j(s) = i(s)+1 = j(0)\left[1+a*s^2+b*s^4\right]^{-1} \qquad (9)$$

where a and b are constants to be determined from the data.

At high values of s the x-ray scattering for argon is expected to be the same as the gas scattering which is just an ensemble of non-interacting atoms. Note that scattering at high s values reflects scattering from two centers that are relatively close, namely intra-atomic electrons. Deviations from the independent atom scattering or gas scattering reflects structure or preferred positions which occur at lower values of the scattering parameter, s.

Therefore, experimental data were obtained in this work to sufficiently large values of s so that the comparison to the gas scattering could be made and I(s) could then be scaled to the same frame of reference as $f^2(s)$.

In this experiment an upper value of 2θ equal to 60° using Mo Kα radiation was sufficient and the experimental scattering behaved as the gas scattering for larger scattering angles.

B. General Data Analysis

The scattered radiation from a cell and argon sample as the result of being irradiated by a monochromatic beam of x-rays may be written as:

$$I_{ca}(2\theta) = N_a P(2\theta)\left[I_a^c(2\theta)A_a^c(2\theta)+I_a^i(2\theta)A_a^i(2\theta)\right]$$

$$+ N_c P(2\theta)\left[I_c^c(2\theta)A_c^c(2\theta)+I_c^i(2\theta)A_c^i(2\theta)\right] \qquad (10)$$

where 2θ is the scattering angle, N_a and N_c are normalization constants, $I_a^c(2\theta)$ and $I_a^i(2\theta)$ are the coherent and incoherent (Compton[14]) scattering from the argon sample, $A_a^c(2\theta)$ and $A_a^i(2\theta)$ are the coherent and incoherent absorption factors for the argon, $I_c^c(2\theta)$ and $I_c^i(2\theta)$ are the coherent and incoherent scattering from the cell, $A_c^c(2\theta)$ and $A_c^i(2\theta)$ are the coherent and incoherent absorption factors for the cell, and $P(2\theta)$ is the polarization factor given by:[14]

$$P(2\theta) = \tfrac{1}{2}\left[1+\cos^2(2\theta)\right] \qquad (11)$$

The quantity to be determined from data in Eq. (10) is $I_a^c(2\theta)$ which is I(s) in Eq. (1).

In order to determine the cell scattering, the empty cell pattern was measured every time in a separate

experiment. The empty cell scattering may be written as:

$$I_{ec}(2\theta) = N_c P(2\theta)\left[I_c^c(2\theta)A_{ec}^c(2\theta)+I_c^i(2\theta)A_{ec}^i(2\theta)\right] \quad (12)$$

where the subscript ec denotes empty cell.

Note that it appears that the distinction must be made between coherent and incoherent radiation because of the absorption factors which are wavelength dependent, with the incoherent wavelength, λ', given by:[14]

$$\lambda' = \lambda + 0.024\left[1-\cos(2\theta)\right] \quad (13)$$

where λ is the coherent wavelength. However, upon calculating absorption factors as described in Appendix D for this particular experiment for Mo Kα radiation, the fact emerged that for the cell, the difference between the incoherent and coherent absorption factors, with or without the sample present, was small and on the order of 0.002 at 60° 2θ. This fact may also be observed in a previous thesis.[2]

At this point in the data analysis the distinction between the coherent and incoherent absorption factors for the cell was ignored. Both types of absorption factors were computed for all experiments to confirm that

the difference was small. This assumption that the coherent and incoherent absorption factors for the cell were equal is the major difference in the data analysis procedure from the previous two theses.[1,2] Note that this assumption was not applied to the sample.

Therefore, letting $A^i_{ec}(2\theta) = A^c_{ec}(2\theta)$, Eq. (12) becomes:

$$I_{ec}(2\theta) = N_c P(2\theta) I^*_c(2\theta) A^c_{ec}(2\theta) \tag{14}$$

where $I^*_c(2\theta)$ is the total scattered radiation from the cell. Also, letting $A^i_c(2\theta) = A^c_c(2\theta)$, Eq. (10) becomes:

$$I_{ca}(2\theta) = N_a P(2\theta)\left[I^c_a(2\theta)A^c_a(2\theta)+I^i_a(2\theta)A^i_a(2\theta)\right]$$

$$+ N_c P(2\theta) I^*_c(2\theta) A^c_c(2\theta) \tag{15}$$

Therefore, to subtract the cell scattering from the cell plus sample scattering, the empty cell data could be divided by $A^c_{ec}(2\theta)$ and multiplied by $A^c_c(2\theta)$ and the subtraction carried out. This was not done.

The subtraction procedure above is correct only if the same amount of radiation was delivered to the two separate experiments and the cell position was the same for both. The x-ray generator did have drift and the

cell did move slightly during the experiments described here.

In order to observe and minimize the effect of the intensity drift, the entire 2θ space under study was scanned many times, with each complete scan requiring one to two hours. Then at the end of the experiment, the scans were simply added together for each 2θ, thus mimicking a multichannel analyzer. This technique had the advantage that the maximum drift in any single scan would be that which had occurred over the time period of that scan.

In order to scale the empty cell data to the cell plus sample data on an intensity basis, the drift in the summed counts for each scan was studied. The advantage of using the summed counts for a scan verses a single Bragg peak or flat region in the scan was that the summed counts yielded a much larger number and in terms of statistics a much smaller drift could be observed.

The actual intensity drift always observed between the empty cell and cell plus sample experiment was on the order of one to two per cent. This seemed to be reasonable for a 24 hour experiment because a new x-ray tube and solid state high voltage rectifiers in the x-ray generator were used.

The actual cell movement observed over the time period of an experiment was usually less than 0.001 inch as indicated by alignment checks before and after the experiment. However, with the cell moving, note that the number of scattering centers in the x-ray beam would change and an apparent intensity drift would then be observed. Also with cell movement, the alignment would change and thus affect the absorption factors.

To ascertain the effect on the data due to a change in absorption factors because of cell movement, the absorption factors were computed from the cell positions at the beginning and end of one experiment and the data subsequently analyzed. The effect was approximately $2^{\circ}K$ on the PY well depth and considered negligible.

The apparent change in intensity as indicated by the summed counts for a scan could not be definitely assigned to either incident intensity drift or cell movement. Since the relative change was never more than one to two per cent, and since the empty cell and cell plus argon were irradiated for the same lengths of count time, and since the total time for the entire experiment was on the order of 24 hours, the empty cell data were usually subtracted off with a scale factor, F, of about unity. The actual F factors used are presented in Table 2.

Hence, the argon scattering alone may be written as:

$$I_a(2\theta) = I_{ca}(2\theta) - F^*A_c^c(2\theta)I_{ec}(2\theta)/A_{ec}^c(2\theta) \qquad (16)$$

where $I_a(2\theta)$ is the total argon intensity. The argon intensity above is also the first term on the right hand side of Eq. (10).

At this point in the data analysis it was necessary to smooth the argon scattering curve and then correct it for distortion. The distortion correction technique requires derivative estimates which were obtained from the smoothed line estimate.

The smoothing technique used is an adaption of the cubic spline interpolation method and this is the first time it has been applied to this type of x-ray data. This smoothing technique fits piecewise cubics to a set of data, but now using least squares criterion and demanding continuity in the function and first derivative over the entire smoothing range. The derivation of this smoothing technique is presented in Appendix D.

However, like any technique, the user must make some decisions relative to its use. In spline smoothing the user must know or estimate the values of the function at the two end points of the data range along with the first derivatives.

For the data analysis here, the value of the function at $2\theta = 0$ simply had to be guessed because of distortion effects, but the derivative was zero because of symmetry. At the upper value of the independent variable the argon scattering curve behaved like the gas or independent atom scattering of x-rays, namely:

$$I_a(s) = N_a P(s) \left[f_a^2(s) A_a^c(s) + I_a^i(s) A_a^i(s) \right] \qquad (17)$$

where the independent variable is now changed to s as defined by Eq. (2), noting that Mo Kα radiation was used. All the quantities on the right hand side of Eq. (17) were known in a particular experiment except the normalization constant, N_a. $I_a(s)$ was easily estimated from the data at large values of s since the curve was relatively flat. Therefore N_a was determined and a derivative estimate was computed for input to the smoothing routine.

Also in using the spline smoothing technique, the user must specify the mesh points, or boundary points, which determine the intervals over which to fit the cubics. The final choice is dependent on how well the smoothed curve appears to approximate the data. This will involve nothing more than the user's judgment. Computing a variance is relatively useless since in any smoothing or curve fitting technique the user can deplete

all degrees of freedom and decrease the variance to zero. The input used to smooth the data for each experiment described here is presented in Table 2.

After the data were smoothed, they were corrected for distortion. The distortion effect arose from the fact that the detector accepted a finite angular spread of scattered radiation. The description of the distortion correction that applied to this experiment is presented in Appendix G.

After the data had been smoothed and corrected for distortion, the structure factor, i(s) could then be determined. At this point the scattering data were still of the form:

$$I_a(s) = N_a P(s)\left[I_a^c(s)A_a^c(s)+I_a^i(s)A_a^i(s)\right] \qquad (18)$$

Here a decision had to be made and that was the point at which i(s) went to zero. This point is referred to as the truncation point. This decision was made by visual examination of the data. The truncation point that was used for all experimental states was in the region of $5 < s < 5.5$ Å^{-1} which roughly corresponded to $2\frac{1}{2}$ oscillations of i(s) or the fifth zero in i(s).

Suppose that the truncation point chosen was s_o, then the assumption was made that the argon scattering,

$I_a(s)$, was described by the gas scattering at that point which then determined the normalization constant:

$$N_a = I_a(s_o)\left\{P(s_o)\left[f^2(s_o)A_a^c(s_o)+I_a^i(s_o)A_a^i(s_o)\right]\right\}^{-1} \qquad (19)$$

This normalization constant may be close to the one used in the smoothing step but not necessarily the same.

With the value of N_a determined, $I_a^c(s)$ could then be determined from the data:

$$I(s) = I_a^c(s) = I_a(s)/N_aP(s)A_a^c(s) - I_a^i(s)A_a^i(s) \qquad (20)$$

where $I_a^i(s)$ is the theoretical value of the incoherent atomic scattering. The structure factor, i(s) was then computed using Eq. (1). The scattering factors used in this thesis are presented in Appendix B.

At this point a consistency check could be made on the choice of the truncation limit or actually N_a. The r = 0 value of g(r)-1 is computed by:

$$g(0)-1 = (2\pi^2\rho)^{-1}\int_0^{s_o} s^2 i(s)ds \qquad (21)$$

Theoretically g(0) = 0 so that the value of the integral should be close to $-2\pi^2\rho$. This is essentially the integral normalization procedure suggested by Krogh-Moe.[46]

Note that the truncation procedure used chopped off a third peak in I(s) because it was not visible. Since the i(s) curves included two positive peaks and three negative peaks, it was anticipated that g(0)-1 would be biased in the negative direction. A rule of thumb criterion in computing i(s) was to demand that the value of g(0)-1 be not greater than -1 or smaller than -3 and preferably between -3 and -2. Therefore a trial and error procedure developed in choosing the truncation point.

Much discussion has ensued about the observability of the third positive peak in i(s) and its effect on the results. Clearly the exclusion or inclusion of this peak will affect the g(0) calculation. Numerical experiments on both of these topics are presented in Section V.

The technique used to Fourier transform the structure factor is that of integrating an analytic approximation. The structure factor was obtained as a set of smoothed points. These points were interpolated using the cubic spline interpolation presented in Appendix E. Appendix F indicates the algebra necessary to use the piecewise cubics in a Fourier transform.

The procedure used to obtain g(r) and c(r) from experimental data is summarized as follows:

1. Compute absorption factors for the observed alignment of the cell in the x-ray beam.

2. Subtract the cell data from the cell plus argon data to obtain the argon scattering.

3. Smooth the argon scattering which involves a guess of the normalization constant.

4. Correct the argon data for distortion effects.

5. Guess a truncation point on the argon scattering curve and compute i(s).

6. Compute g(0), if this value is not acceptable, repeat step 5.

7. Compute g(r) and c(r) and finally the Percus-Yevick potential.

IV. DATA PRESENTATION & DISCUSSION

Table 1. is a cross reference between the date of the experiment and the thermodynamic state. Each experiment is uniquely identified by a date because each thermodynamic state was studied at least twice. Figure 1. is a pressure-density phase diagram for argon locating the thermodynamic states that were studied. Table 3. presents the i(0) values obtained from Levelt[51] and Itterbeck.[52]

The data presented for each of eleven experiments are:

1. Absorption factors, Tables C.1 through C.12 in Appendix C.
2. Intensity measurements after summation of the scans and dual filter subtraction, and the argon spectrum, Tables 4.A through 4.K. (The * by a datum indicates that it was deleted in the smoothing step.)
3. Smoothed argon spectrum before and after the distortion correction, i(s), g(r), c(r) and PY u(r)/k, Tables 5.A through 5.K.

Examples of the raw data on the laboratory frame of reference for the experiments of 2/23/71, 7/28/71 and 12/15/71 are presented in Figures 2. through 4. These data are the starting point for the data analysis to obtain g(r) and c(r). Observe the low angle region in these Figures and note that the empty cell scattering should go to zero at $2\theta = 0$ because beryllium is essentially incompressible. For the data of 2/23/71

this appears to be the case but not for the data of 7/28/71 and 12/15/71. The data in the last two Figures show an enounter of the x-ray main beam. This occurred because the receiving slit on the detector was opened up to insure observation of all of the cell at high values of 2θ and hence prevent any rotation of the data.[1] The upswing of the low angle cell plus sample data of 2/23/71 is due to the isothermal compressibility of argon. The raw data from all experiments were plotted in this manner and the main beam encounter was noted.

The subtraction procedure to obtain the argon scattering did not necessarily recover the argon scattering at low angles when the main beam was encountered as it might be assumed. Therefore the datum that indicated it was contaminated by the main beam was usually deleted.

Also note in Figures 2. through 4. in the region of 20° 2θ that the beryllium peaks are very large relative to the argon scattering. This is the region of the second peak of i(s) for argon.

Figures 5. and 6. present the raw argon spectrum for the data of 11/30/71 and 12/15/71 along with the smoothed line and gas scattering estimate. Note that there is no apparent rotation[1] of the data and these two line estimates coincide at the larger values of s. Also these two Figures give a visual indication of the scatter

of the data. One reason for the apparently large statistical scatter is that there have been three subtractions performed to get to this point, namely, the dual filter subtraction for the empty cell and cell plus sample, and the subtraction of the empty cell data from the cell plus sample data.

From Figures 5. and 6. the decision is to be made relative to the existence of the peaks in i(s). In either Figure the third peak or valley is difficult to determine. There is a deviation from the gas scattering, but remember that this deviation must be multiplied by the independent variable in order to compute the Fourier transform.

Figures 7.A through 7.M and 8.A through 8.M present the various steps performed to obtain g(r), c(r) and the PY potential for the data of 11/30/71 and 12/21/71. The structure factor, i(s), in each of these sets of Figures includes two positive peaks. This is to be contrasted in the numerical experiments with a parallel presentation of the 12/21/71 data with three peaks in i(s), hence the meaning of the ❷ on the 12/21/71 Figures.

Figures 7.A and 8.A each indicate the magnitude of the distortion correction relative to the uncorrected curve for the sample-detector distance used. This correction is not large but this is to be contrasted in

the numerical experiments with the sample-detector distance used by Mikolaj.[1]

Figures 7.B and 8.B present the structure factor computed by Eq. (1). Note the isothermal compressibility effect on the 12/21/71 data as a decrease in i(0) relative to that of 11/30/71.

In the following discussion of Figures 7. and 8. only the alphabetic identification will be referred to. Figures C and D present the kernels of the Fourier transforms of $r\left[g(r)-1\right]$ and rc(r). The $r\left[g(r)-1\right]$ kernels are rather uniform in appearance, but the rc(r) kernels show a dominant feature in the region of 1 Å^{-1}. As the isothermal compressibility decreases, this feature becomes more pronounced.

Figures E through J present the actual curves to be integrated to obtain $r\left[g(r)-1\right]$ and rc(r) for r = 3.8, 5.2 and 7.2 Å. These quantities are then just the corresponding kernels multiplied by sin(sr). The area under the curve in the r = 3.8 Å Figures is approximately g(r)-1 or c(r) since the lead constant on the integral, $(2\pi^2\rho r)^{-1}$, is close to unity. The 3.8 Å value of r is approximately where the maximum of g(r) and c(r) occur.

Consider now the 5.2 Å Figures where 5.2 Å is just midway between the first and second peaks of g(r). The observation to be made is that the positive and negative

contributions to the integral are not small and to compute g(r) or c(r) the difference of two relatively large areas must be obtained and this is prone to errors. Any error in determining i(s) in a small region of s space, for example around $2\theta = 20^{\circ}$, could easily alter the result. This region of r space is where the subsidiary peak appears in g(r) and a corresponding second peak in c(r).

Figures G and J present the curves to be integrated to obtain $r\left[g(r)-1\right]$ and rc(r) for r = 7.2 Å. This is the region in r space where the second peak in g(r) appears. Note the dominant feature in the c(r) integrand around 1 $Å^{-1}$.

Figures K and L present the g(r)-1 and c(r) estimates up to r = 10 Å. The final Figures, M, present the PY potentials for these two states.

A summary of the Percus-Yevick well depths, the main peak height of i(s), g(r), c(r) and the width of the main i(s) peak at i(s) = 0 is presented in Figures 9. through 13. and Table 6.

V. NUMERICAL EXPERIMENTS

A. The Distortion Effect

It was previously noted in the Data Presentation that the distortion correction applied to the data in this work was relatively small. The reason for the correction being small is that the sample-detector distance used was large relative to the sample length. However, an interesting effect may be demonstrated if a set of data that has been corrected is numerically distorted back to a smaller sample-detector distance, thus mimicking the experimental conditions of Mikolaj,[1] and then computing g(r), c(r) and the PY potential. The distortion correction is described in Appendix G.

It is assumed that the sample-detector distance used by Mikolaj was on the order of 4.8 inches.

Tables 7.A through 7.D present the results of numerical experiments on the effect of distortion carried out on four sets of real data. These results are to be compared with the corresponding correct data in Tables 5.A through 5.K.

The result of computing g(r), c(r) and the PY potential from data that appears as if they were obtained with a sample-detector distance of 4.8 inches is a marked decrease in the PY well depth. For the particular thermodynamic states studied, this error is

on the order of 15°K. This error is also density dependent as may be inferred from the derivation of the correction procedure. The correction is slope sensitive because the detector is an averager and biased to high angles in the configuration used.

The numerical distortion experiment carried out on the data of 6/23/71 is presented in plotted form in Figures 14.A through 14.G. The most marked effect is seen in Figure 14.D which shows the change in the kernels of the Fourier transform of rc(r). It is true that both g(r) and c(r) change in the same direction upon correcting for distortion, but note that si(s) is divided by 1+i(s) to compute c(r), and in the region of 1 $\mathring{A}^{-1}$, i(s) is less than zero, thus errors are magnified and the change in c(r) is greater than in g(r).

Table 8. summarizes the results of the numerical experiments on distortion relative to the PY well depths for four experiments.

The distortion phenomenon explains why Mikolaj's computed PY well depths are too small and the apparent slope of these well depths verses density is too steep.[21,35]

B. Subsidiary Peak Phenomenon

During the course of working up the data in this thesis the so-called subsidiary peak[2,4,40-44] sometimes appeared. The appearance was not at all consistent,

but an example of how it may occur was obtained in the data of 6/23/71 which are presented in Table 9.

The results for this set of data are plotted in Figures 15.A through 15.E. On each of these Figures there are two curves, one which yields the subsidiary peak and one which does not. The decision to be made is the choice between the two smoothed curves in Figure 15.A which represent the data on the laboratory frame of reference.

It is interesting to note that there is a second peak in c(r) when there is a subsidiary peak in g(r) for this set of data, hence, the local minimum on the outer wall of the PY potential.

This demonstration does not present evidence either pro or con relative to the existence of the subsidiary peak. However, of all of the data presented in this thesis, there are few occurrences of the subsidiary peak and duplicate efforts did not yield the same subsidiary peak. It may be said that the reproducibility of the subsidiary peak at the present time is nonexistent.

C. The Effect of Uncertainties in Smoothing Data in the Low Angle Region

During the course of examining the data from these experiments, a few experimental measurements presented PY well depths that were markedly too shallow or too deep. For quite some period of time the explanation was not

known. With the aid of duplicate experiments on the thermodynamic states studied, it was guessed that the reason had something to do with the low angle region of the data space.

Now a set of data has been prepared that shows the sensitivity of c(r), but not g(r), to the smoothed line estimate in the low 2θ region. The data of 7/28/71 presented in Figures 16.A through 16.G show two parallel work ups where everything is essentially the same except that the first two data points in Figure 16.A are deleted for one of the curves.

The reason for deleting data in this region is that the detector had encountered the x-ray main beam. Refer back to Figure 3. which is a plot of the raw data for the experiment of 7/28/71 and note the increasing empty cell intensity with decreasing angle. Contrast this observation against the raw data for the experiment of 2/23/71 which show the correct empty cell intensity behavior.

The important Figure to observe in this sequence is 16.D which is a plot of the kernels of the Fourier transform of rc(r). The difference between the two curves is relatively large around $s = 0.5$ Å^{-1}, and the sine wave that multiplies these curves for the evaluation of the integral to obtain c(r) for $r = 3.8$ Å does not depress this region. Observe Figure 16.F which is the

c(r) plot and finally Figure 16.G which shows the difference in the PY potentials. The ❶ and ❷ on these Figures denote the same set of data in the sequence.

Qualitatively, c(r) increases as the smoothed line estimate of the argon spectrum in the low s region is biased upward. The effect on g(r) for the same bias of the smoothed line estimate is nil. Therefore, the effect on the PY potential is a net decrease.

Table 10.A presents the data plotted in Figures 16.A through 16.G. Table 10.B presents the data from the experiment of 8/4/71 which yielded a PY well depth that was too shallow as contrasted against the data of the same experiment presented in Table 5.E. The only difference in these two sets of data again is the low angle smoothed line estimate.

D. Truncation, The Existence of a Third Peak in i(s) at Various Pressures and the Effect of Neglecting It

The truncation of the structure factor, i(s), was determined by what could be observed from the raw data on the laboratory frame of reference such as those presented in Figures 5. and 6. To this date, argon spectra such as these have never been presented in this form. These spectra are the argon scattering as observed by the detector. No corrections have been made and only the cell scattering has been subtracted off.

The size of the oscillations in the data above

$4\frac{1}{2}$ Å^{-1} are on the order of the scatter of the data. To be emphasized is the fact that in the ensuing data analysis the gas scattering is subtracted from the data and the result multiplied by the independent variable, thus errors are also multiplied.

The structure factor is state dependent. For two thermodynamic states on an isotherm, i(s) for the higher pressure state is expected to have larger peak heights due to an increase in packing over the lower pressure state.

Three thermodynamic states on the 127°K isotherm were studied. The pressures of these states were 54.4, 36.8 and 18.7 atm. Therefore, these data can be used to infer information about the observability of the third peak in i(s) and the effect of truncating it.

The experiment of 12/15/71 was conducted at 54.4 atm and 127°K and the argon spectrum is presented in Figure 6. This Figure indicates that there might possibly be an observable third peak in i(s). Therefore, to determine the effect of neglecting the third peak, or truncating it, these data were worked up with and without it.

Figures 17.A through 17.D and Table 11.A present i(s), g(r), c(r) and the PY potential for this case. The structure factors in Figure 17.A show a slight difference over the entire range of s because the

imposed normalization for g(0) was not exactly the same for both. Note that including a third peak increases the integral of $s^2i(s)$ and it is also anticipated that both g(r) and c(r) will increase in the region of r = 3.8 to 4.0 Å.

Figures 17.B and 17.C present the computed g(r) and c(r) functions. The functions in each Figure that are larger in the region of r = 3.8 Å correspond to the structure factor with three positive peaks.

Figure 17.D presents the PY potentials with the ❸ on this Figure designating the potential corresponding to the structure factor with three peaks. The difference in the minima is seen to be on the order of $2^{\circ}K$.

Table 11.B presents a similar treatment for the data of 12/21/71 whose thermodynamic state is the same as that of 12/15/71. These data show a third peak in i(s) that has a markedly decreased period of oscillation from the other peaks. Note that Verlet[40] indicates the oscillations should be regular at these and higher values of s.

Therefore, when data are obtained at lower pressures and higher temperatures for argon, it is anticipated that i(s) will show decreased peak heights and the effect of neglecting a third positive peak should not present errors greater than those just observed. The effect on the PY potential is minimal.

E. Effect of g(0) Being Significantly Different from Zero

In the Data Analysis Section it was stated that the computed g(0) value was being used as a guide to yield information about the normalization of i(s). To determine the effect of the choice of the normalization criterion used, a study was carried out allowing g(0) to assume positive values significantly different from zero to observe the effect on g(r), c(r) and the PY potential.

The data of 11/30/71, which include in the structure factor two positive peaks, were reworked and the g(0) value forced positive by truncating i(s) at a different value of s. Figures 18.A through 18.D and Tables 12.A through 12.B present two parallel work ups for i(s) which give g(0) values of about +3 and +6. Note in these Figures that the effect on g(r) at r = 3.8 Å is somewhat less than on c(r). The PY well depth for the +3 case is about 114°K and for the +6 case about 109°K.

Also note that in forcing g(0) positive that the third valley in i(s) almost disappeared. This is in contrast to the behavior expected by Verlet.[40]

Compare these well depths to the 11/30/71 data in Table 5.H where the well depth is 120°K for g(0) ≈ -0.5. The overall difference is not negligible.

Actually, the value of g(0) cannot be discussed without taking into account truncation. If a third peak had been included in the set of data used in this numerical experiment, g(0) would have been larger.

Therefore, to estimate an upper bound on the contribution to g(0) from a neglected third peak in i(s), consider the following. The third valley of i(s) in the 11/30/71 data in Table 5.H was multiplied by -1 and shifted up in s space by 1.12 Å^{-1} to mimic a third peak. Integrating $s^2 i(s)$ over this assumed third peak and multiplying by $(2\pi^2\rho)^{-1}$ yielded about 4.5. Using this as an extreme upper bound, g(0) would be expected to be about -3.5 neglecting the third peak in i(s).

Note that the amplitude of each successive oscillation of i(s) appears to decrease by about a factor of two, and also in this particular case the third valley appears to span too great a range in s space. Therefore, to be more realistic, neglecting the third peak should yield g(0) on the order of -2.

This experimental evidence indicates that positive g(0) values are not plausible when a third peak in i(s) is neglected. Also, if three peaks and valleys are included, it is plausible to expect g(0) to be close to zero. Peaks higher in s space are not expected to significantly alter g(0).

Therefore, if argon data for the states studied are presented that yield positive $g(0)$ values significantly different from zero, for example +10, then the PY well depth will be shallow by approximately 15°K. If a third peak is included in $i(s)$, then there will be three negative and three positive peaks and the computed $g(0)$ value should be quite close to zero. The assumed negative bias of $g(0)$ in this work appears to be reasonable.

F. Effect on $g(r)$ and $c(r)$ Using Post- vs. Pre-cell Alignment for Computing Absorption Factors

In the Data Analysis it was stated that the cell moved during the course of an experiment. The cell position in the x-ray main beam must be known to compute absorption factors. In order to evaluate the effect of such movement on final results, the data of 9/28/71 were worked up with both sets of absorption factors. The post-alignment was approximately 0.001 inch lower.

The changes in $g(r)$ and $c(r)$ were not large, $g(r)$ being either 2.09 or 2.06 at 3.8 Å, and $c(r)$ being either 1.21 or 1.18 at 3.9 Å. The PY well depth changed by approximately 2°K at 4.0 Å. Table 13. presents the data worked up with the post-alignment absorption factors designated as (II) and Table 5.G presents the pre-alignment case designated as (I). The absorption factors for each case may be found in Appendix C.

Therefore, cell movement during an experiment did not significantly affect the results.

VI. CONCLUSIONS AND RECOMMENDATIONS

A summary of the PY well depths, main peak heights of i(s), g(r) and c(r) is presented in Figures 9. through 12. These Figures give an estimate of the experimental reproducibility. These results are best estimates based on the numerical experiments presented. There is no reason to believe that the scatter in the final results is due to any cause other than the scatter in the data on the laboratory frame of reference.

The following question arises. Will the results change appreciably, for example, $\pm 10^{\circ}K$ on the PY well depths, if better experimental or numerical techniques were developed and used? The answer, though somewhat subjective, is no for the following reasons.

The divergence correction relies on the stated assumption of a nondivergent, or perfect, main beam. It is estimated that a change of not more than a $5^{\circ}K$ increase in the well depth would occur if the main beam divergence was considered. This estimate is based on the fact that the x-ray target to sample distance is greater than the sample to detector distance and in the configuration used, an error of $5^{\circ}K$ would have occurred if the data were not corrected for the sample to detector distance. Also the main beam was collimated.

It should be noted that the atomic scattering

factors used are based on a free atom and do not take into account the fact that neighbors are present. The effect of this approximation on the results is not obvious, but a significant effect is not expected.

The lack of data in the low s region and the need for interpolation to s = 0 possibly results in an error in c(r). Numerical experiments on this aspect suggest that an error of 10°K in the computed well depths is possible, but the sign of this error is not evident. This problem is definitely important because of the compressibility of argon for the thermodynamic states studied, and hence, the effect on the kernel of the Fourier transform of rc(r).

The effect of double scattering[53,54] was not considered. This phenomenon arises from the fact that a photon may actually be scattered twice rather than once before entering the detector. The possible paths then could be cell to cell, sample to sample, cell to sample and sample to cell. The effect of this phenomenon on the final results was not investigated, but a significant effect is not expected.

At this point, it is anticipated that there is no other important experimental phenomenon that has not been considered or mentioned.

On the basis of the data and results presented in

this thesis, the following conclusions relative to current statistical mechanical theories of fluids may be drawn:

1. The Percus-Yevick well depths, u(r)/k, for argon computed from measured g(r) and c(r) functions are in the range of 105 to 120°K for the five states of argon studied. Because of the narrow density range studied, 0.91 to 1.135 gm/cc, these well depths should only be interpreted as estimates of the effective pair potential in this density range and extrapolation is not recommended.

2. Given current estimates of the zero density pair potential and of the effective pair potential in the presence of a weak three-body force, the Percus-Yevick equation predicts a state dependent potential because it does not take into account non-additive effects. The PY well depths for this set of data are in reasonable agreement with the theoretical work of Rowlinson, et al,[35,36] as presented in Figure 19.

3. The Mikolaj-Pings[38] well depths are too shallow by at least 15°K because the raw experimental data were not corrected for distortion as described in Appendix G.

Recommendations for improving the experimental and numerical techniques are:

1. The scattering contributions due to the beryllium

cell must be minimized to observe liquid structure above $s = 5\ \text{Å}^{-1}$. This may be accomplished by the use of a beryllium single crystal cell.

2. Low angle data which can be obtained on a low angle goniometer are needed to improve the accuracy of the direct correlation function. This is indicated in numerical experiments on the effect of uncertainties in low angle data smoothing.

3. The effect of the finite incident beam divergence should be investigated with the possibility of removing the incident sollers to increase incident x-ray intensity.

4. In the analysis of x-ray data for fluids of the type studied here, $g(0)$ should be close to zero.

REFERENCES

1. P. G. Mikolaj, "An X-ray Diffraction Study of the Structure of Fluid Argon," doctoral thesis, California Institute of Technology, Pasadena, California (1965).

2. S. C. Smelser, "An X-ray Diffraction Study of the Structure of Argon in the Dense Liquid Region," doctoral thesis, California Institute of Technology, Pasadena, California (1969).

3. D. G. Henshaw, D. G. Hurst and N. K. Pope, Phys. Rev. 92, 1229(1953).

4. D. G. Henshaw, Phys. Rev. 105, 976(1957).

5. K. Lark-Horowitz and E. P. Miller, Nature 147, 460(1940).

6. N. S. Gingrich and C. W. Thompson, J. Chem. Phys. 36, 2398(1963).

7. R. W. Harris and G. T. Clayton, Phys. Rev. 153, 229(1967).

8. L. A. DeGraff and B. Mozer, J. Chem. Phys. 55, 4967(1971).

9. H. L. Frisch and Z. W. Salsburg, ed., Simple Dense Fluids, Academic Press, N. Y.(1968).

10. H. N. V. Temperly, J. S. Rowlinson and G. S. Rushbrooke, ed., Physics of Simple Liquids, North-Holland Pub. Co., Amsterdam(1968).

11. V. N. Filipovich, Soviet Phys.-Tech. Phyd. 1, 391, 409(1965).

12. R. W. James, The Optical Principles of the Diffraction of X-rays, G. Bell and Sons, London, England(1962).

13. H. H. Paalman and C. J. Pings, Rev. Mod. Phys. 35, 398(1963).

14. A. Guinier, X-ray Diffraction in Crystals, Imperfect Crystals, and Amorphous Bodies, W. H. Freeman and Co., San Francisco(1963).

15. L. S. Ornstein and F. Zernike, Proc. Acad. Sci. (Amsterdam) 17, 793(1914).

16. L. Goldstein, Phys. Rev. 84, 466(1951).

17. J. K. Percus and G. J. Yevick, Phys. Rev. 110, 1(1958).

18. C. J. Pings, Discussions Faraday Soc. 43, 89(1967).

19. J. A. Barker and A. Pompe, Aust. J. Chem. 21, 1683(1968).

20. J. A. Barker, D. Henderson and W. R. Smith, Phys. Rev. Lett. 21, 134(1968).

21. D. A. Copeland and N. R. Kestner, J. Chem. Phys. 49, 5214(1968).

22. H. W. Graben and R. Fowler, Phys. Rev. 177, 288(1969).

23. H. W. Graben, Phys. Rev. Lett. 20, 529(1968).

24. O. Sinanolgu, Adv. Chem. Phys. 12, 283(1967).

25. R. D. Present, J. Chem. Phys. 47, 1793(1967).

26. M. Ross and B. J. Alder, J. Chem. Phys. 47, 4129(1967).

27. A. E. Sherwood, A. G. DeRocco and E. A. Mason, J. Chem. Phys. 44, 2984(1966).

28. H. W. Graben, R. D. Present and R. D. McCullough, Phys. Rev. 144, 140(1966).

29. L. Jansen, Adv. Quant. Chem. 2, 119(1965).

30. A. D. McLachlan, Discussions Faraday Soc. 40, 239(1965).

31. T. Kihara, Adv. Chem. Phys. 1, 267(1958).

32. B. M. Axilrod and E. Teller, J. Chem. Phys. 11, 2999(1943).

33. G. S. Rushbrooke and M. Silbert, Molec. Phys. 12, 505(1967).

34. J. S. Rowlinson, Molec. Phys. 12, 513(1967).

35. G. Casanova, R. J. Dulla, D. A. Jonah, J. S. Rowlinson and G. Saville, Molec. Phys. 18, 589(1970).

36. R. J. Dulla, J. S. Rowlinson and W. R. Smith, Molec. Phys. 21, 299(1971).

37. J. M. Parson, P. E. Siska and Y. T. Lee, J. Chem. Phys. 56, 1511(1972).

38. P. G. Mikolaj and C. J. Pings, J. Chem. Phys. 46, 1401(1967), J. Chem. Phys. 46, 1412(1967).

39. J. A. Barker, D. Henderson and W. R. Smith, Molec. Phys. 17, 579(1969).

40. D. Levesque and L. Verlet, Phys. Rev. Lett. 20, 905(1968).

41. P. L. Fehder, J. Chem. Phys. 52, 791(1970).

42. D. Stripe and C. W. Tompson, J. Chem. Phys. 36, 3921(1962).

43. J. A. Campbell and J. H. Hildebrand, J. Chem. Phys. 11, 334(1943).

44. G. T. Clayton and L. Heaton, Phys. Rev. 121, 649(1961).

45. A. A. Khan, Phys. Rev. 136, A1260(1964).

46. J. Krogh-Moe, Acta. Cryst. 9, 951(1956).

47. H. L. Daneman and G. C. Mergner, Rev. Sci. Instr. 39, 1498(1968).

48. S. Y. Wu, "Study of Equilibrium Critical Phenomena in Fluid Argon," doctoral thesis, California Institute of Technology, Pasadena, California (1971).

49. T. L. Hill, Statistical Mechanics, McGraw-Hill Book Co., N. Y.(1956).

50. J. L. Walsh, J. H. Ahlberg and E. N. Nilson, Journal of Math. & Mech. 11, 225(1962).

51. A. Michels, J. M. H. Levelt and G. J. Wolkers, Physica 24, 769(1956).

52. A. Van Itterbeck, O. Verbeke and K. Staes, Physica 29, 742(1963).

53. B. E. Warren and R. L. Mozzi, Act. Crysta. 21, 459(1966).

54. S. L. Strong and Roy Kaplow, Act. Crysta. 23, 38(1967).

55. W. I. Honeywell, "X-ray Diffraction Studies of Dense Fluids," doctoral thesis, California Institute of Technology, Pasadena, California (1964).

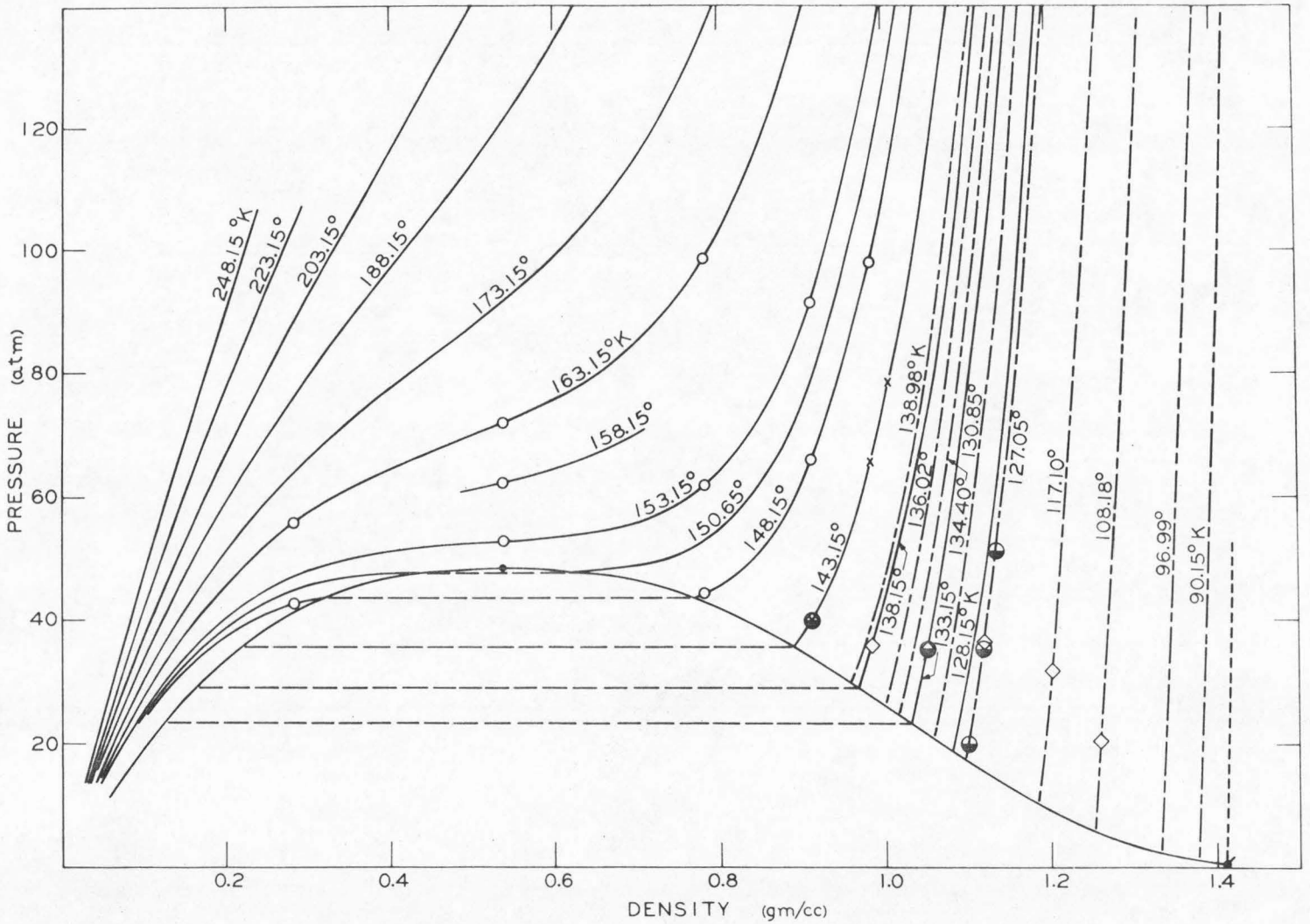

Figure 1. Argon pressure-density diagram showing locations of experimental states, ◒ this work, ○ Mikolaj,[1] ◇ Smelser,[2] X Honeywell.[55]

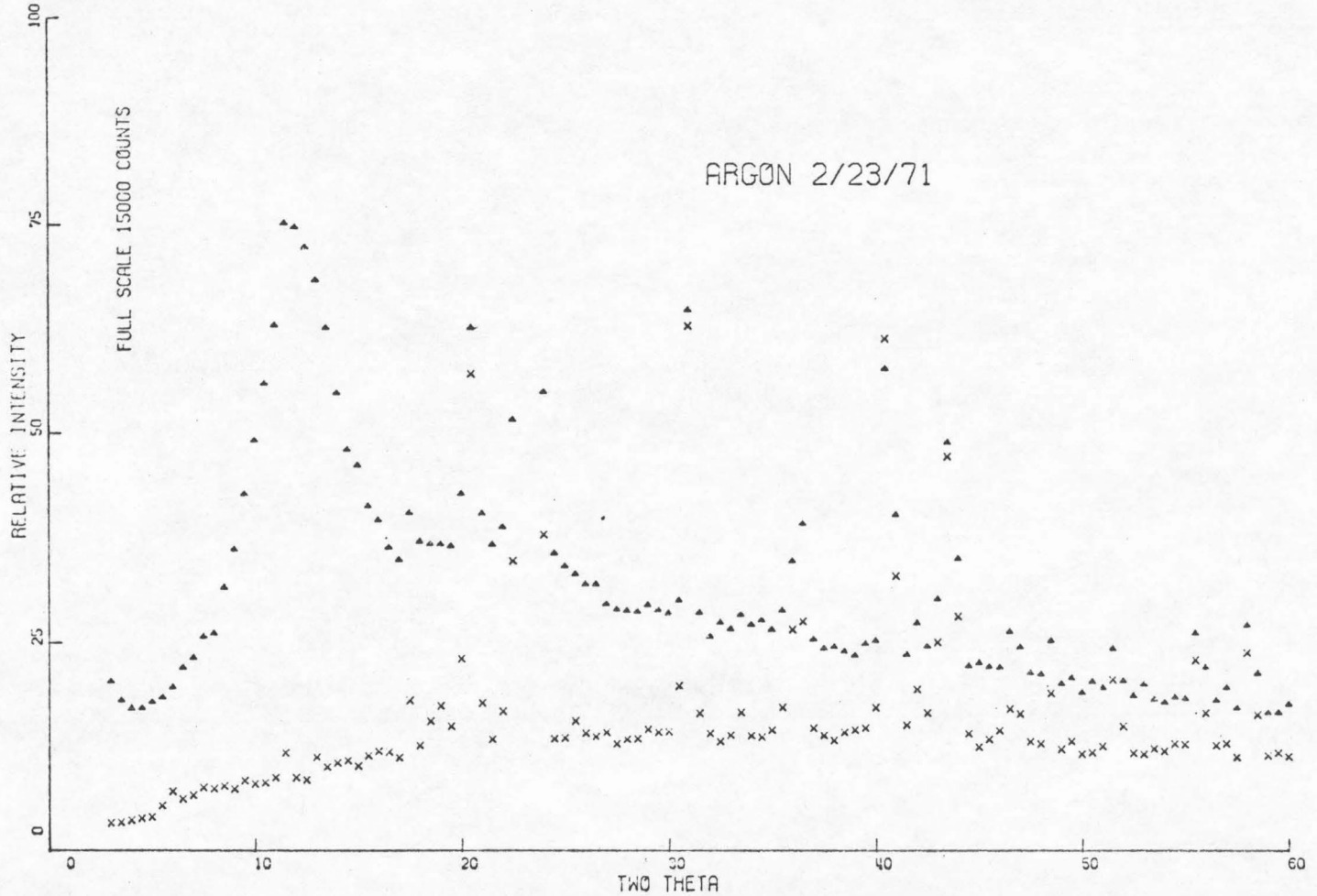

Figure 2. Example of raw data, X = empty cell, ▲ = cell plus argon.

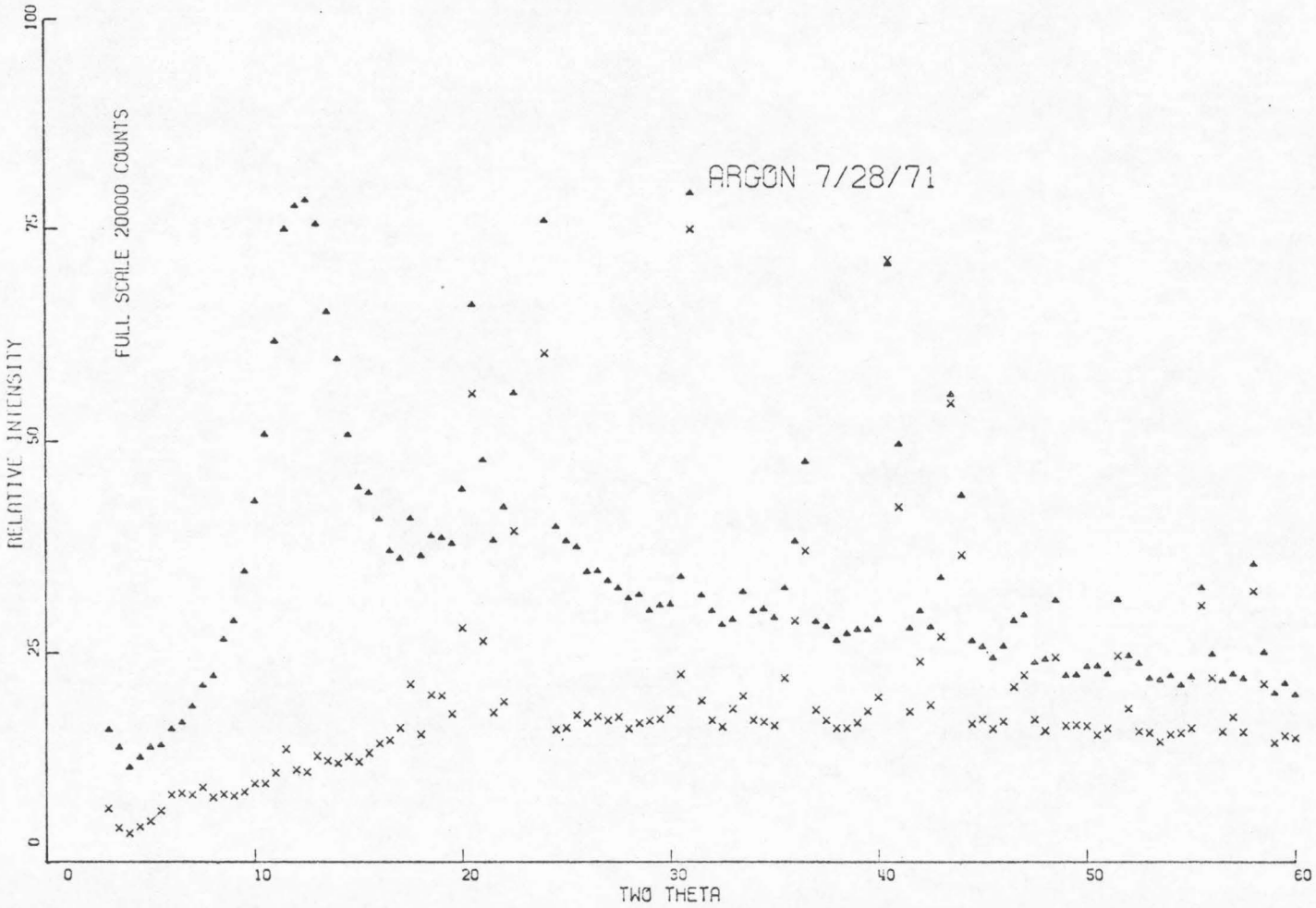

Figure 3. Example of raw data, X = empty cell, ▲ = cell plus argon.

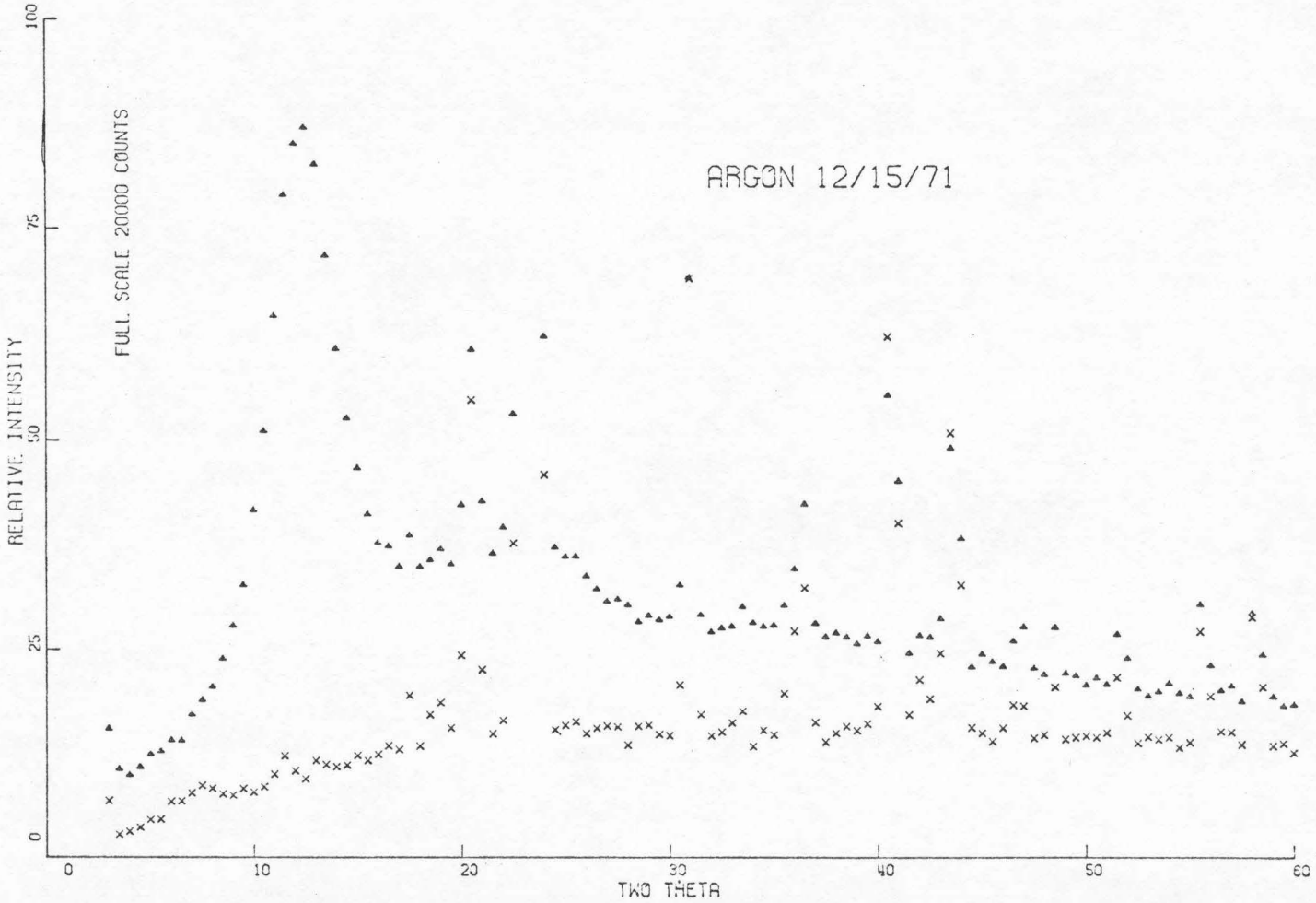

Figure 4. Example of raw data, X = empty cell, ▲ = cell plus argon.

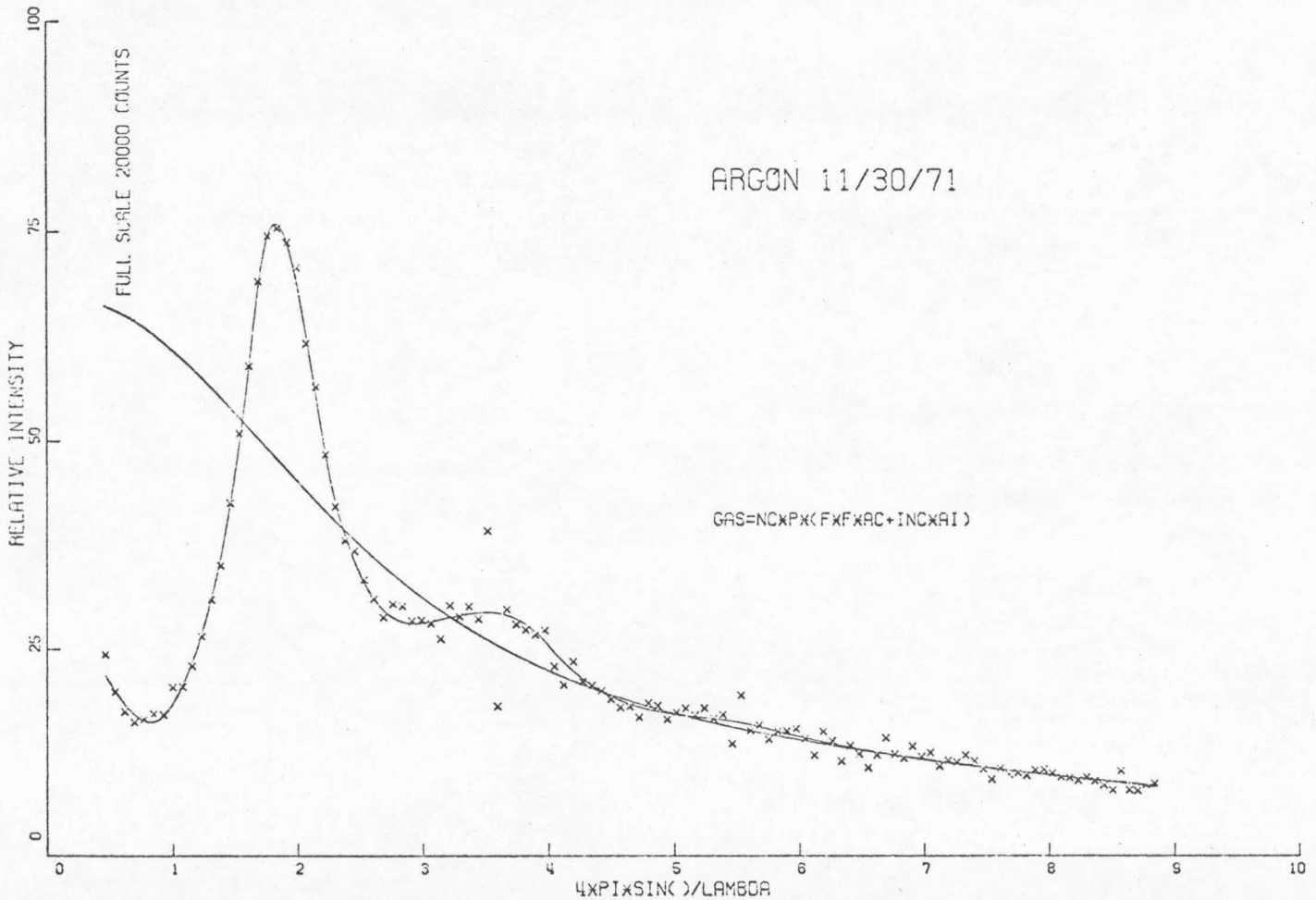

Figure 5. Example of argon spectrum, smoothed line estimate and gas scattering estimate.

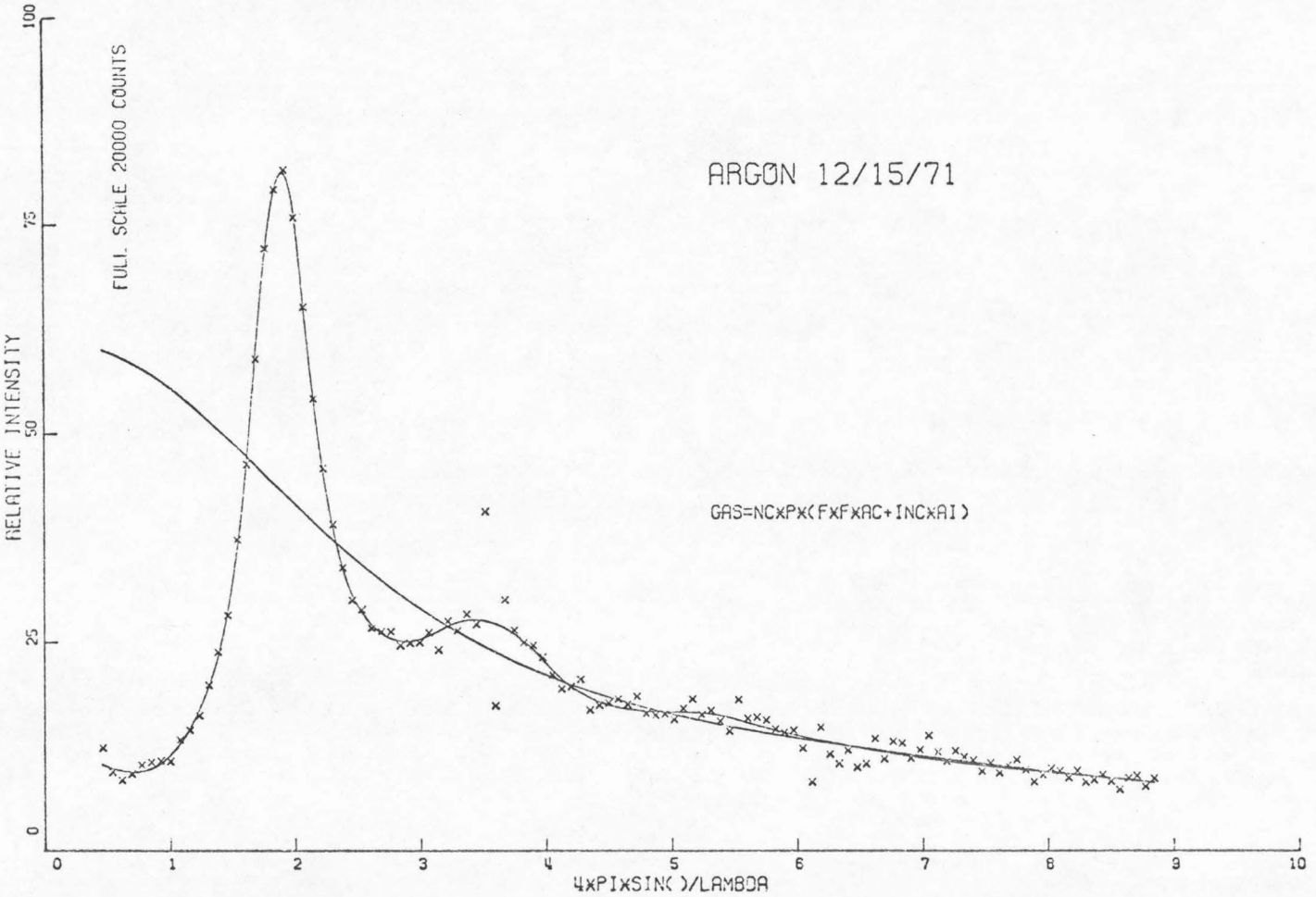

Figure 6. Example of argon spectrum, smoothed line estimate and gas scattering estimate.

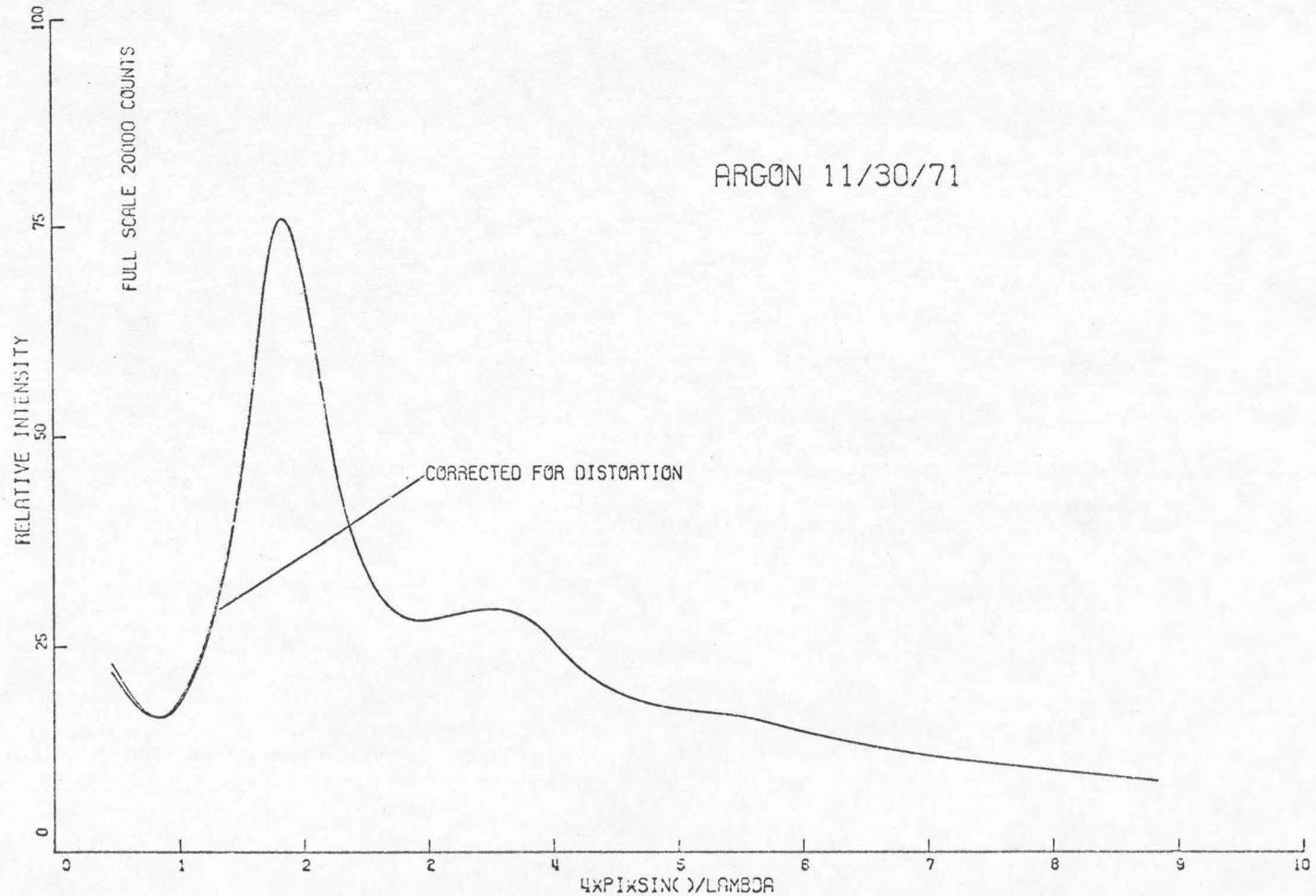

Figure 7.A (through 7.M). Example of data analysis, smoothed and distortion corrected argon spectrum.

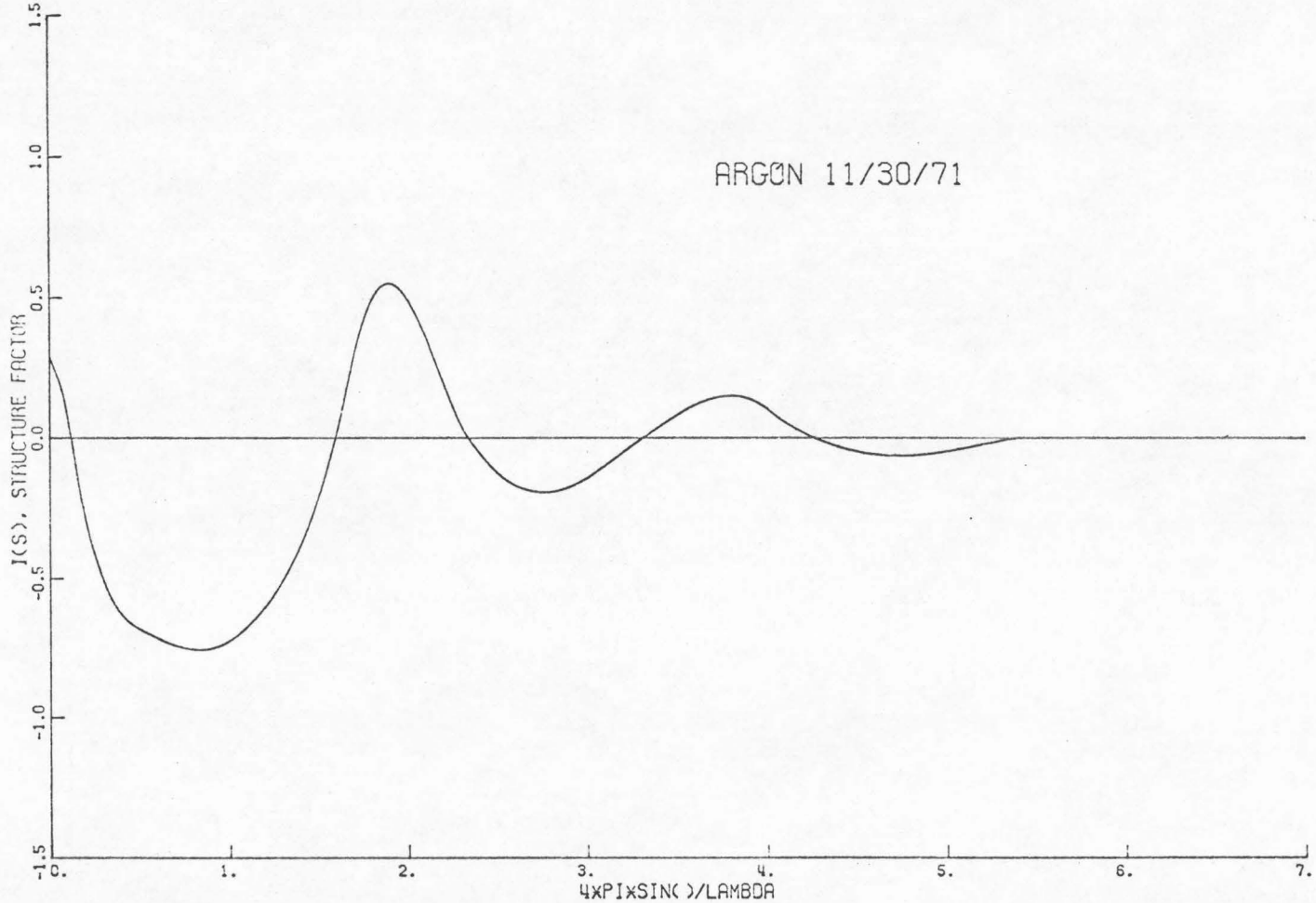

Figure 7.B. Structure factor.

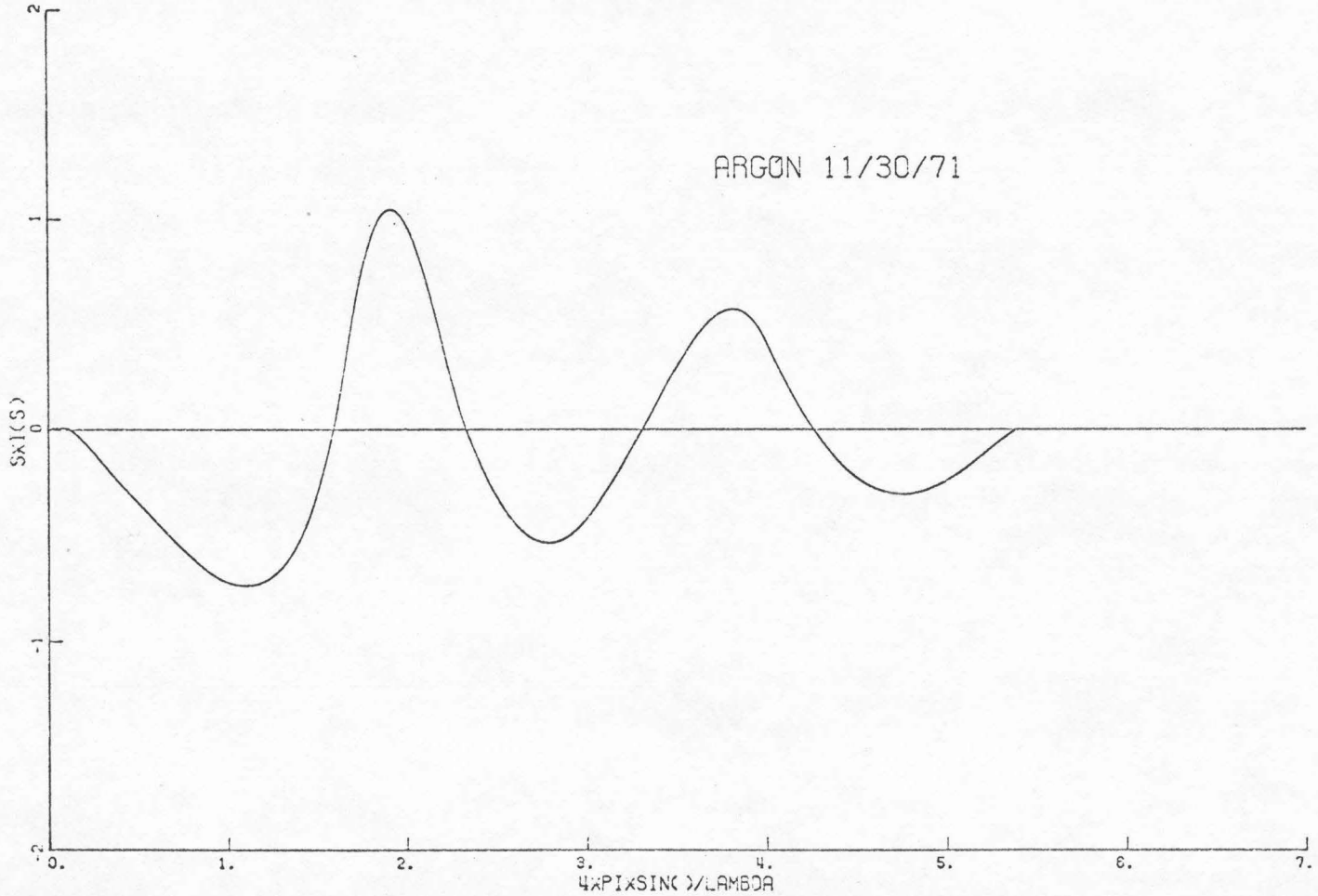

Figure 7.C. Kernel of Fourier transform of $r\left[g(r)-1\right]$.

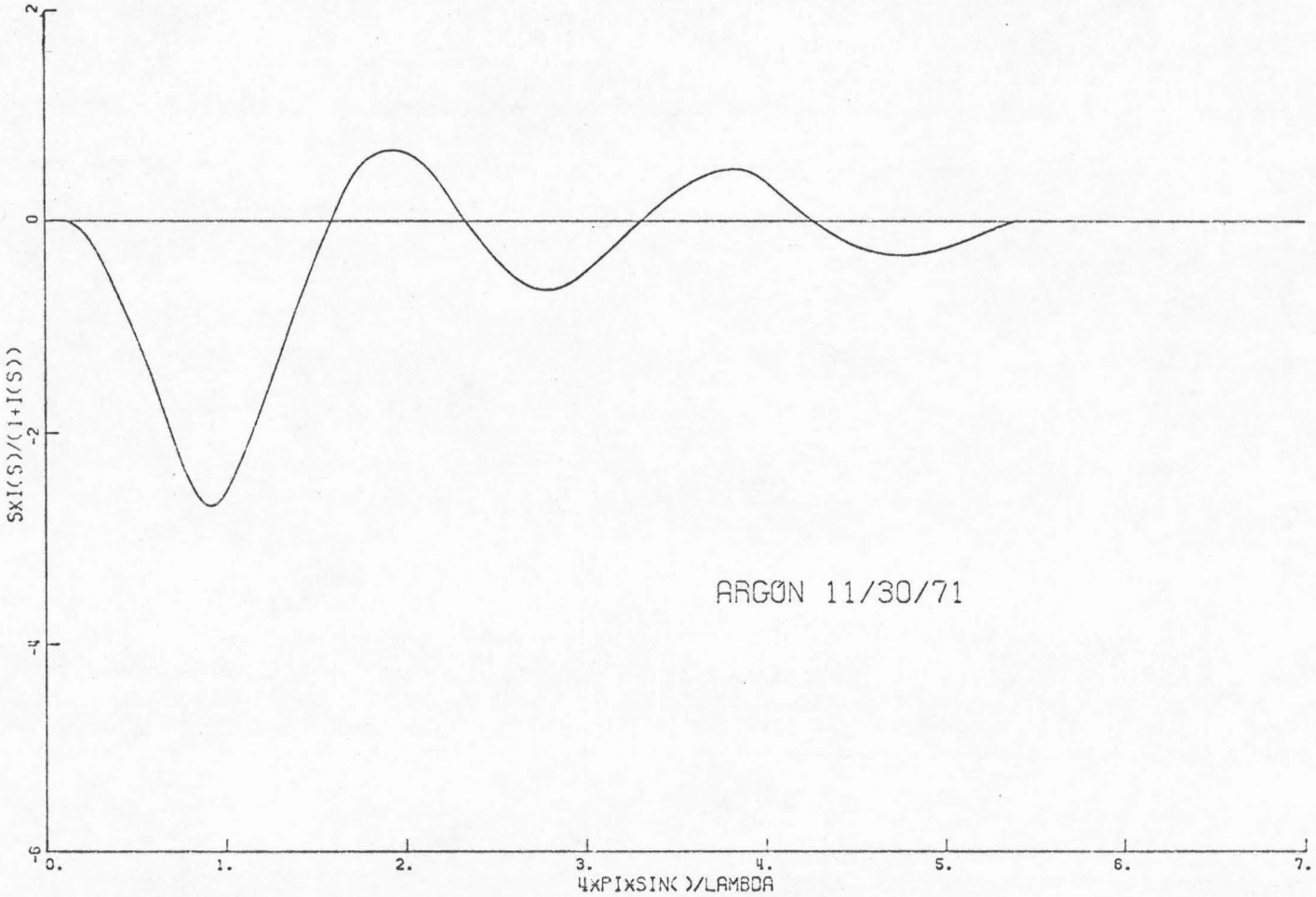

Figure 7.D. Kernel of Fourier transform of rc(r).

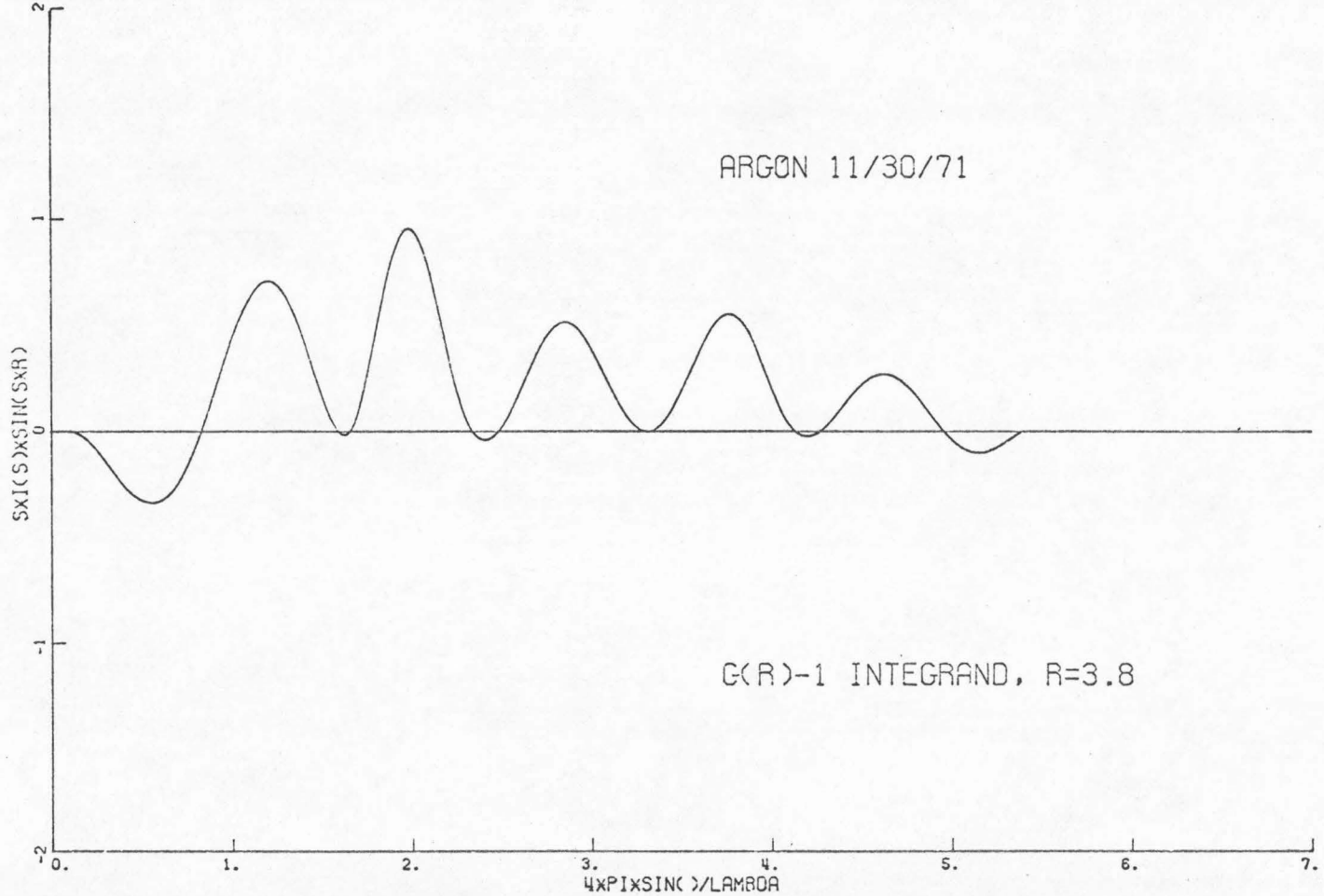

Figure 7.E. Integrand for $r\left[g(r)-1\right]$, r = 3.8 Å.

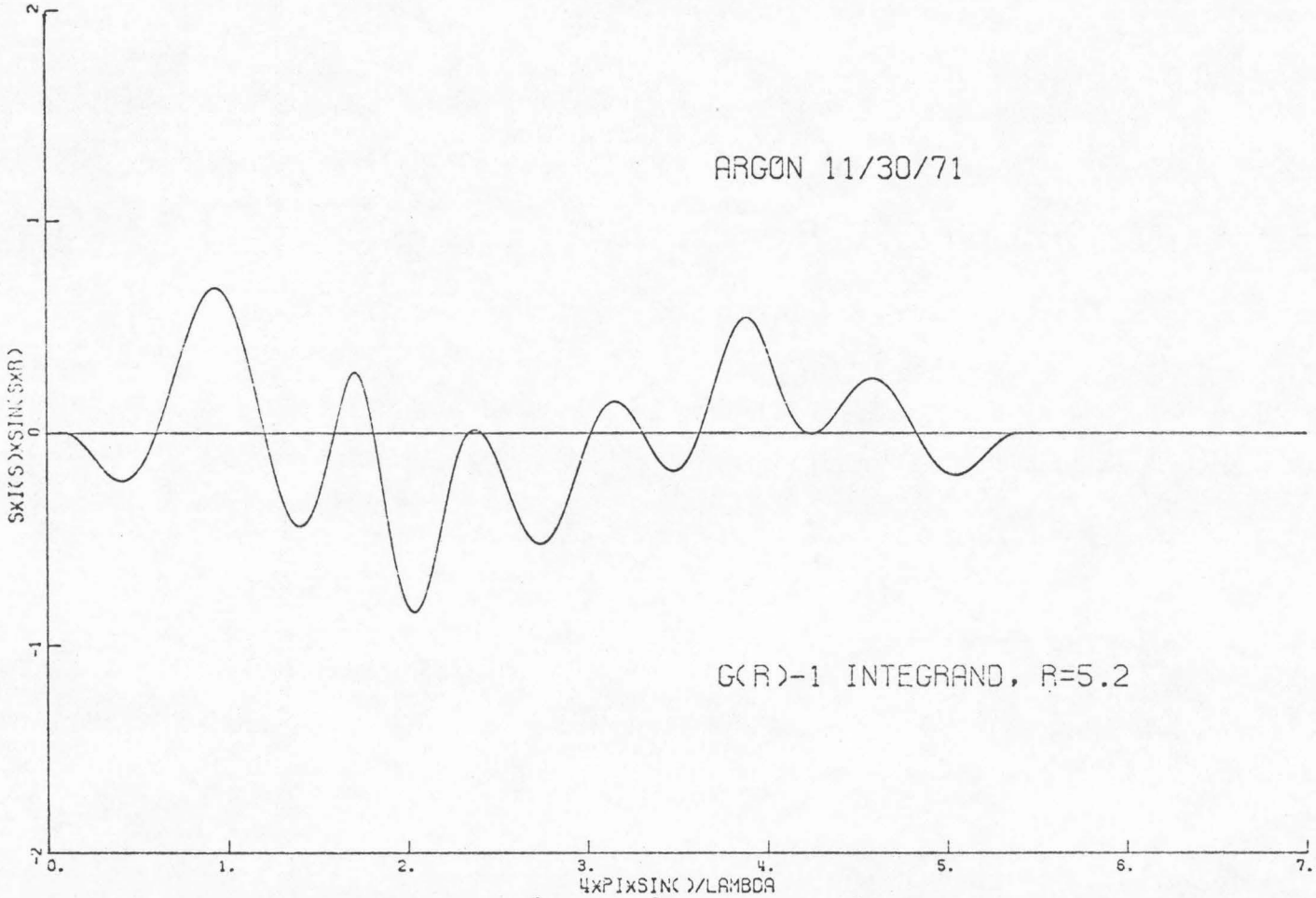

Figure 7.F. Integrand for $r\left[g(r)-1\right]$, r = 5.2 Å.

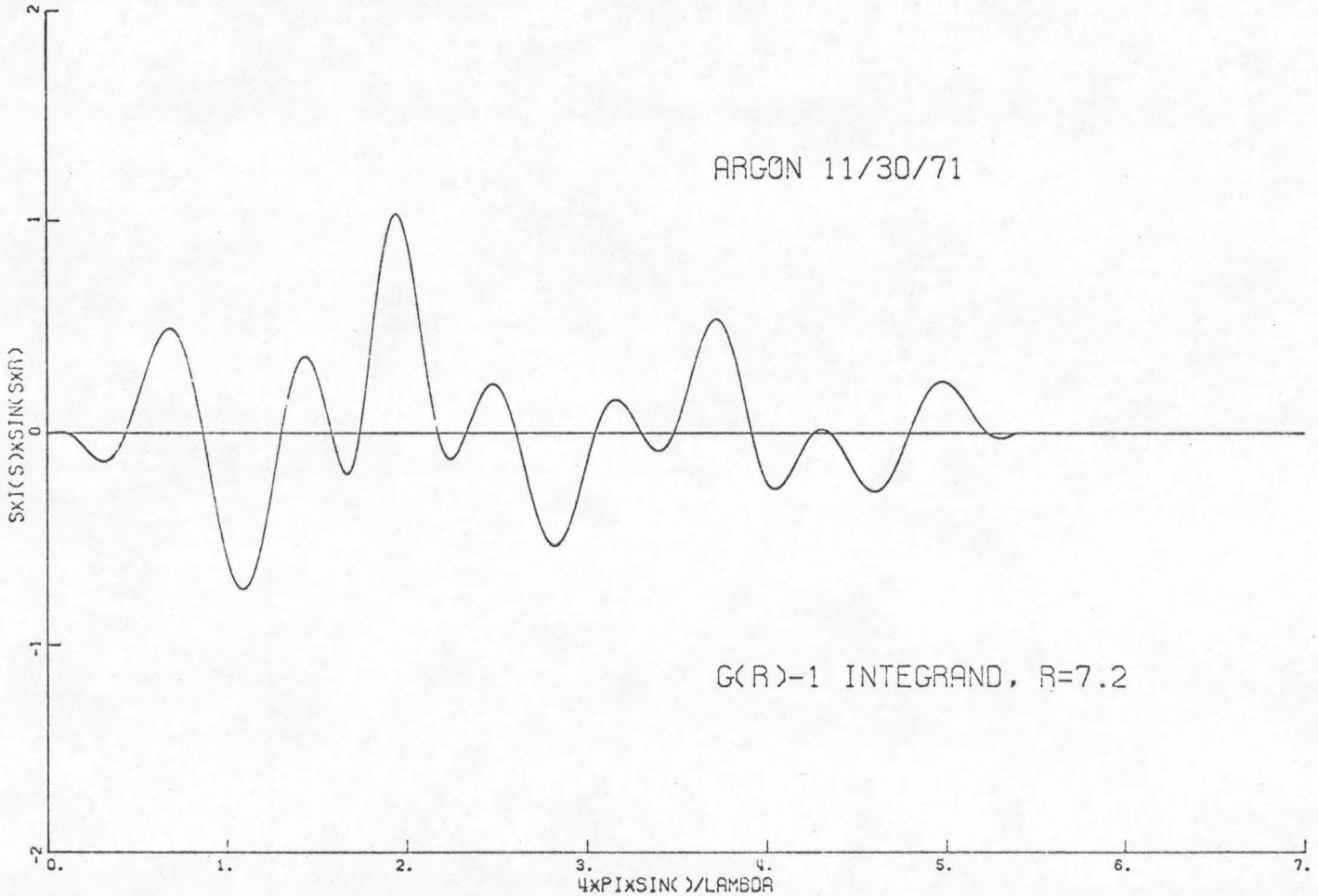

Figure 7.G. Integrand for r g(r)-1 , r = 7.2 Å.

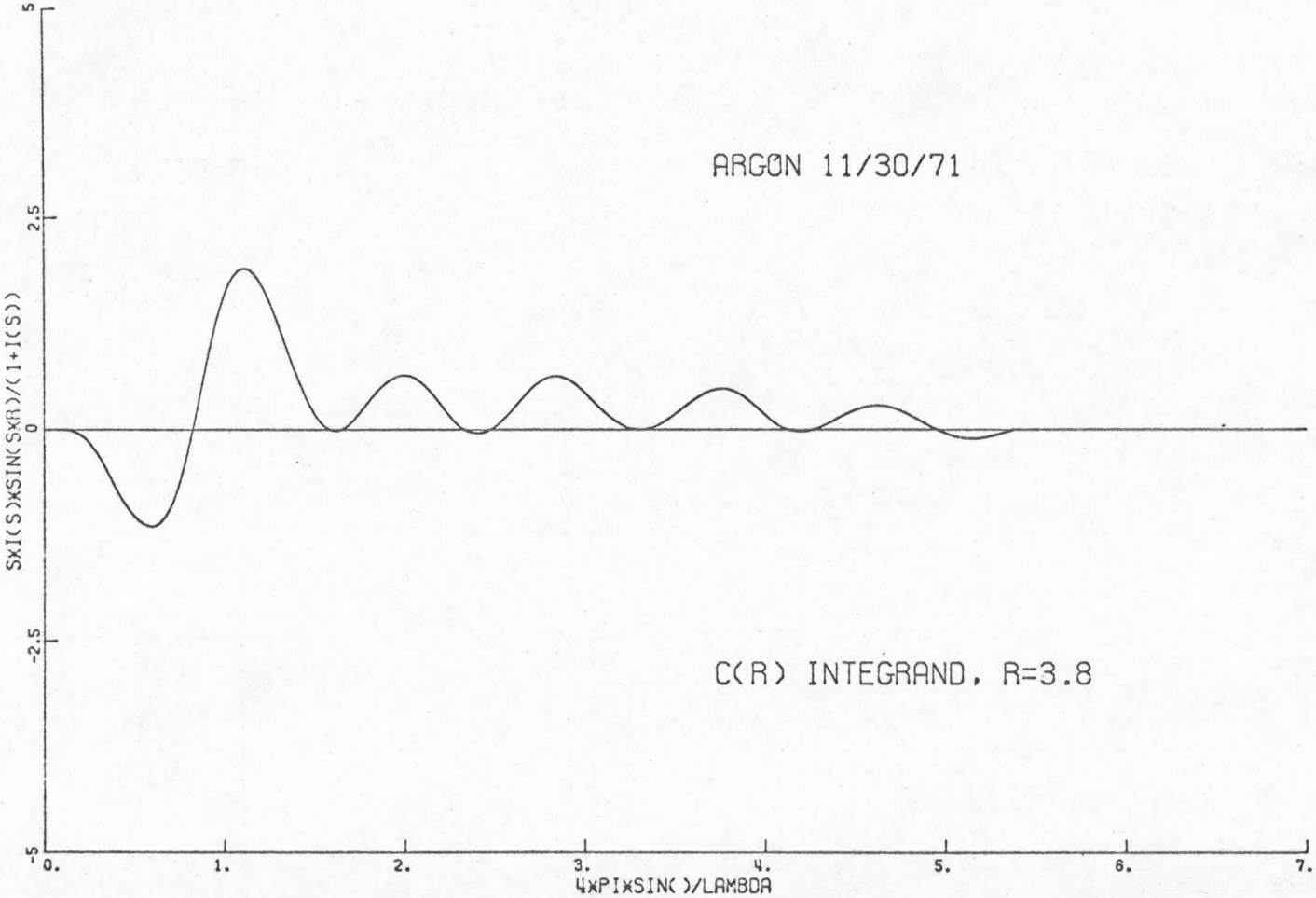

Figure 7.H. Integrand for rc(r), r = 3.8 Å.

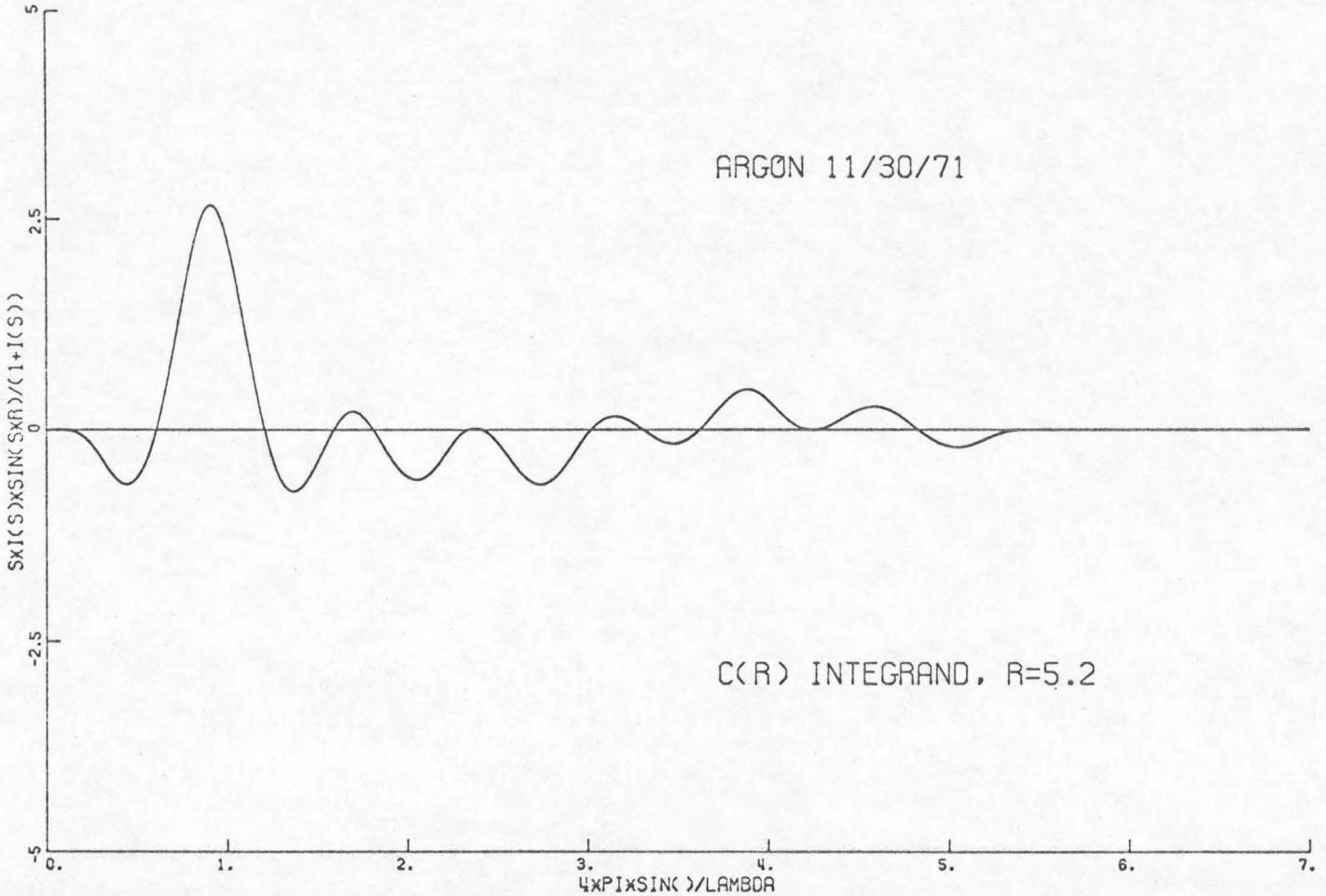

Figure 7.I. Integrand for rc(r), r = 5.2 Å.

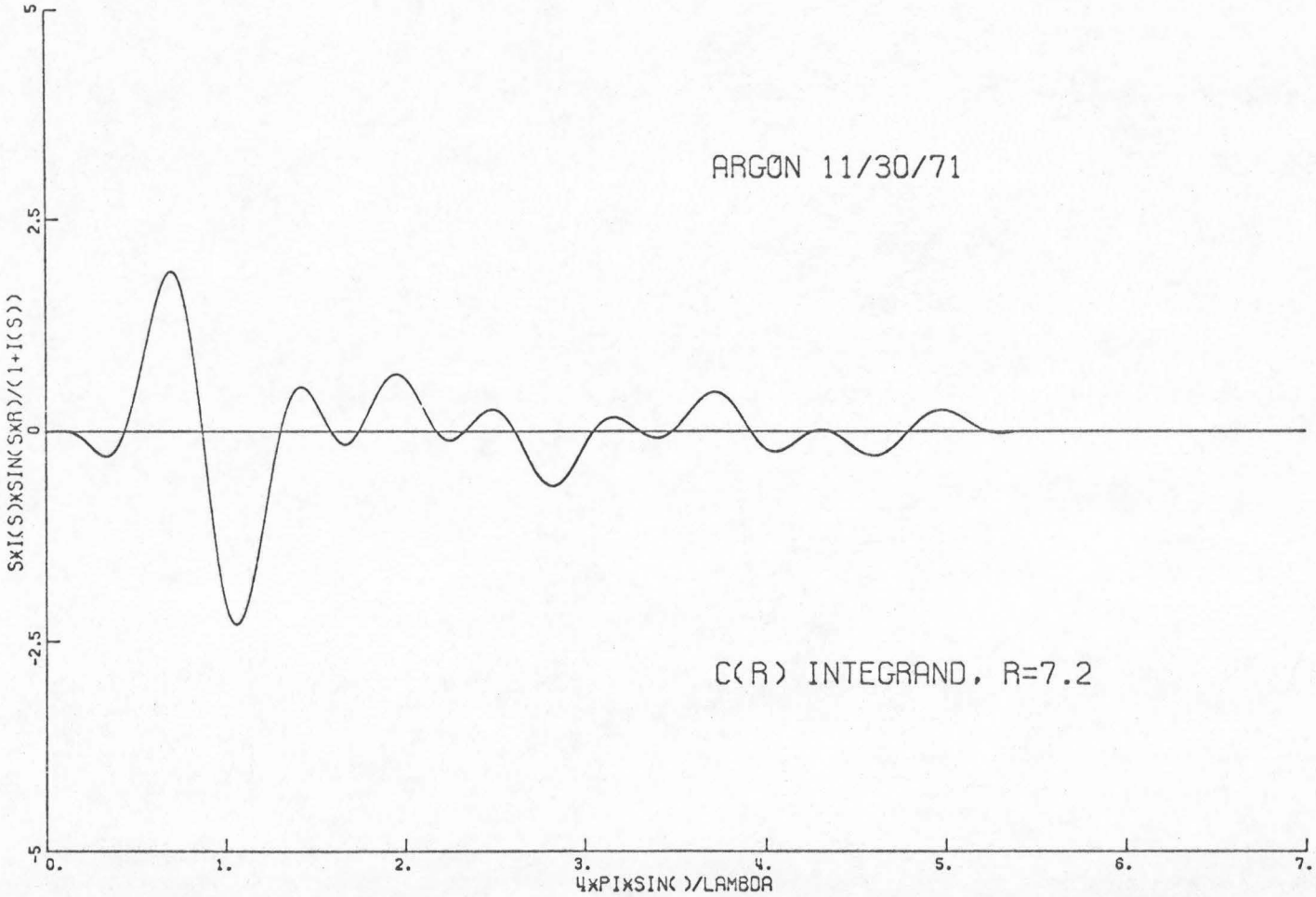

Figure 7.J. Integrand for rc(r), r = 7.2 Å.

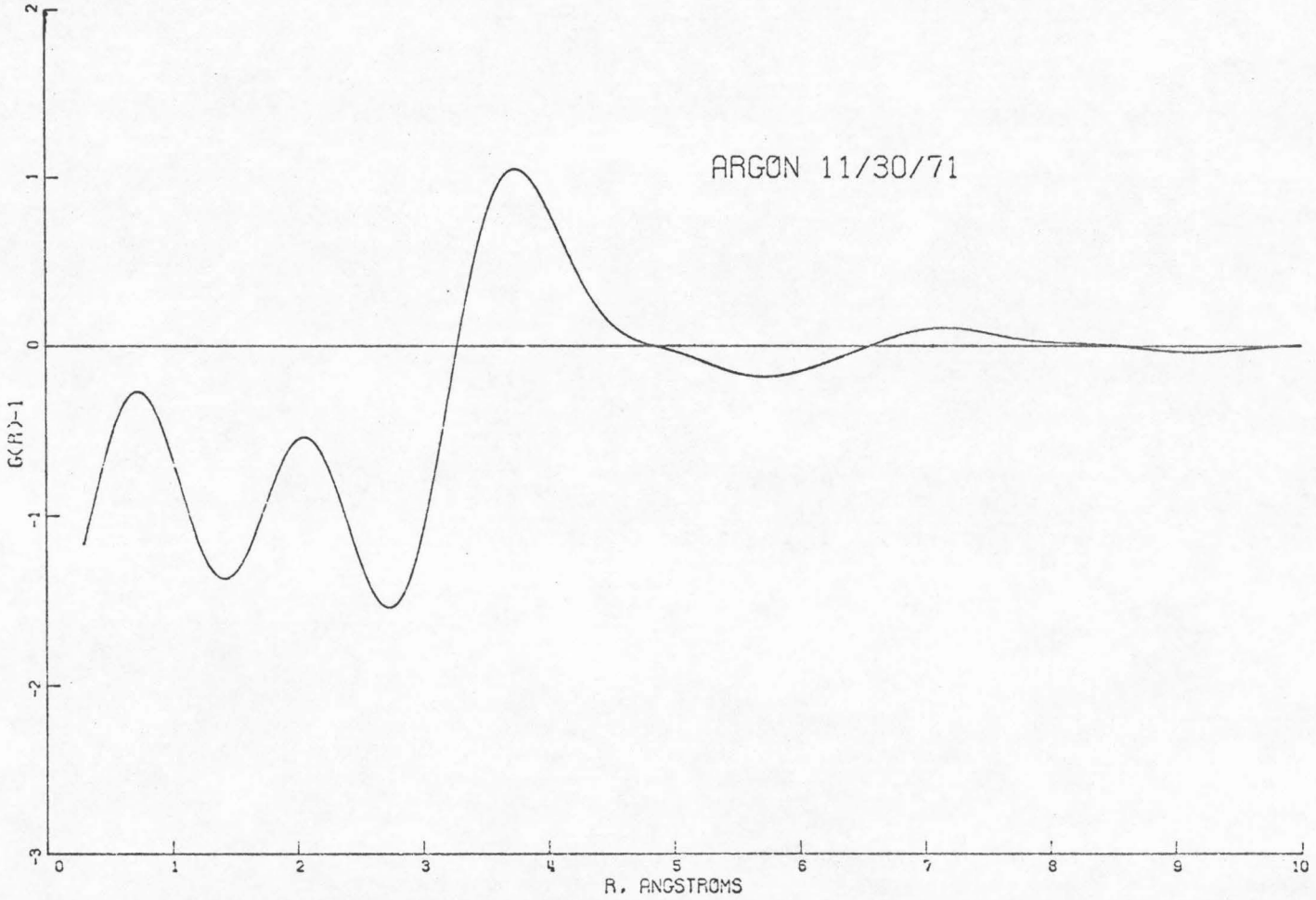

Figure 7.K. Radial distribution function, g(r).

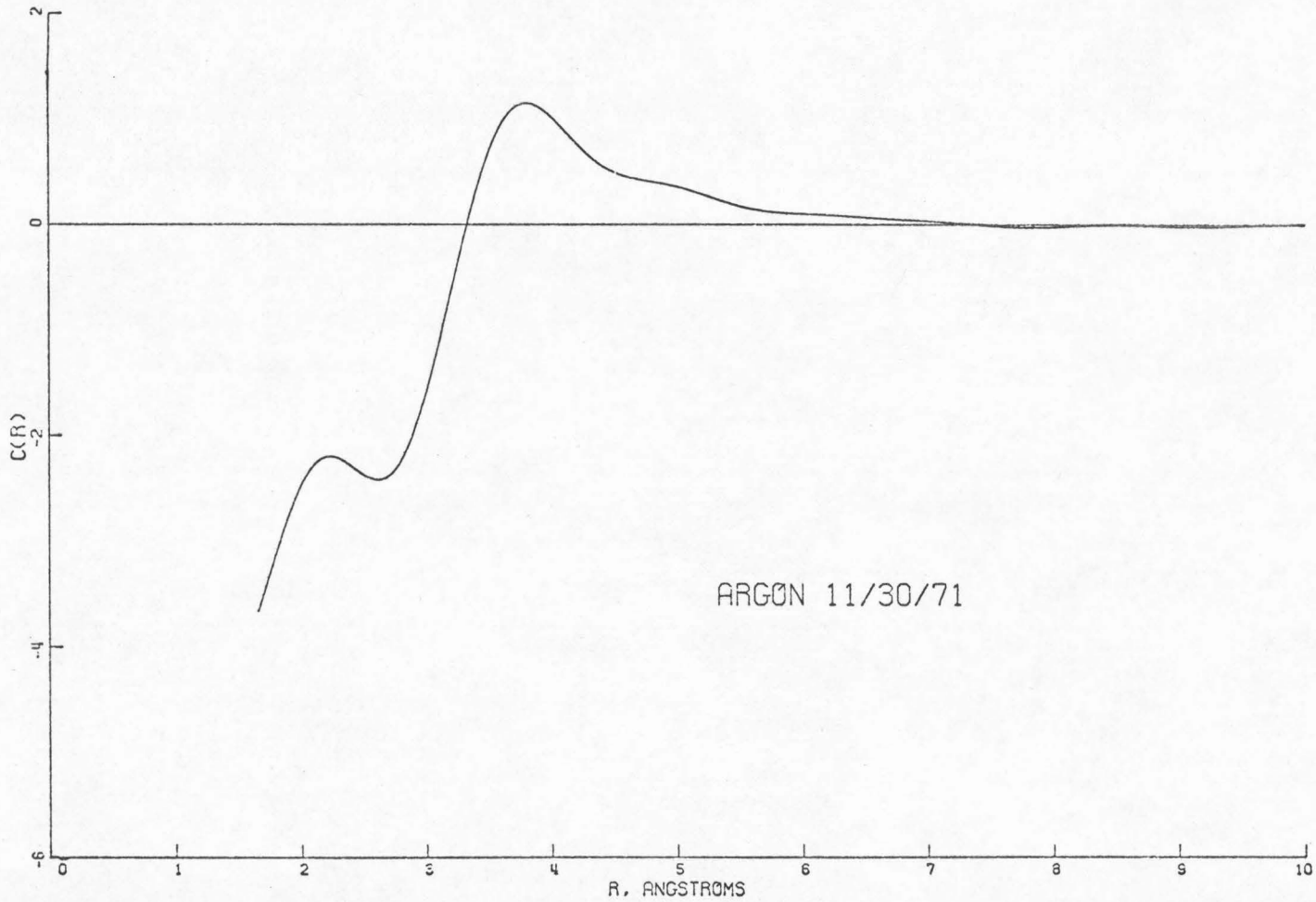

Figure 7.L. Direct correlation function, c(r).

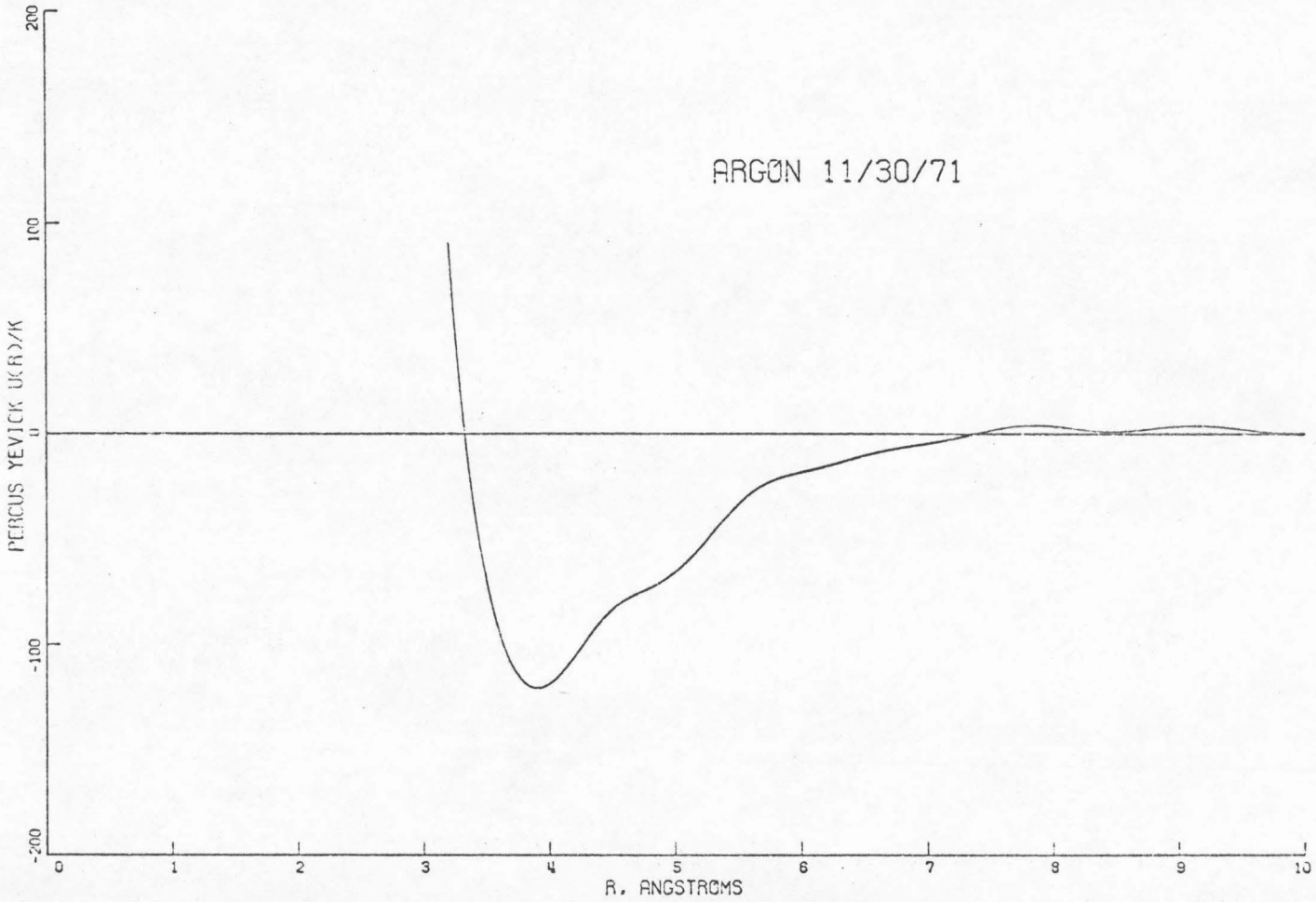

Figure 7.M. Percus-Yevick potential estimate, u(r)/k (^{o}K).

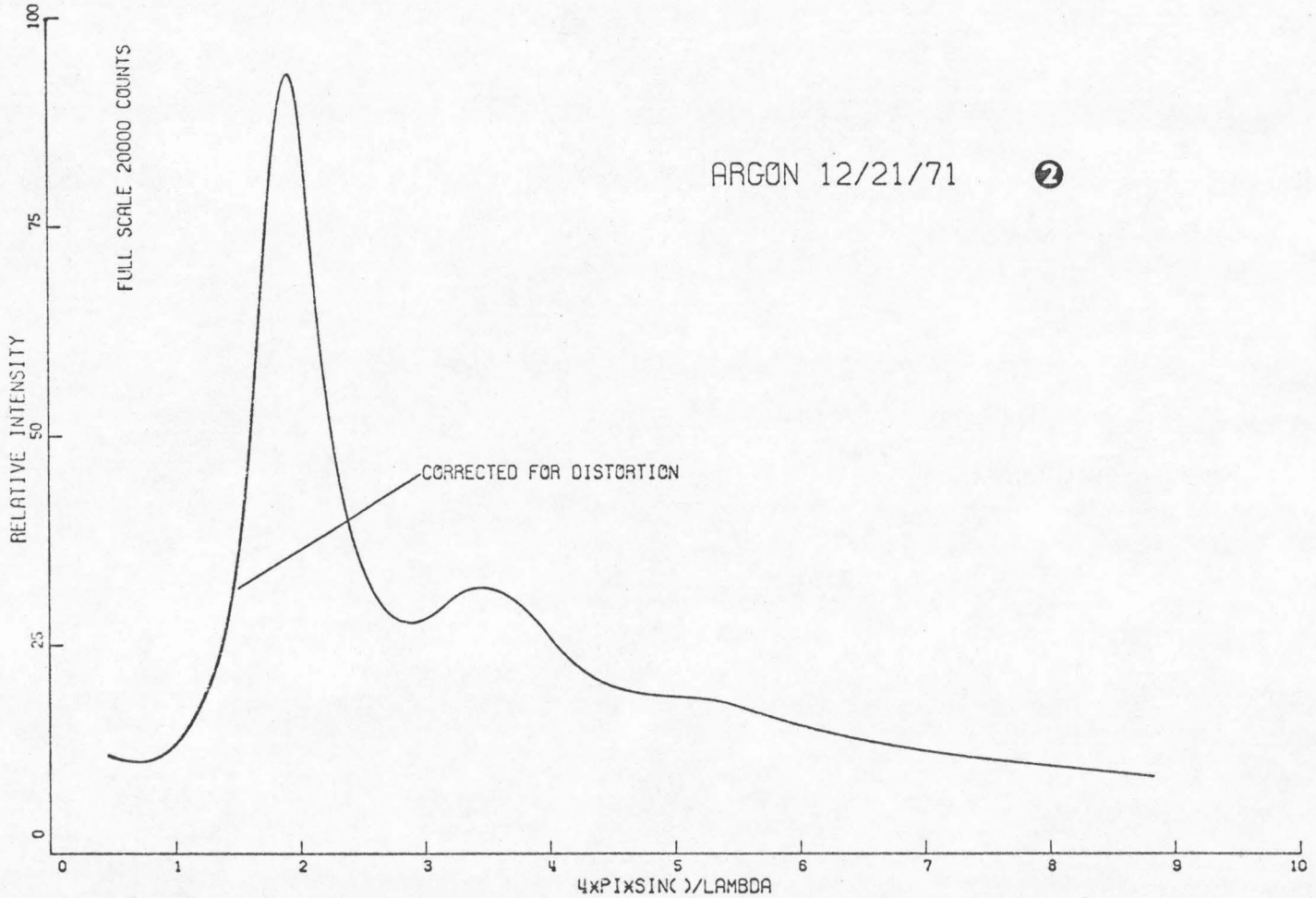

Figure 8.A (through 8.M). Example of data analysis, smoothed and distortion corrected argon spectrum.

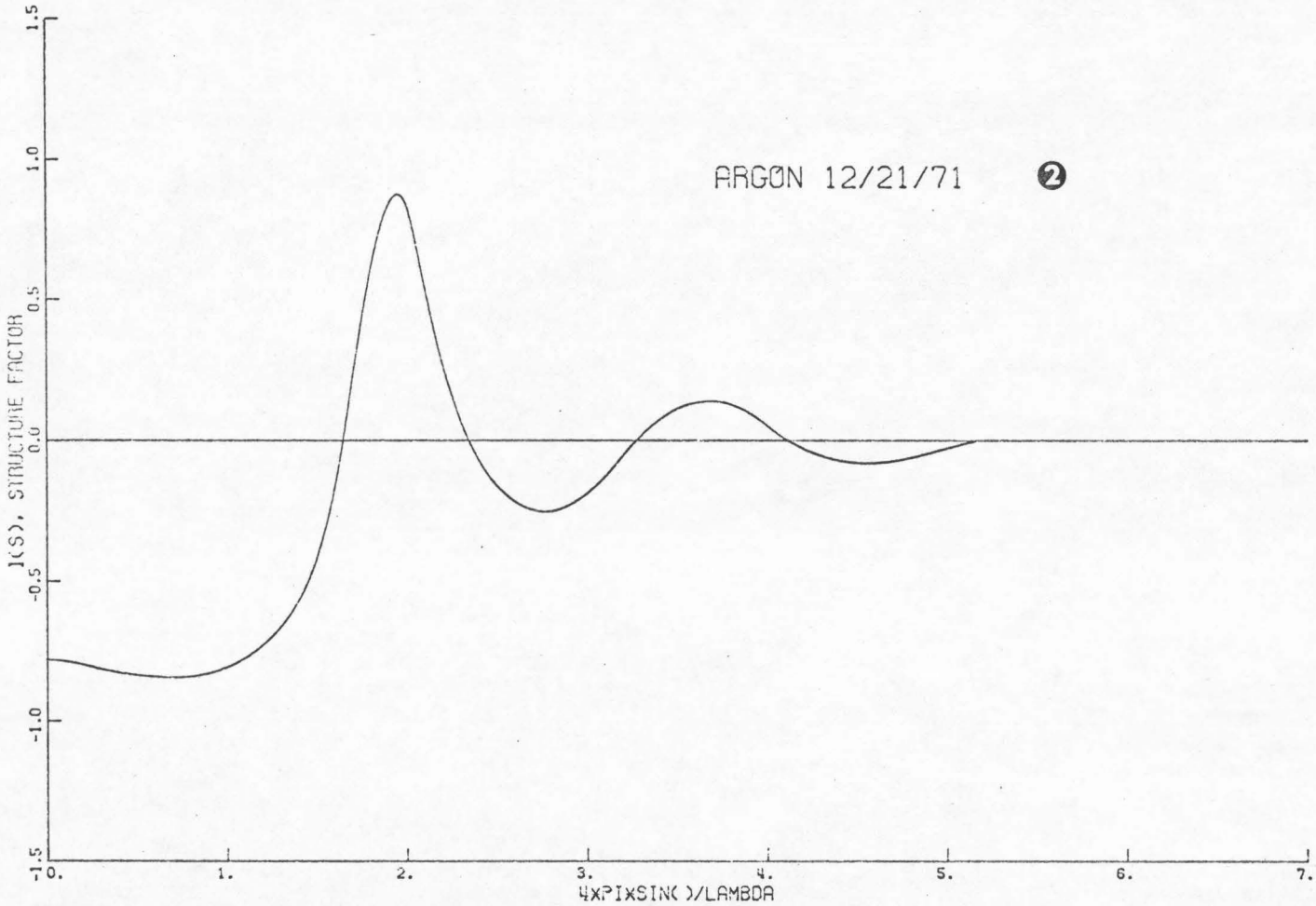

Figure 8.B. Structure factor.

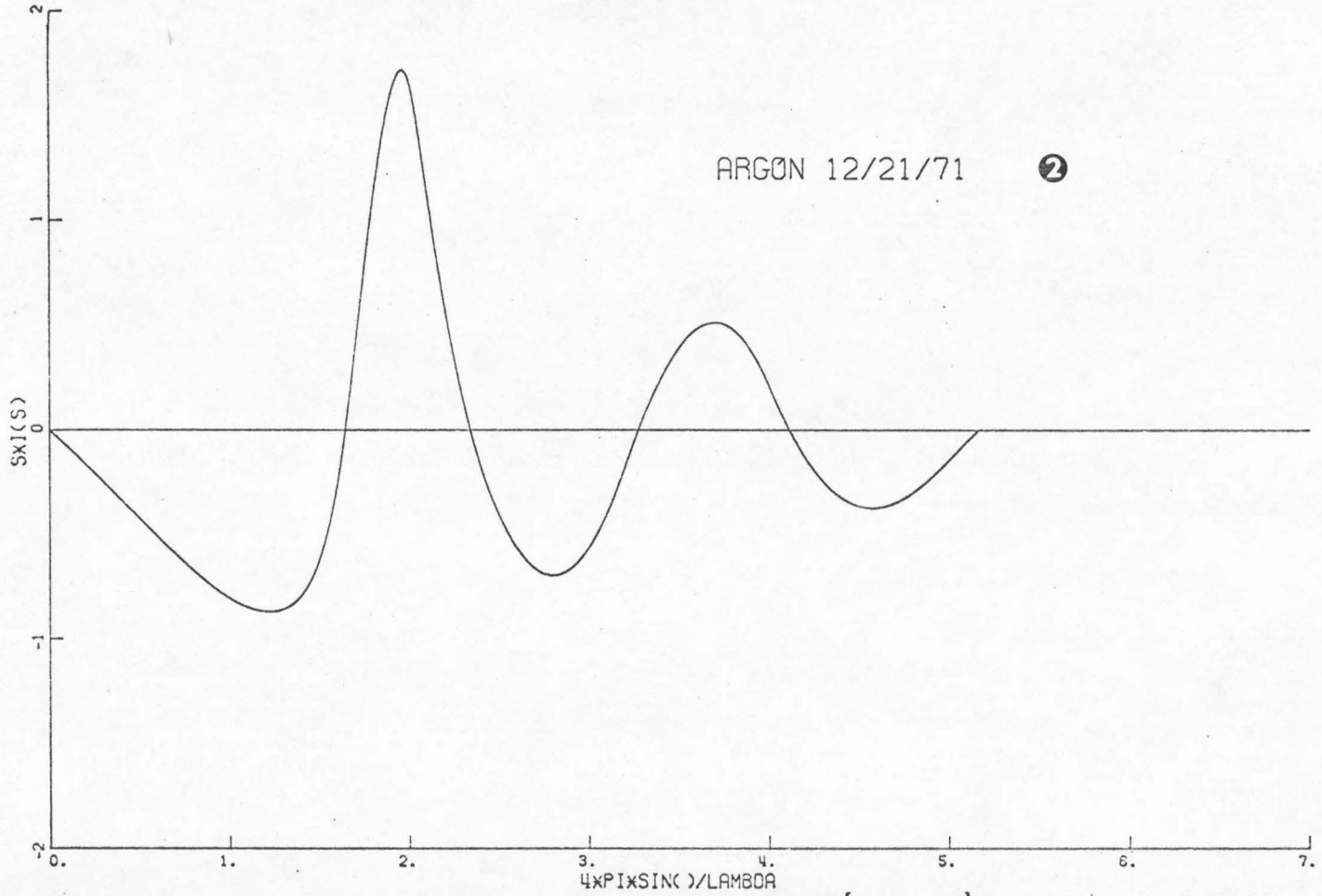

Figure 8.C. Kernel of Fourier transform of $r\left[g(r)-1\right]$.

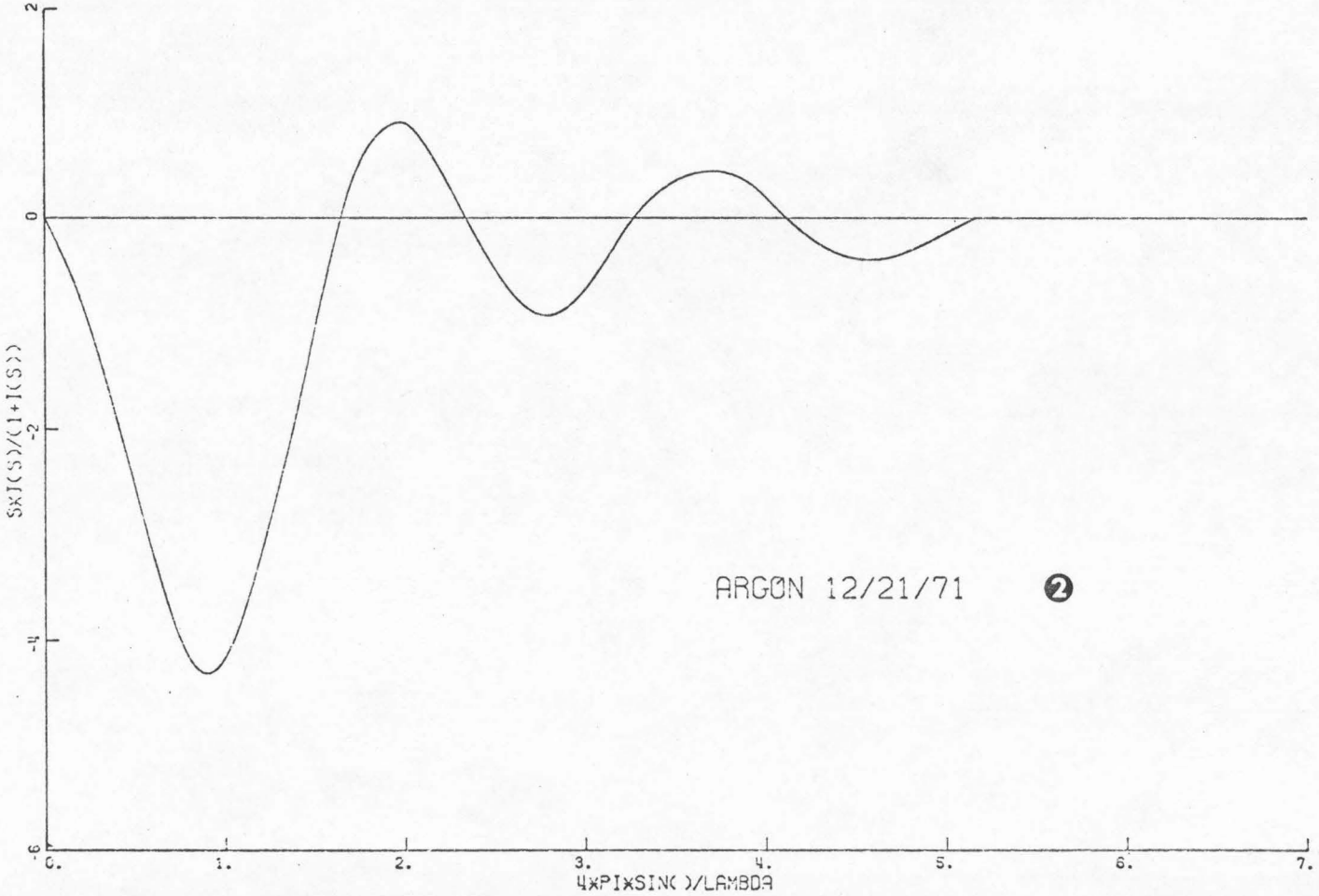

Figure 8.D. Kernel of Fourier transform of rc(r).

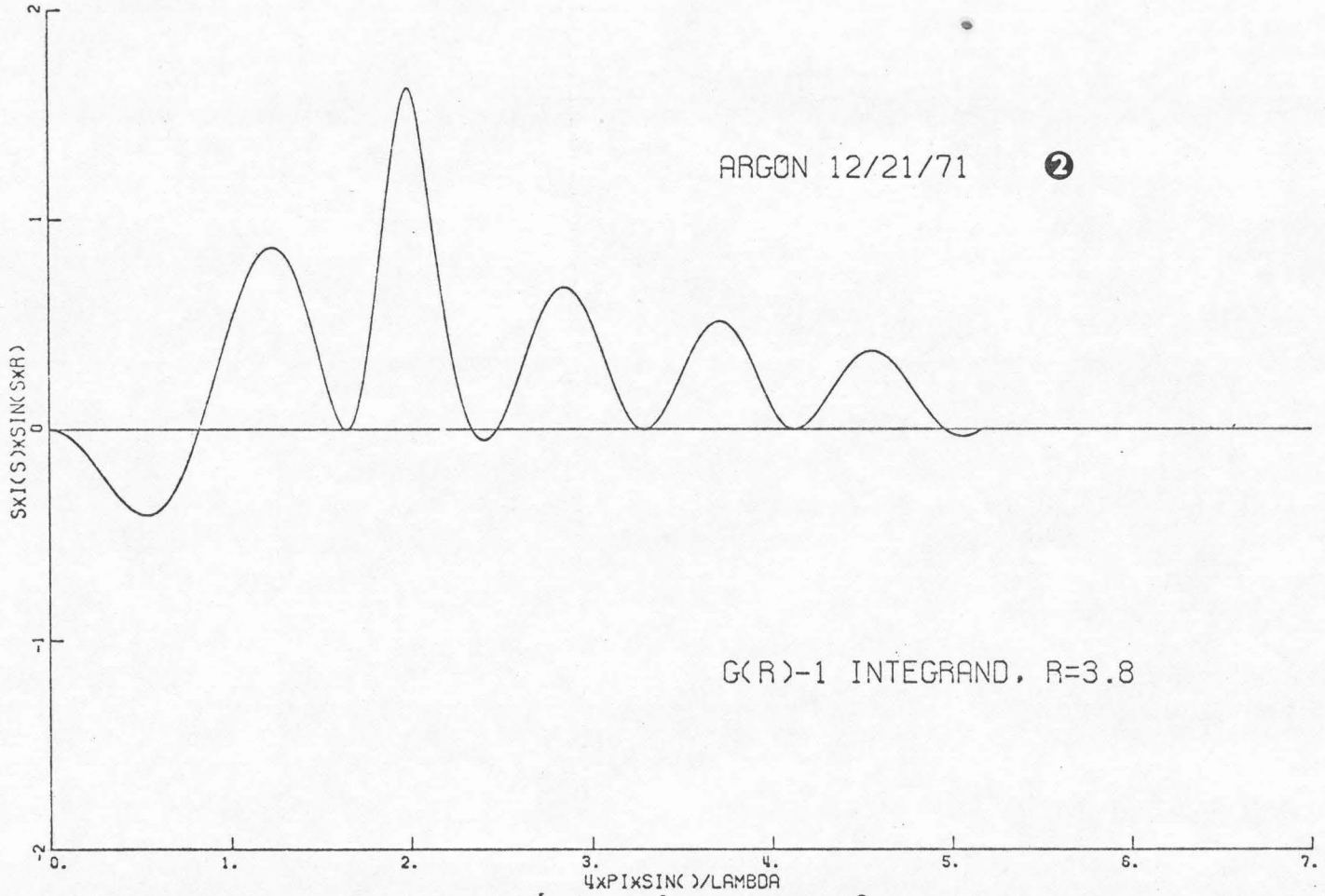

Figure 8.E. Integrand for $r\left[g(r)-1\right]$, r = 3.8 Å.

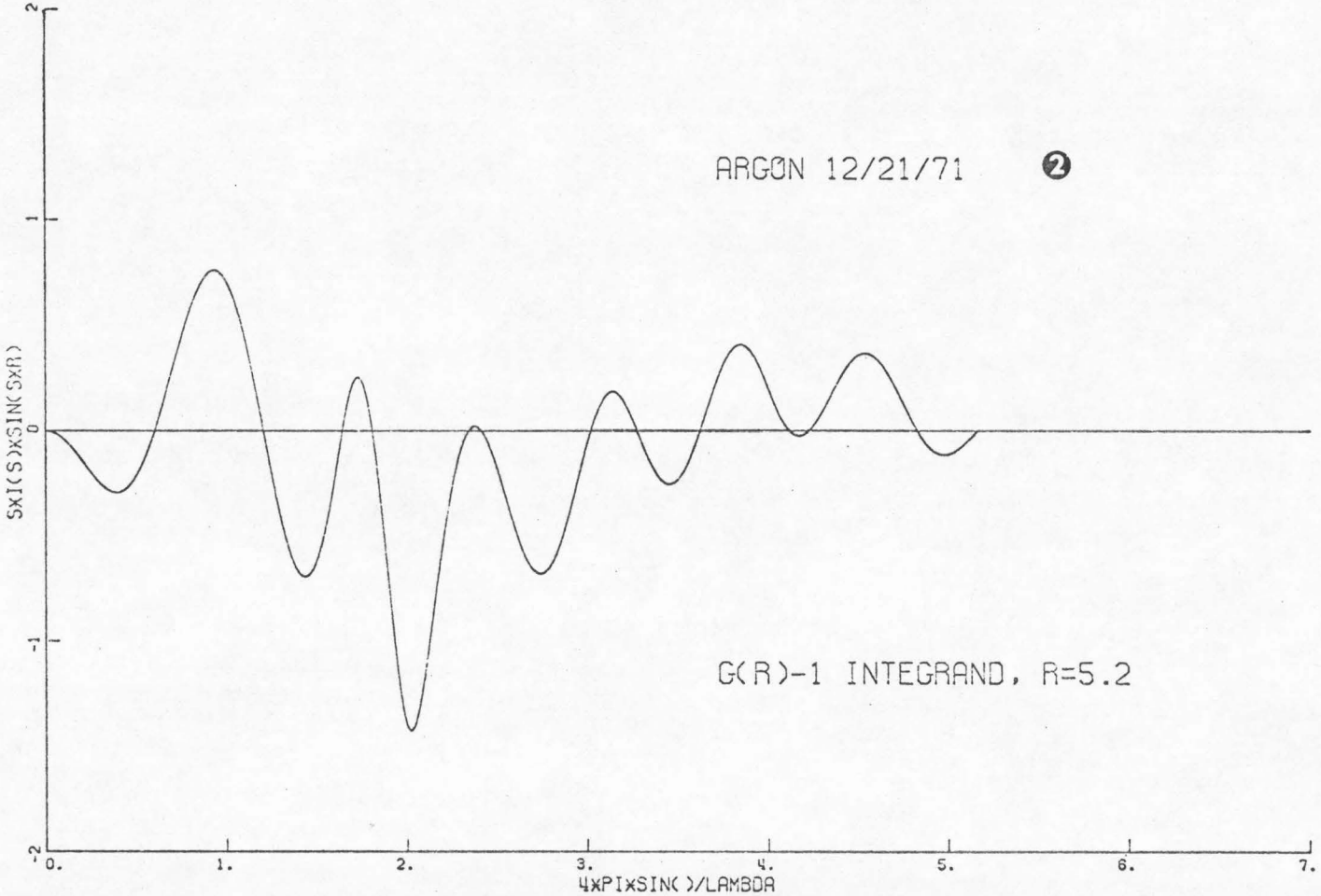

Figure 8.F. Integrand for $r\left[g(r)-1\right]$, r = 5.2 Å.

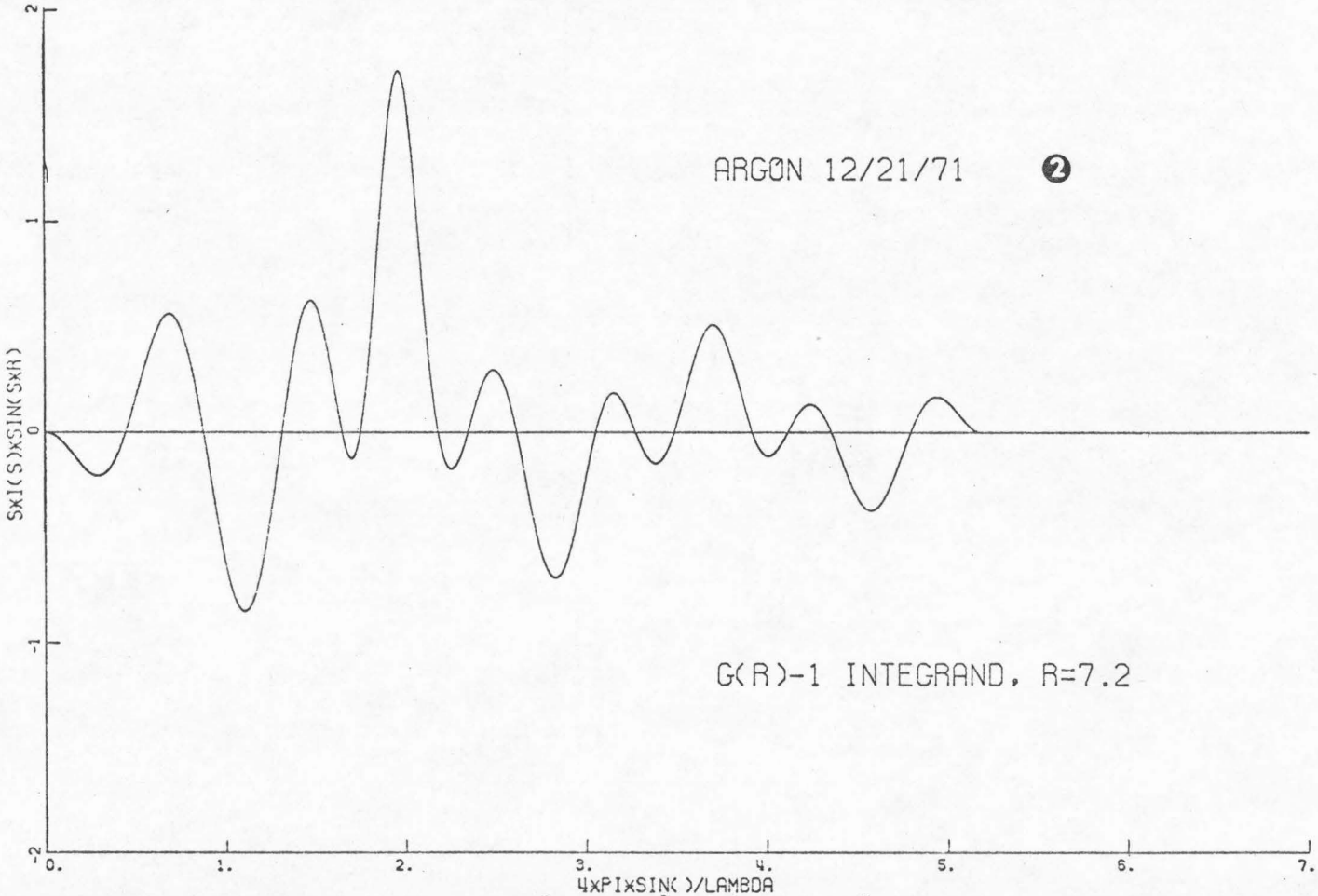

Figure 8.G. Integrand for $r\left[g(r)-1\right]$, r = 7.2 Å.

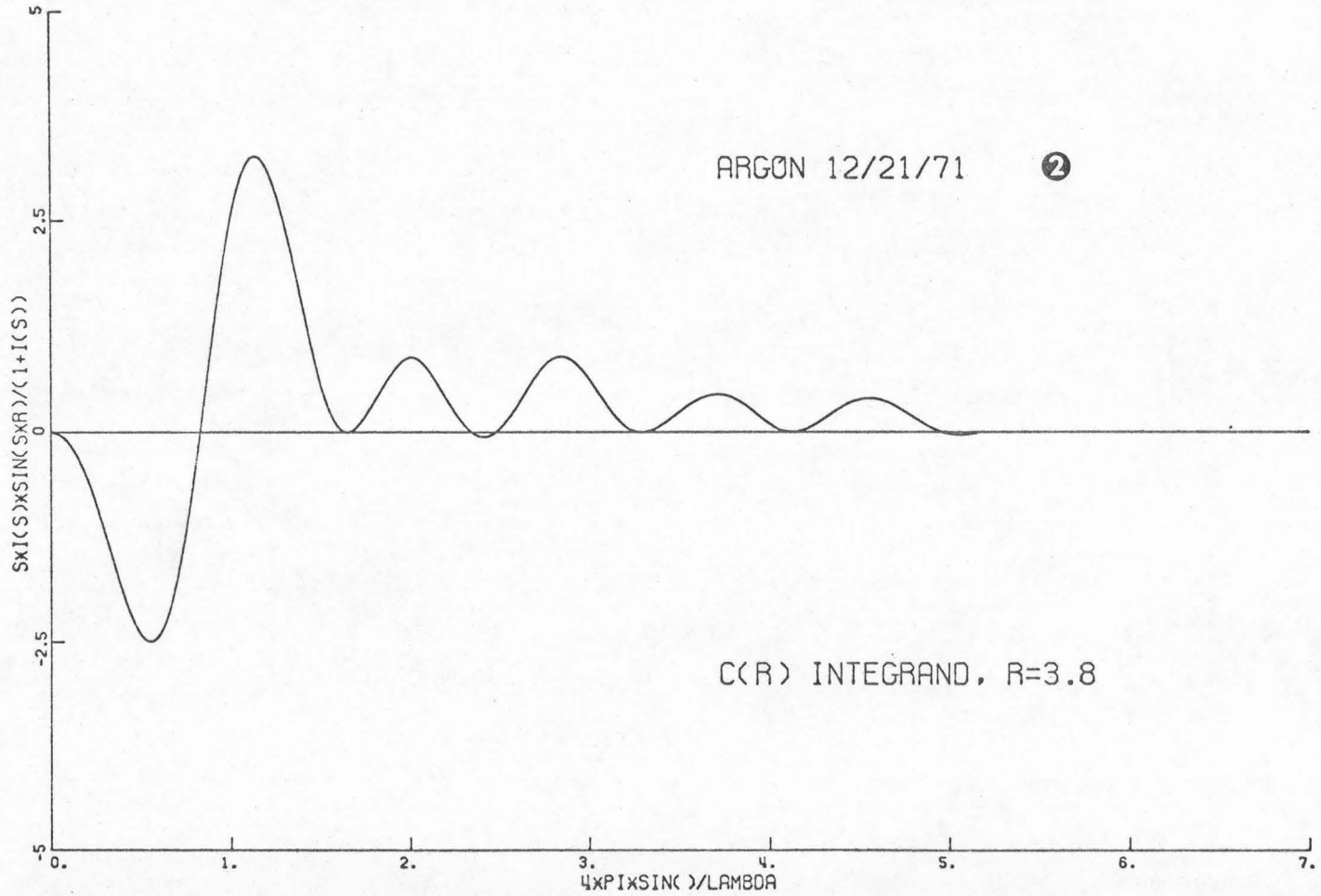

Figure 8.H. Integrand for rc(r), r = 3.8 Å.

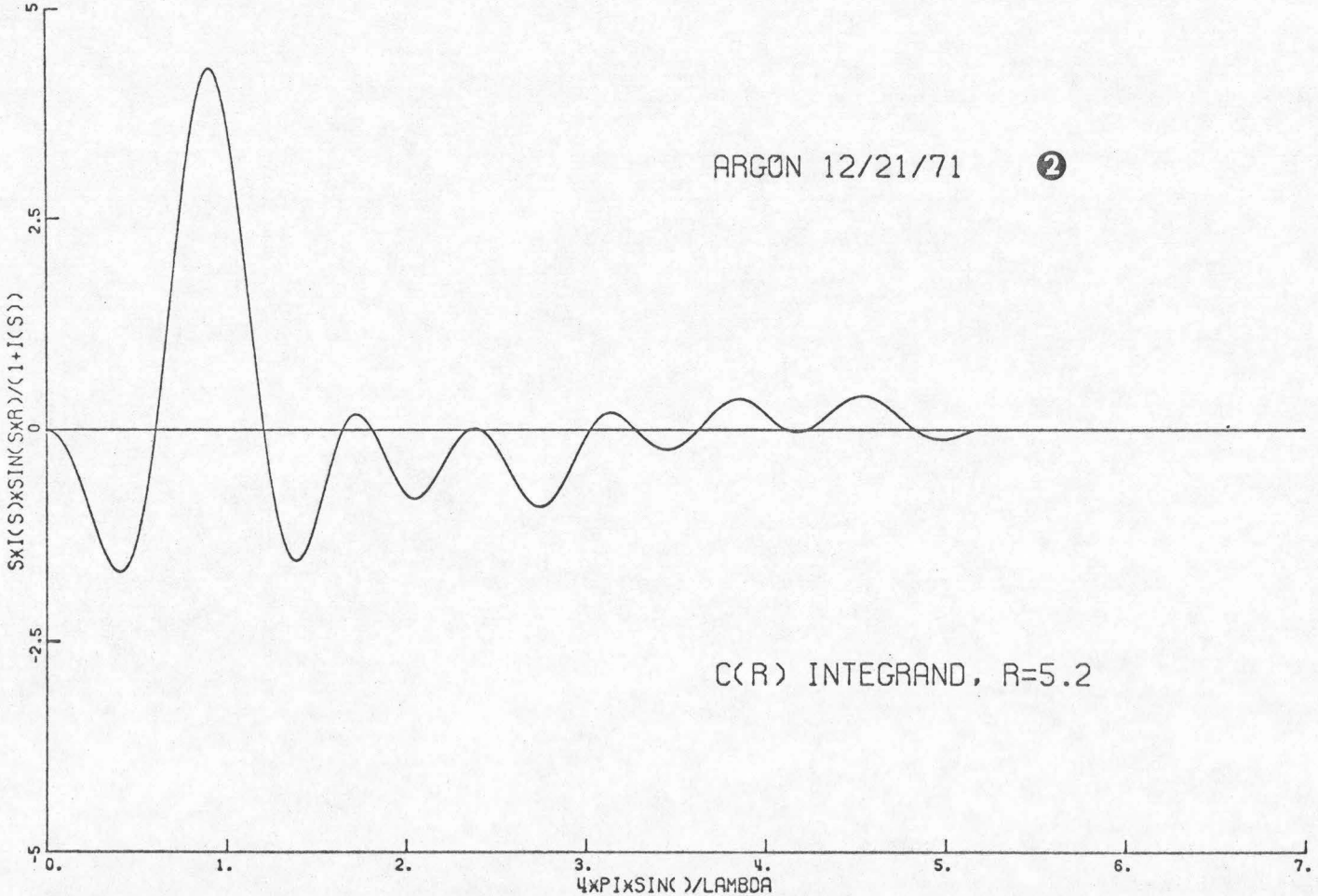

Figure 8.I. Integrand for rc(r), r = 5.2 Å.

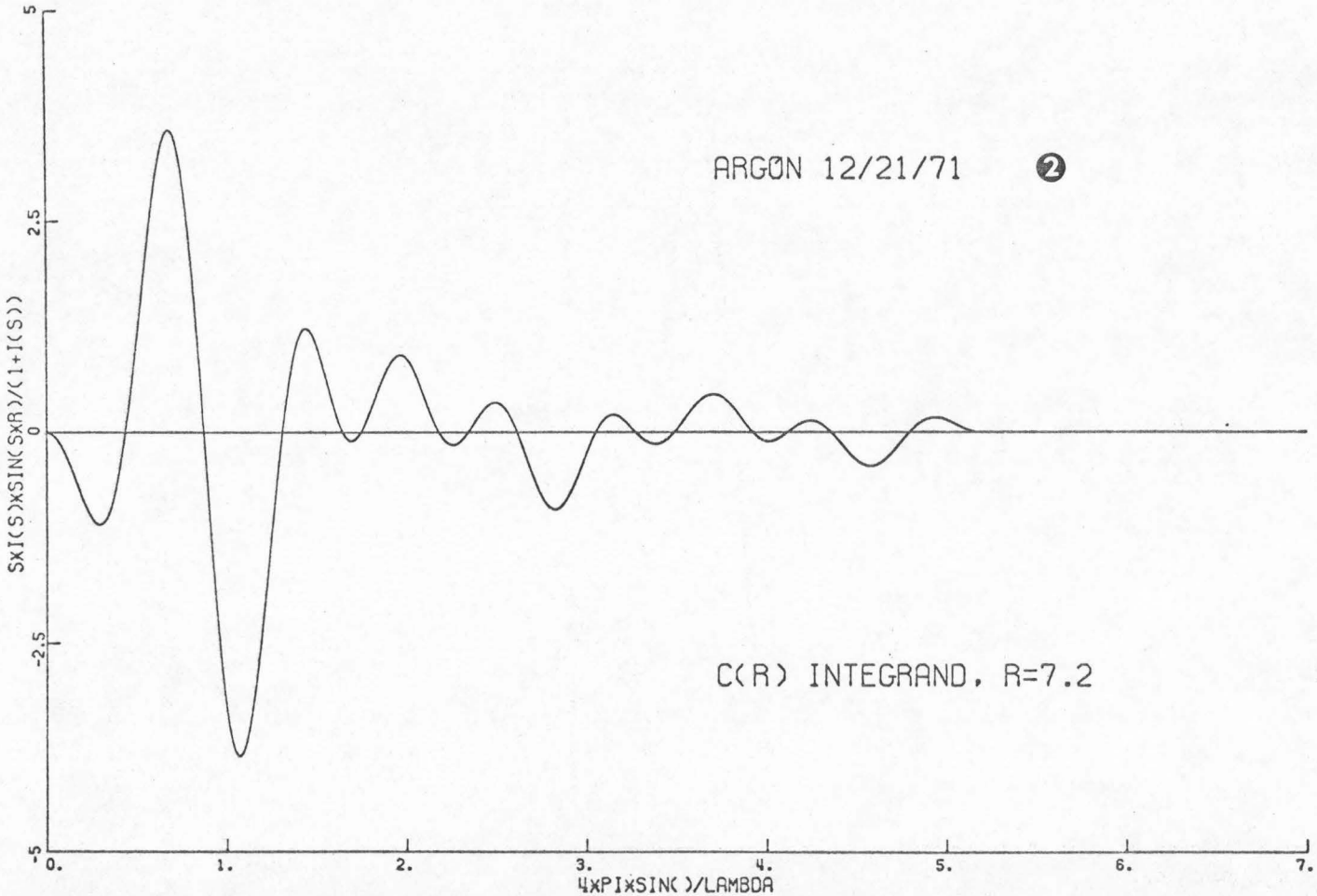

Figure 8.J. Integrand for rc(r), r = 7.2 Å.

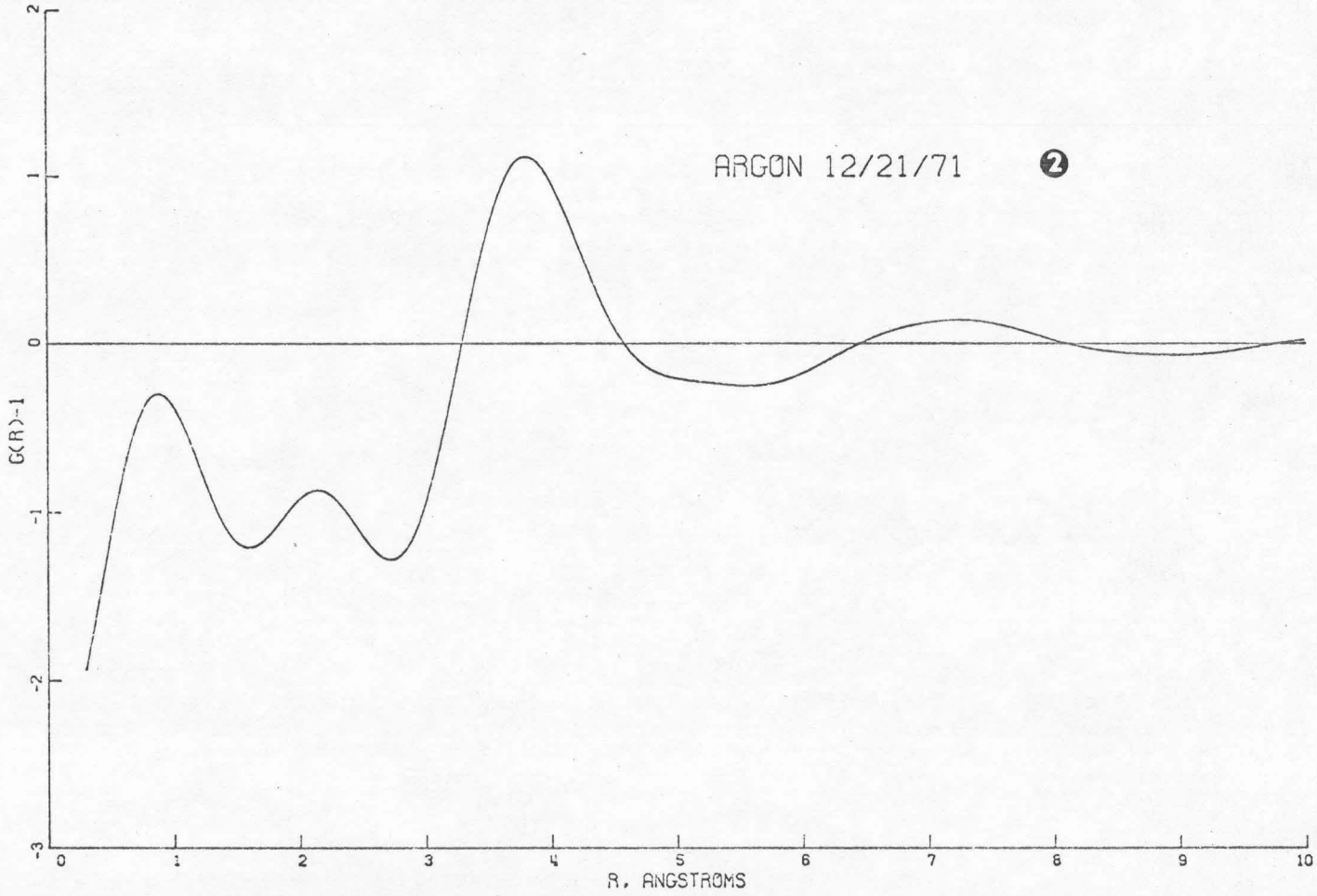

Figure 8.K. Radial distribution function, g(r).

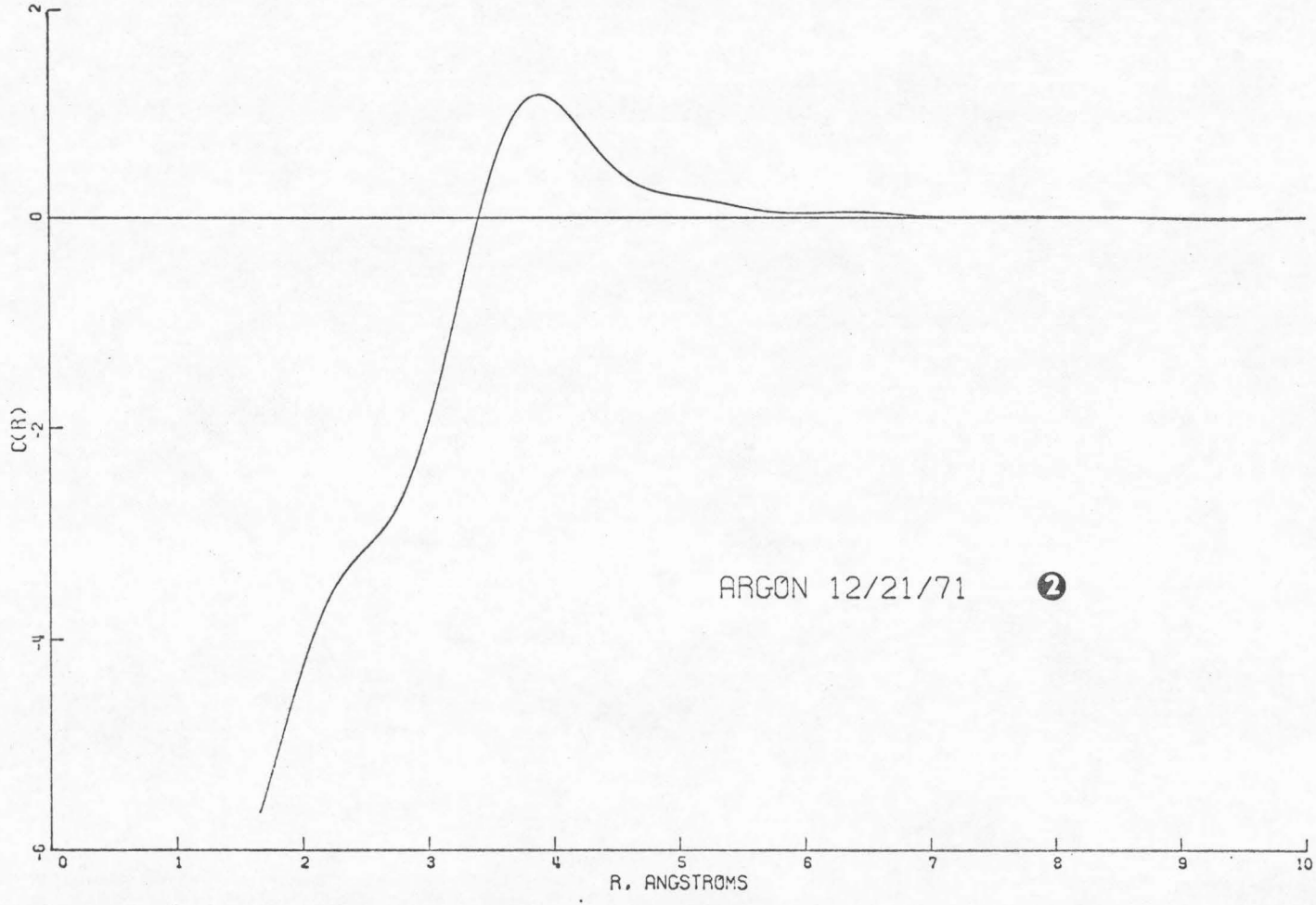

Figure 8.L. Direct correlation function, c(r).

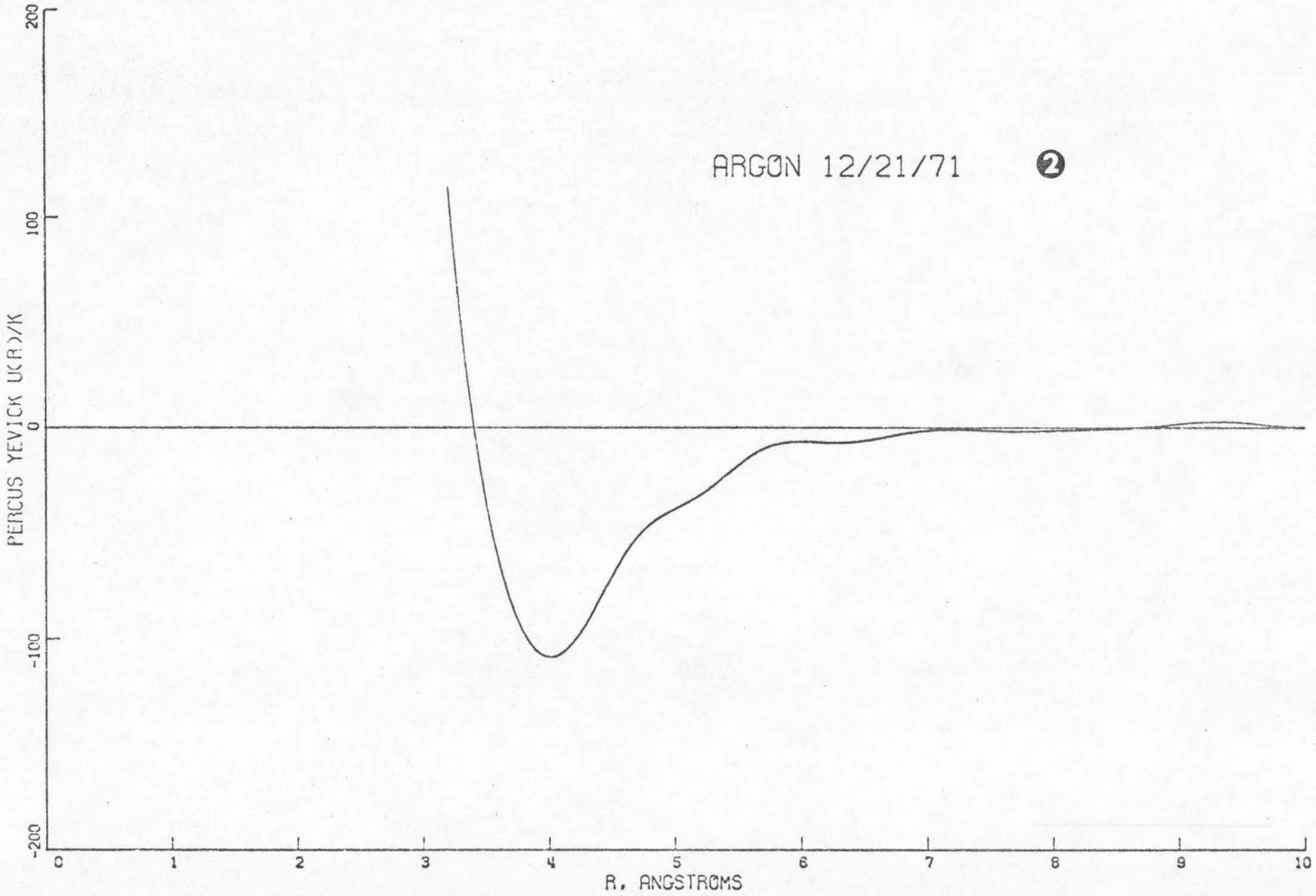

Figure 8.M. Percus-Yevick potential estimate, u(r)/k (^{o}K).

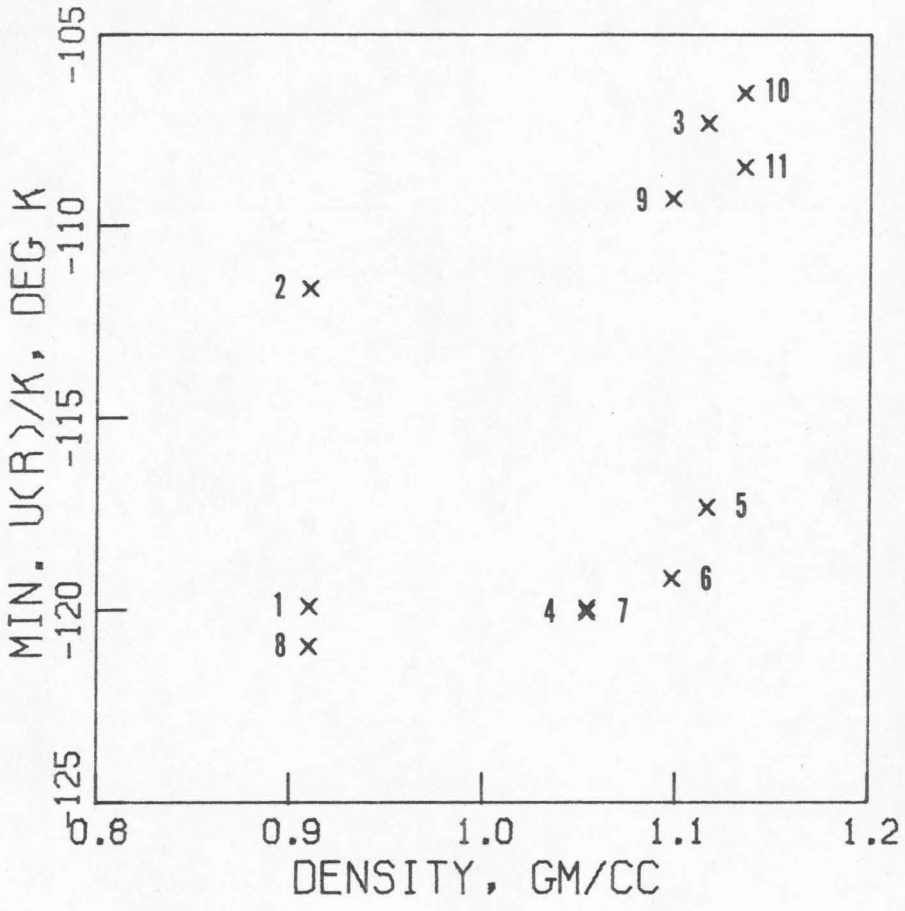

Figure 9. Computed Percus-Yevick well depth for each experiment (See Table 1. for identification of points.).

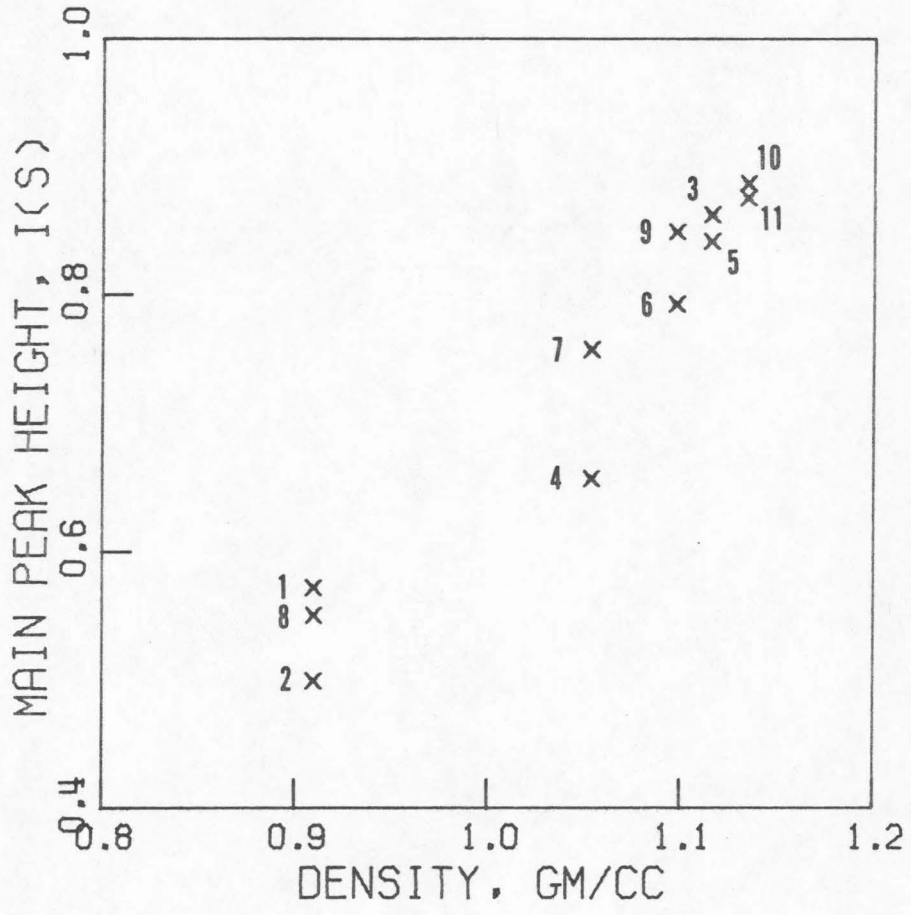

Figure 10. Main peak height of i(s) for each experiment (See Table 1. for identification of points.).

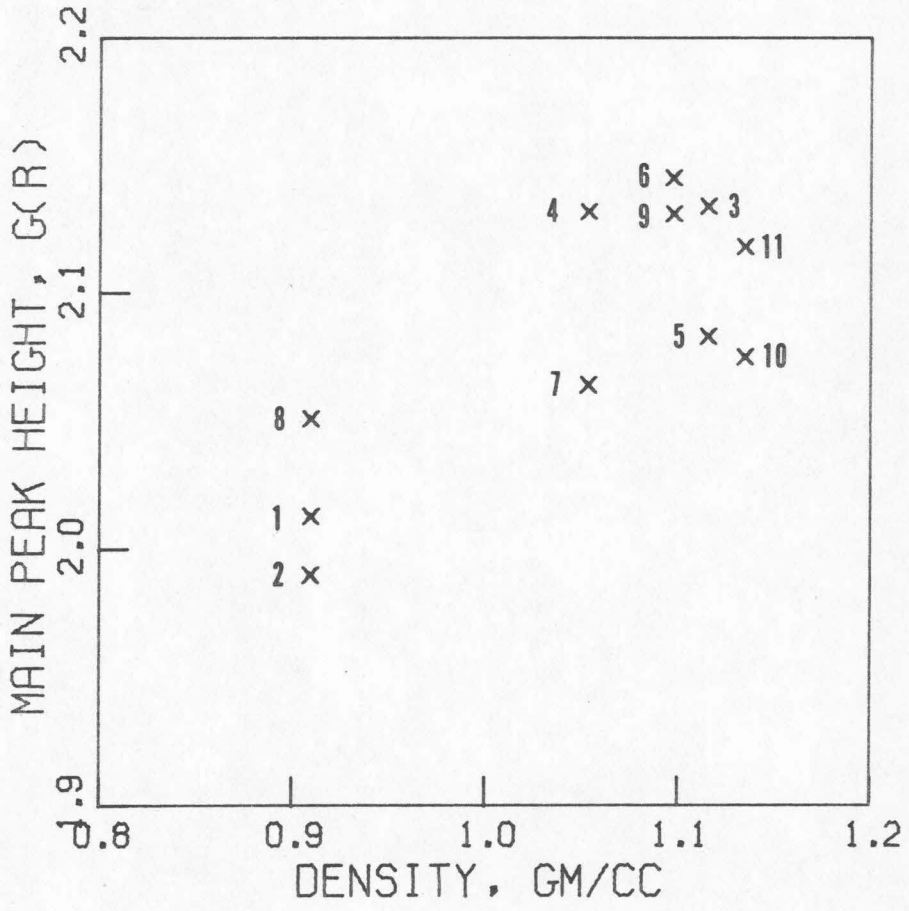

Figure 11. Main peak height of g(r) for each experiment (See Table 1. for identification of points.).

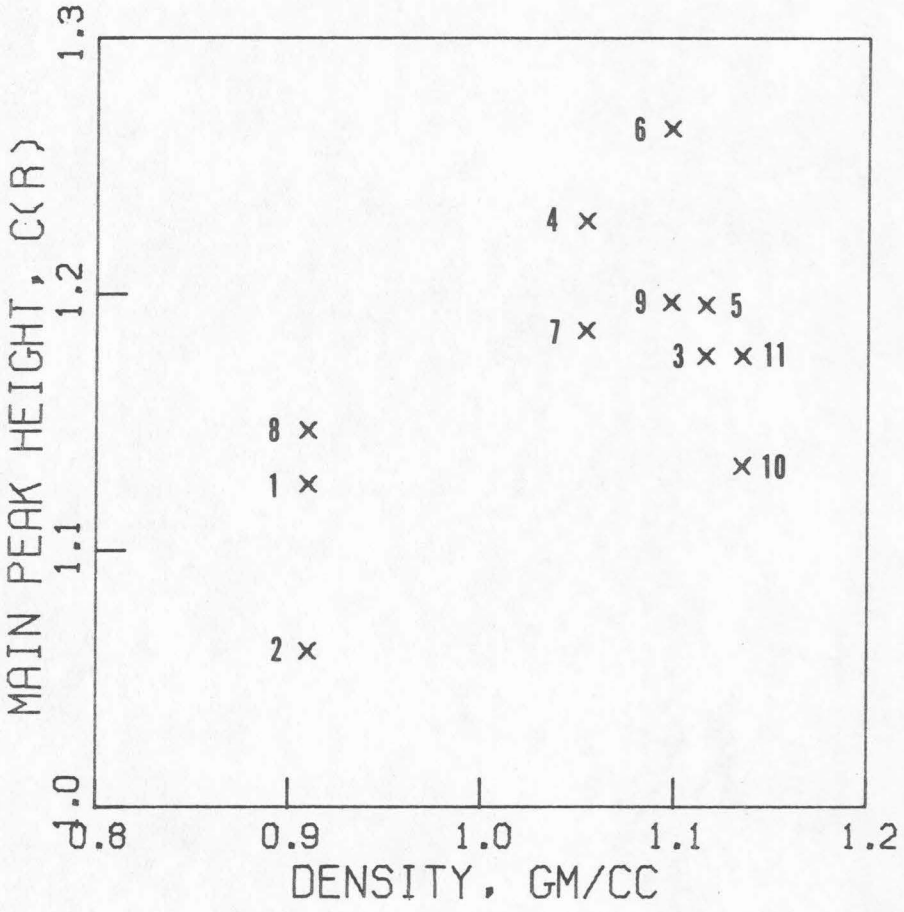

Figure 12. Main peak height of c(r) for each experiment (See Table 1. for identification of points.).

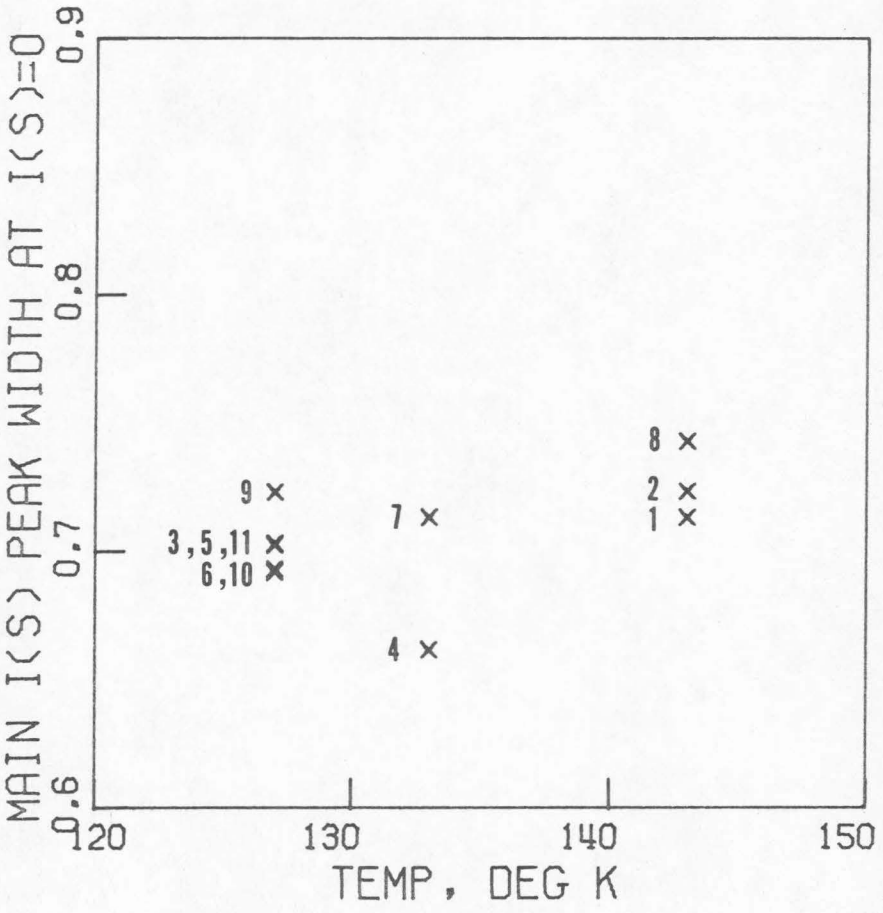

Figure 13. Width of main peak of i(s) at i(s) = 0 for each experiment (See Table 1. for identification of points.).

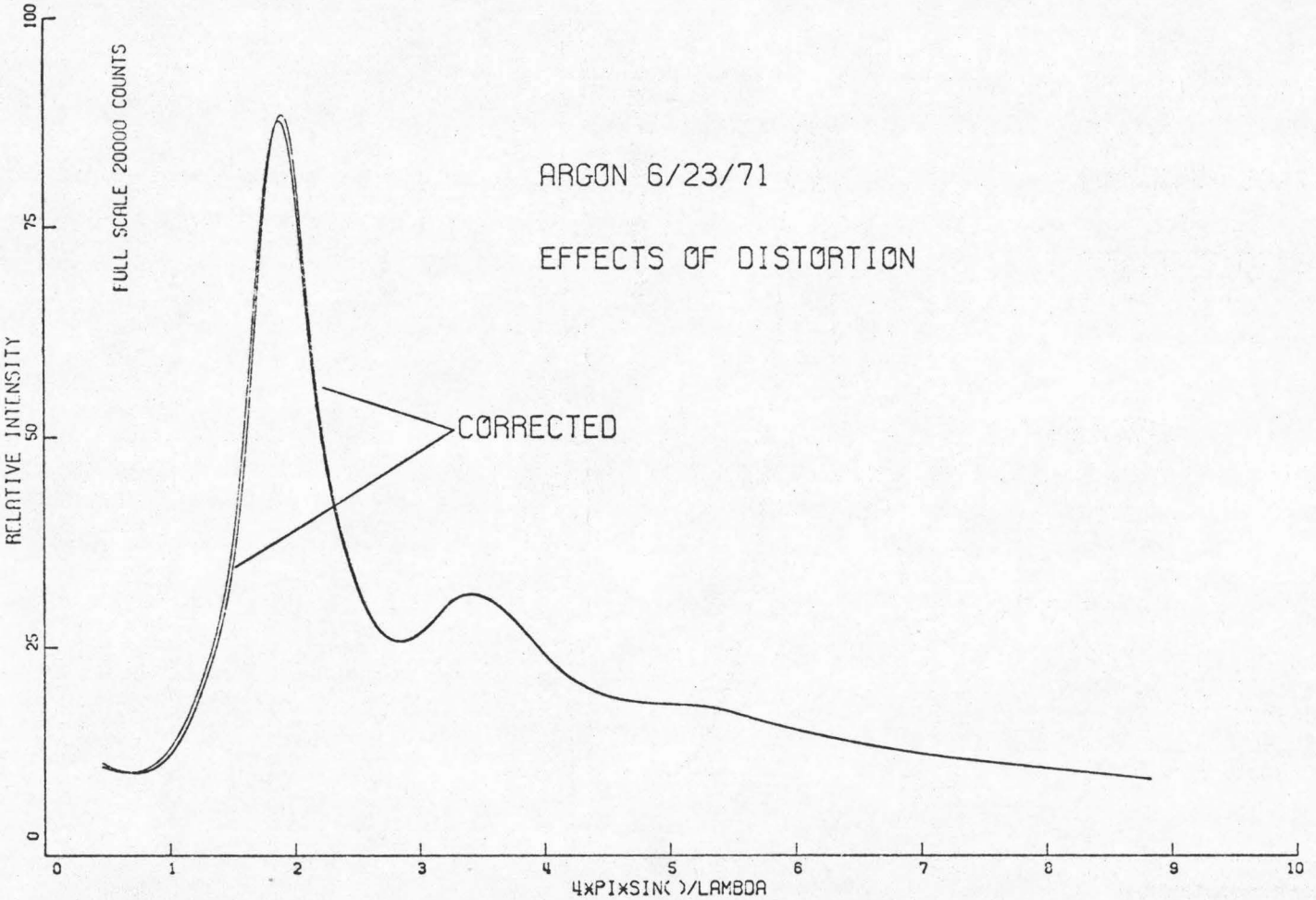

Figure 14.A (through 14.G). Numerical experiment on effect of distortion, corrected and uncorrected argon spectrum.

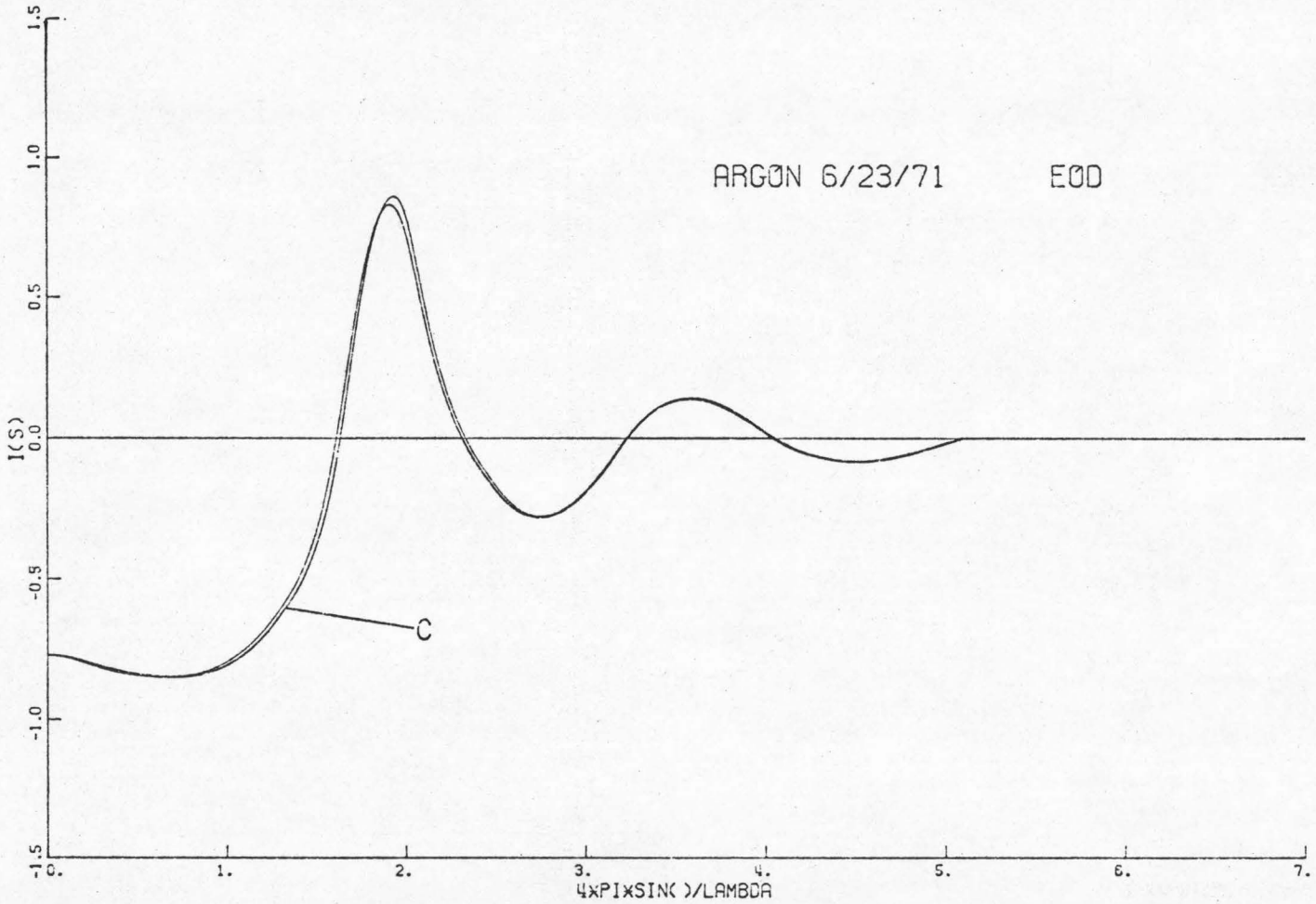

Figure 14.B. Structure factor, i(s), corrected (C) and uncorrected for distortion.

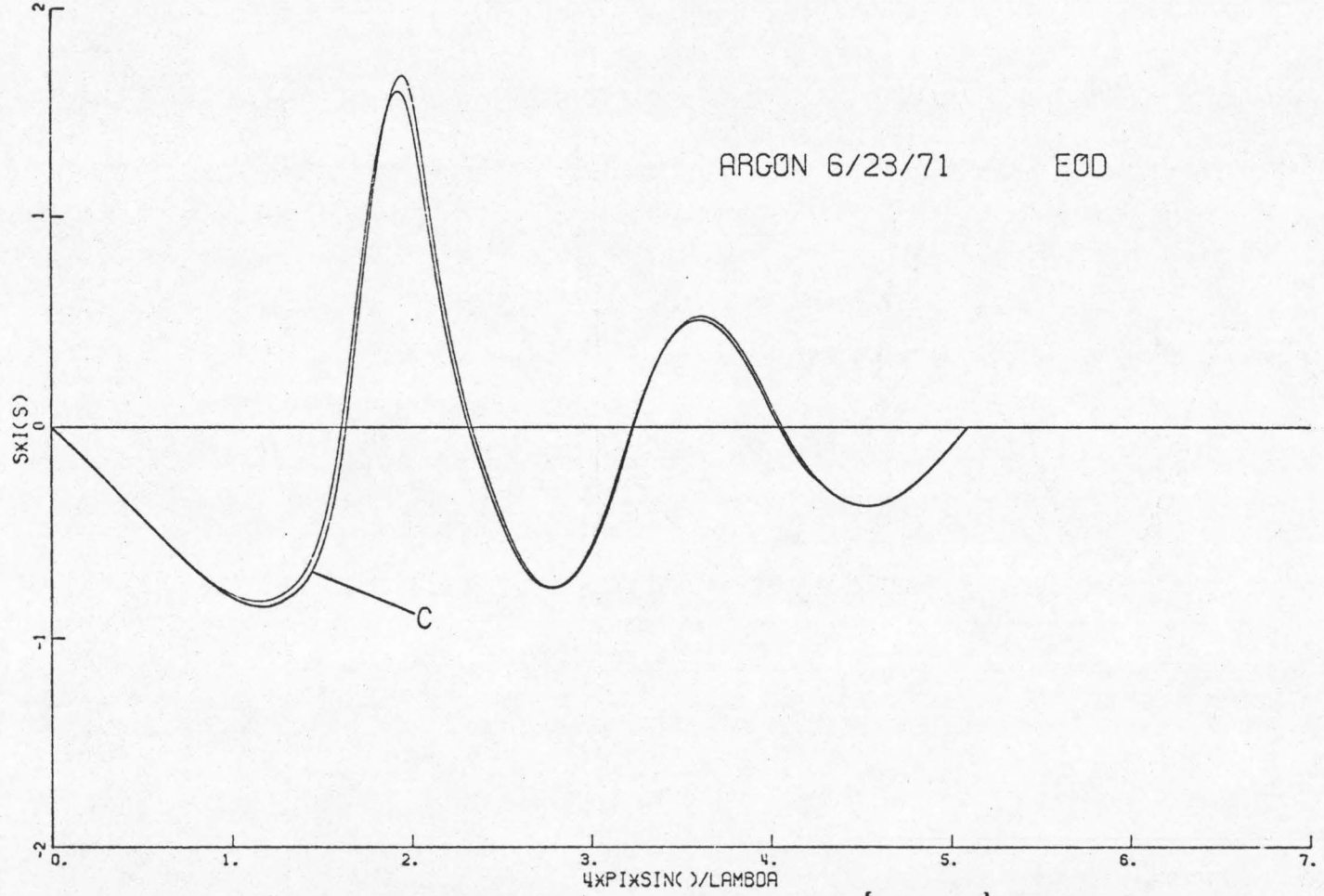

Figure 14.C. Kernel of Fourier transform of $r\left[g(r)-1\right]$, corrected (C) and uncorrected for distortion.

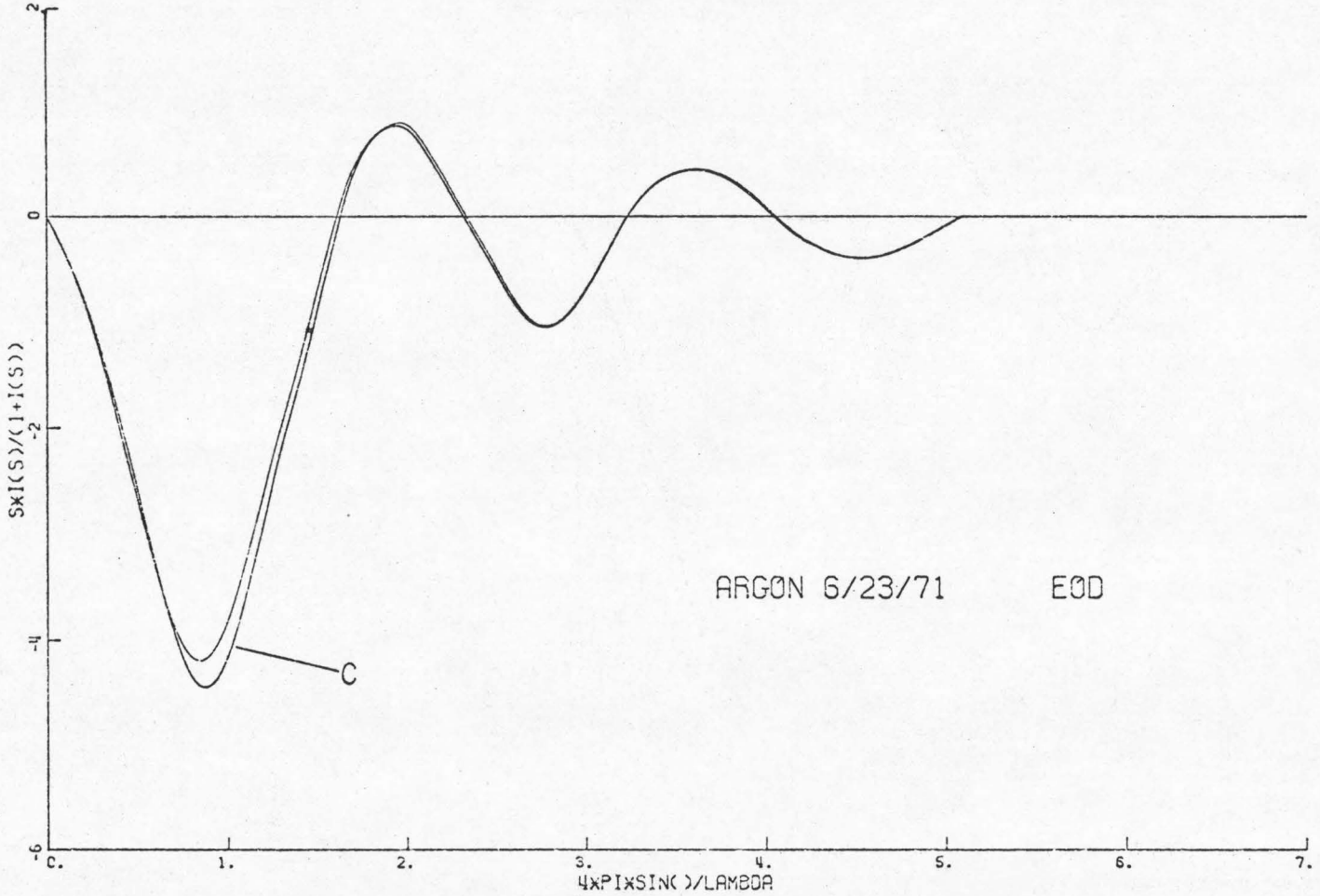

Figure 14.D. Kernel of Fourier transform of rc(r), corrected (C) and uncorrected for distortion.

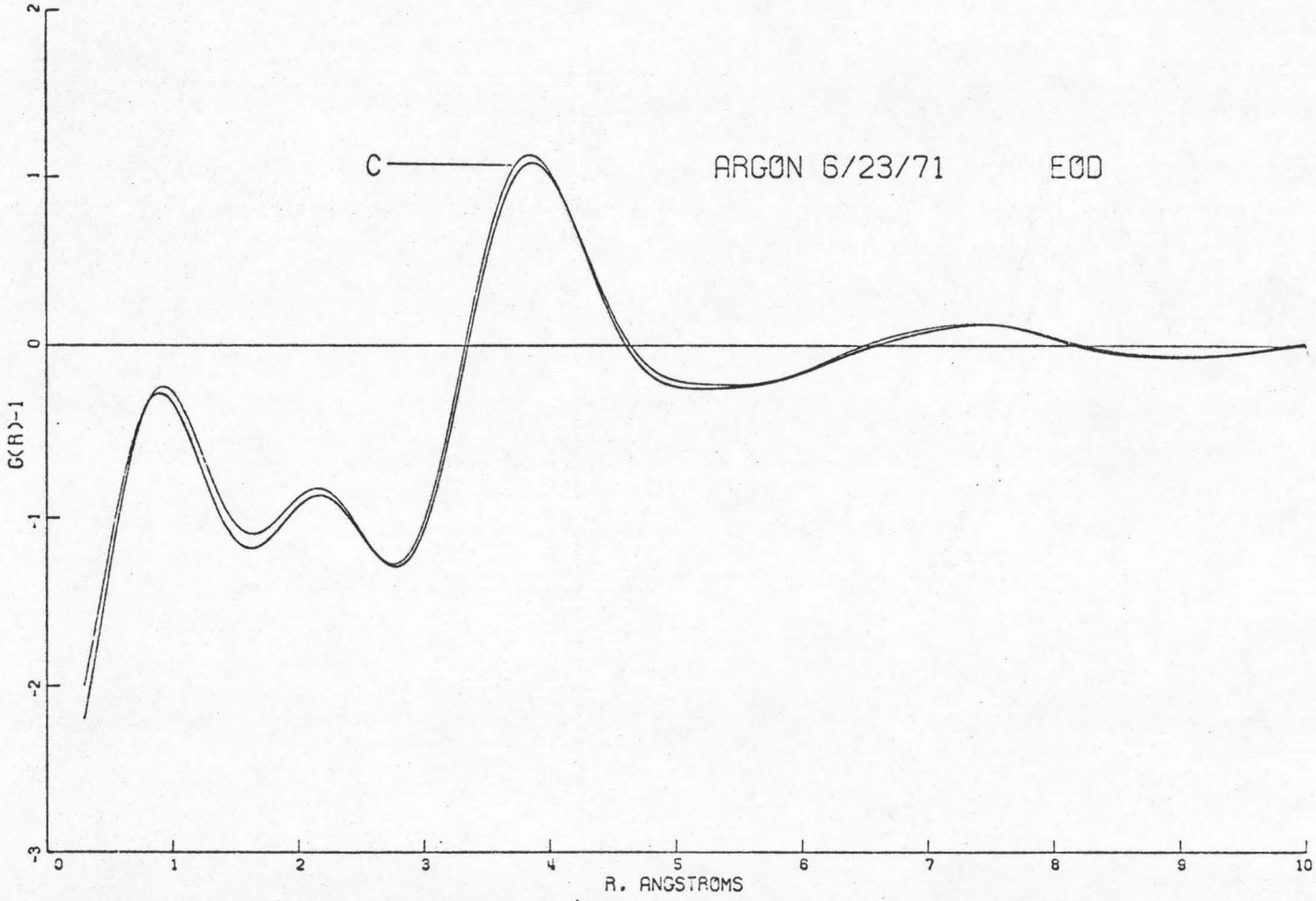

Figure 14.E. Radial distribution function, g(r), corrected (C) and uncorrected for distortion.

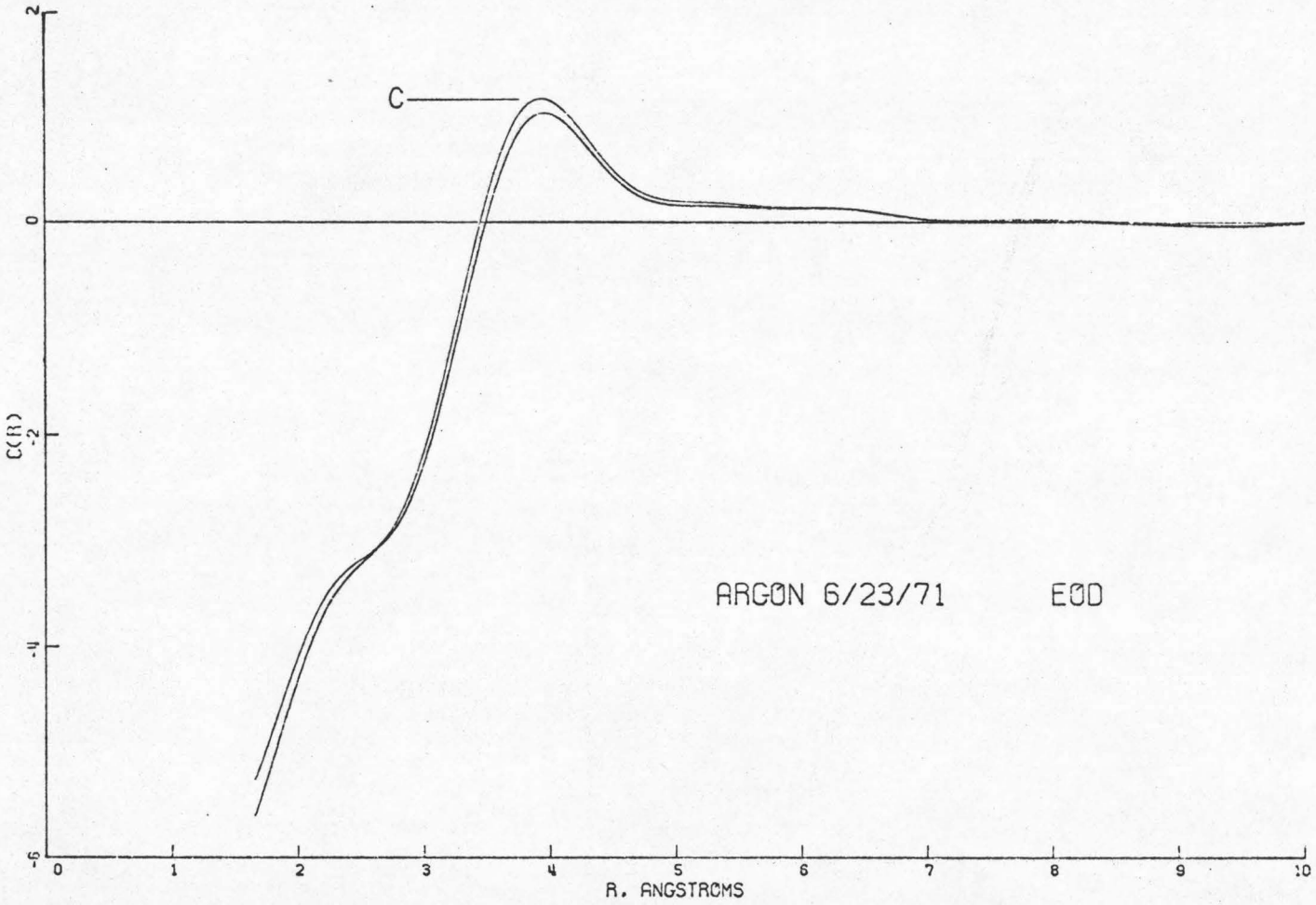

Figure 14.F. Direct correlation function, c(r), corrected (C) and uncorrected for distortion.

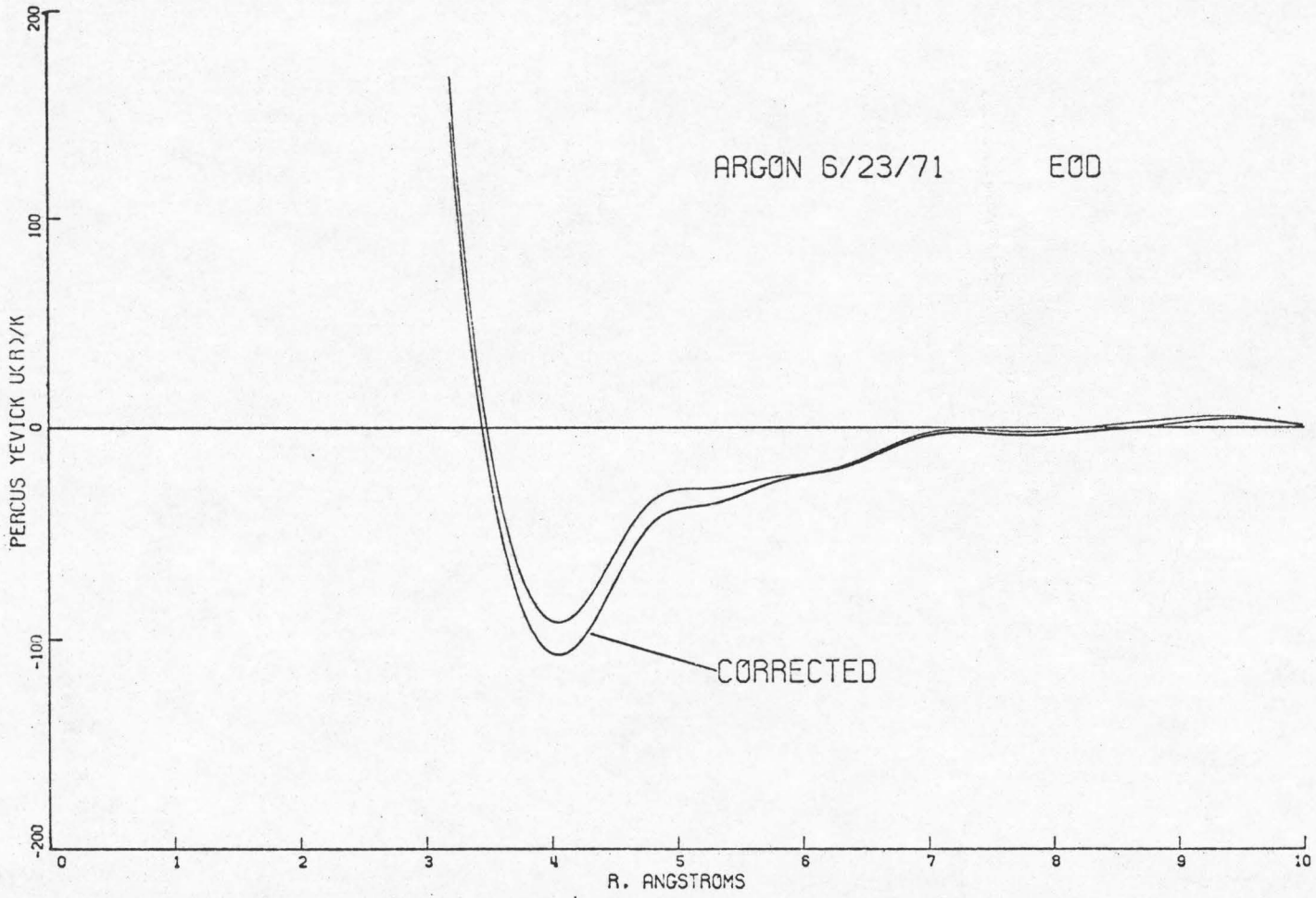

Figure 14.6. Percus-Yevick potential, u(r)/k (^{o}K), corrected and uncorrected for distortion.

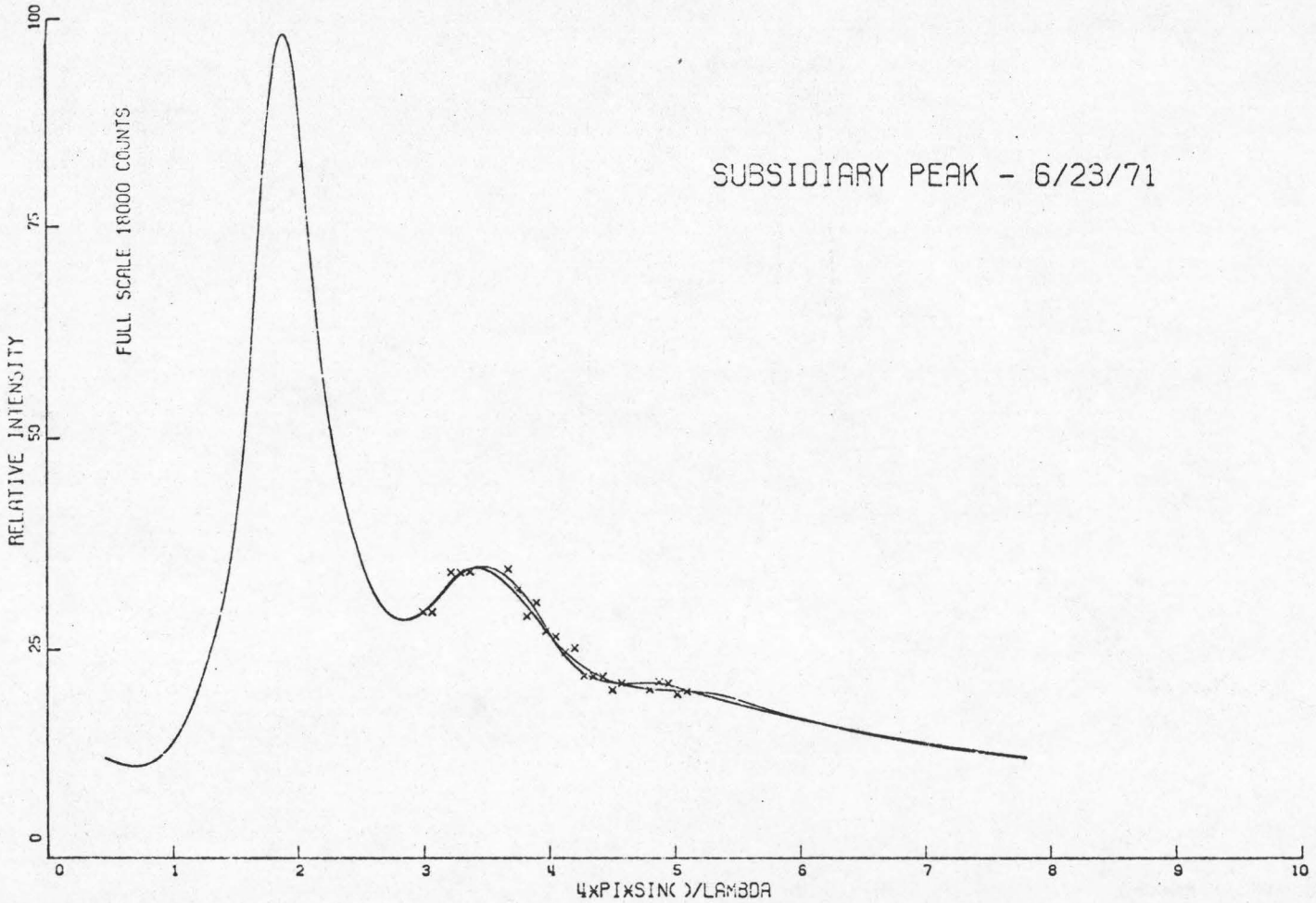

Figure 15.A (through 15.E). Numerical experiment on the subsidiary peak in g(r), one smoothed spectrum above yields the subsidiary peak.

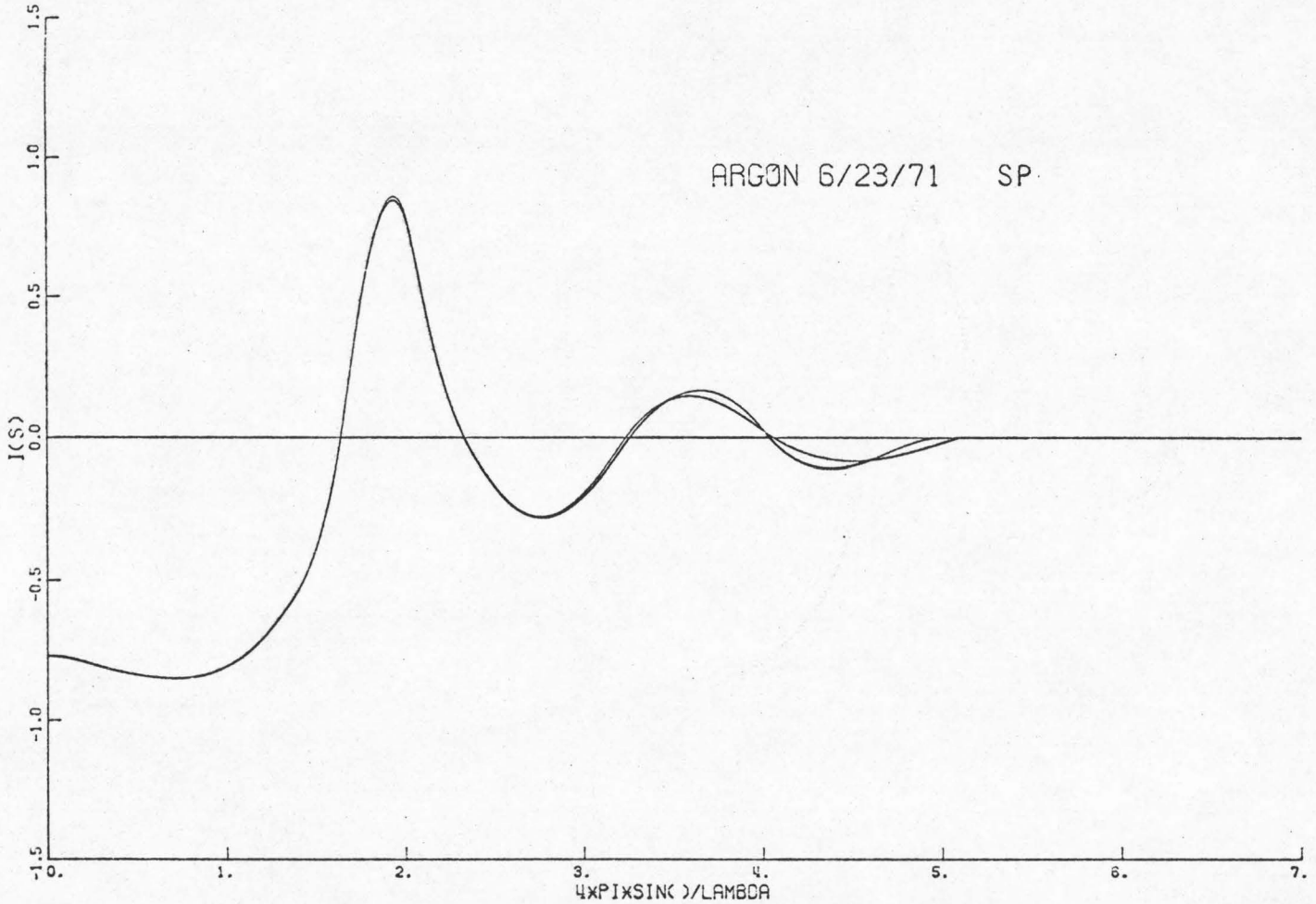

Figure 15.B. Structure factors, i(s), computed from smoothed argon spectra in Figure 15.A.

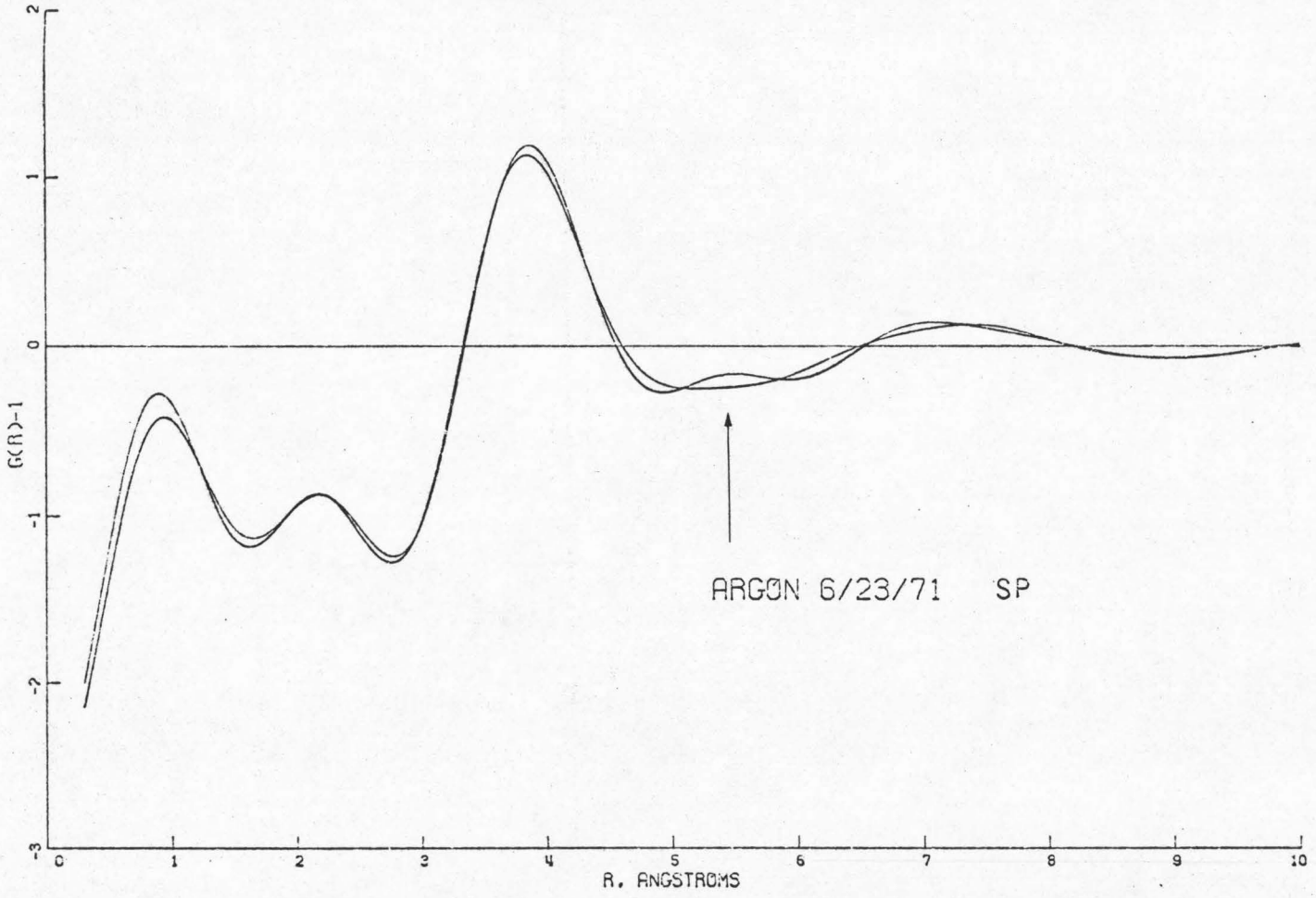

Figure 15.C. Radial distribution functions, g(r), computed from structure factors, i(s), in Figure 15.B, illustrating the subsidiary peak.

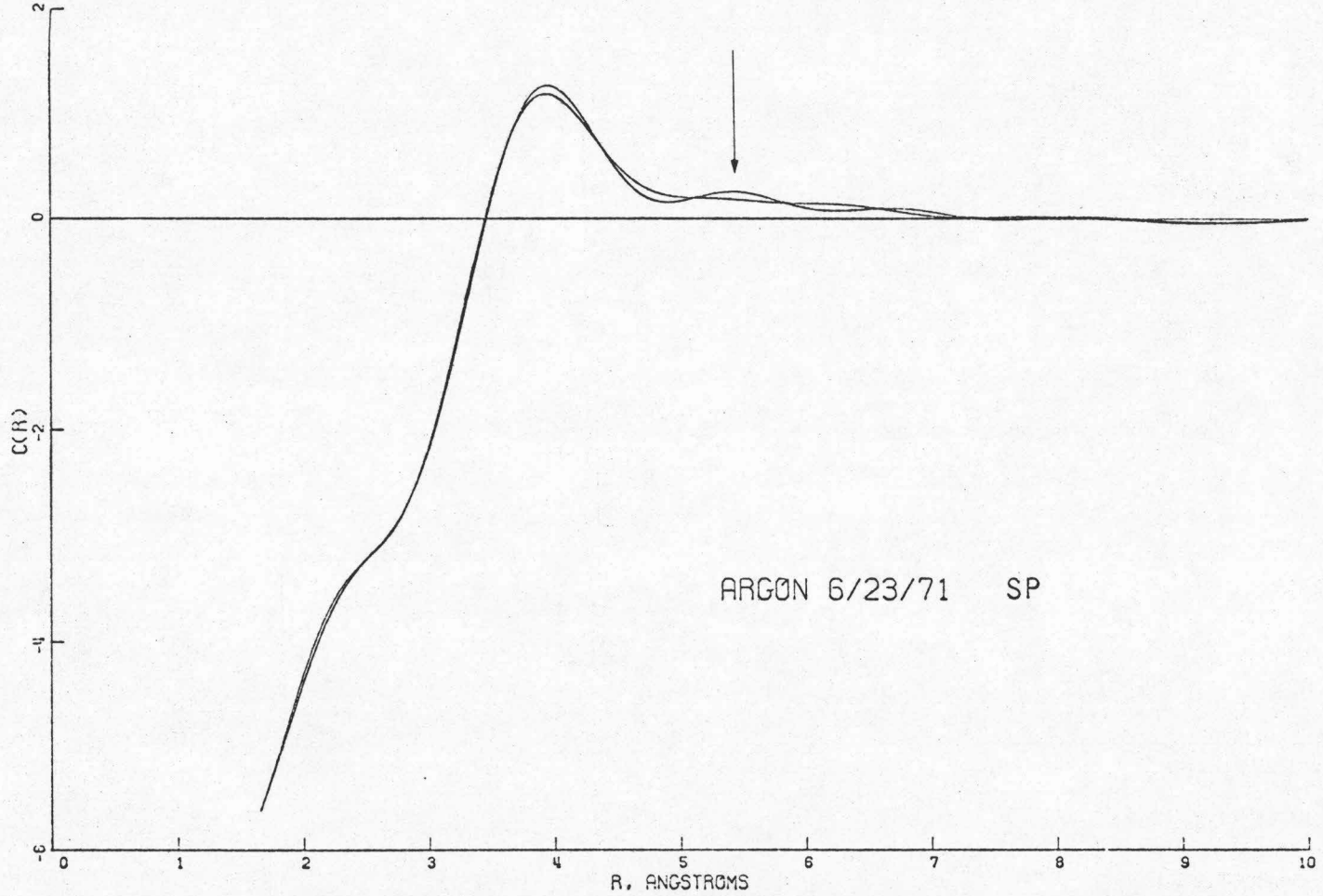

Figure 15.D. Direct correlation functions, c(r), computed from structure factors, i(s), in Figure 15.B, second peak in c(r) correlates with subsidiary peak in g(r).

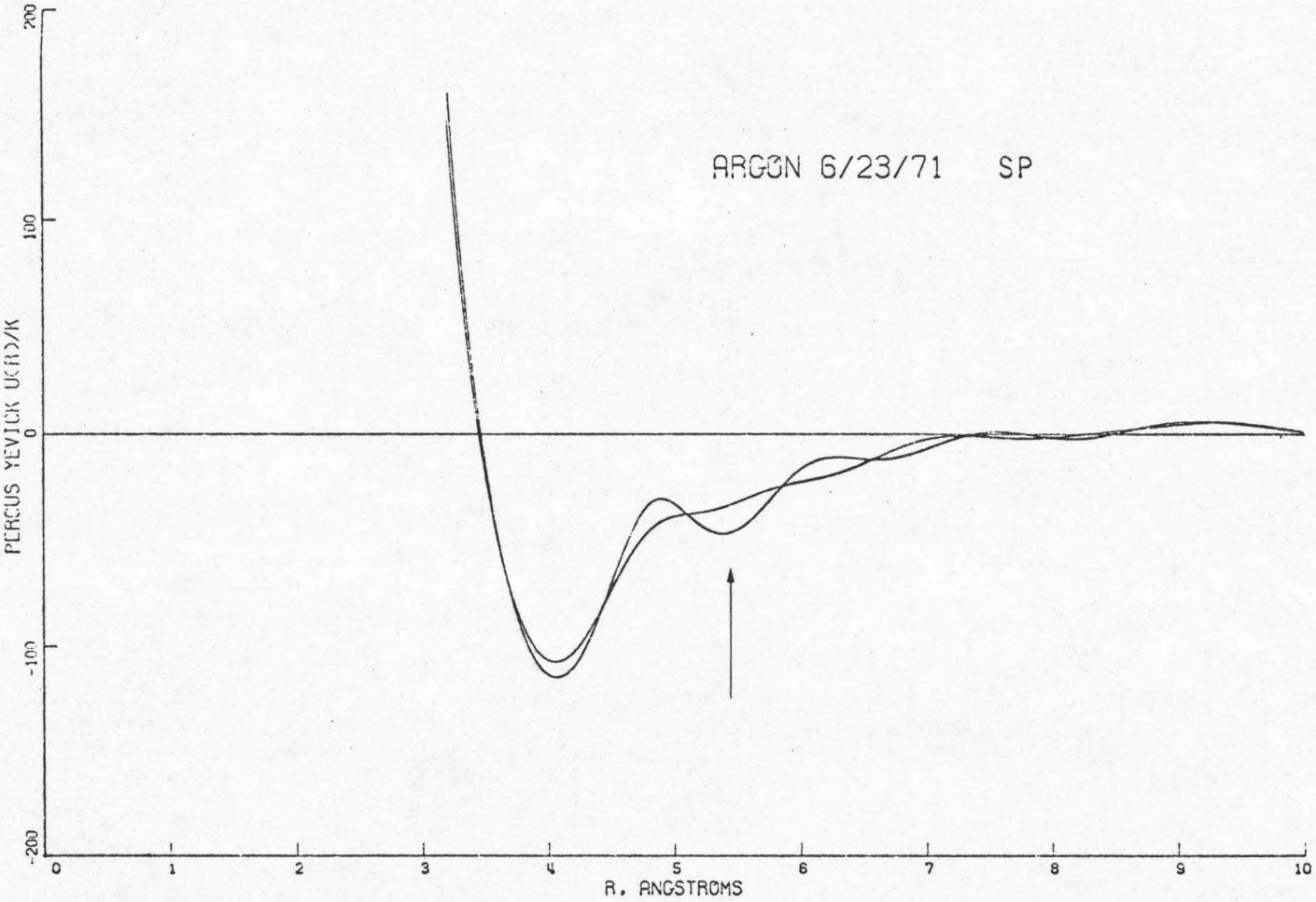

Figure 15.E. Percus-Yevick potentials, u(r)/k ($^{\circ}$K), computed from g(r) and c(r) in Figures 15.C and 15.D, local minimum in potential correlates with subsidiary peak in g(r).

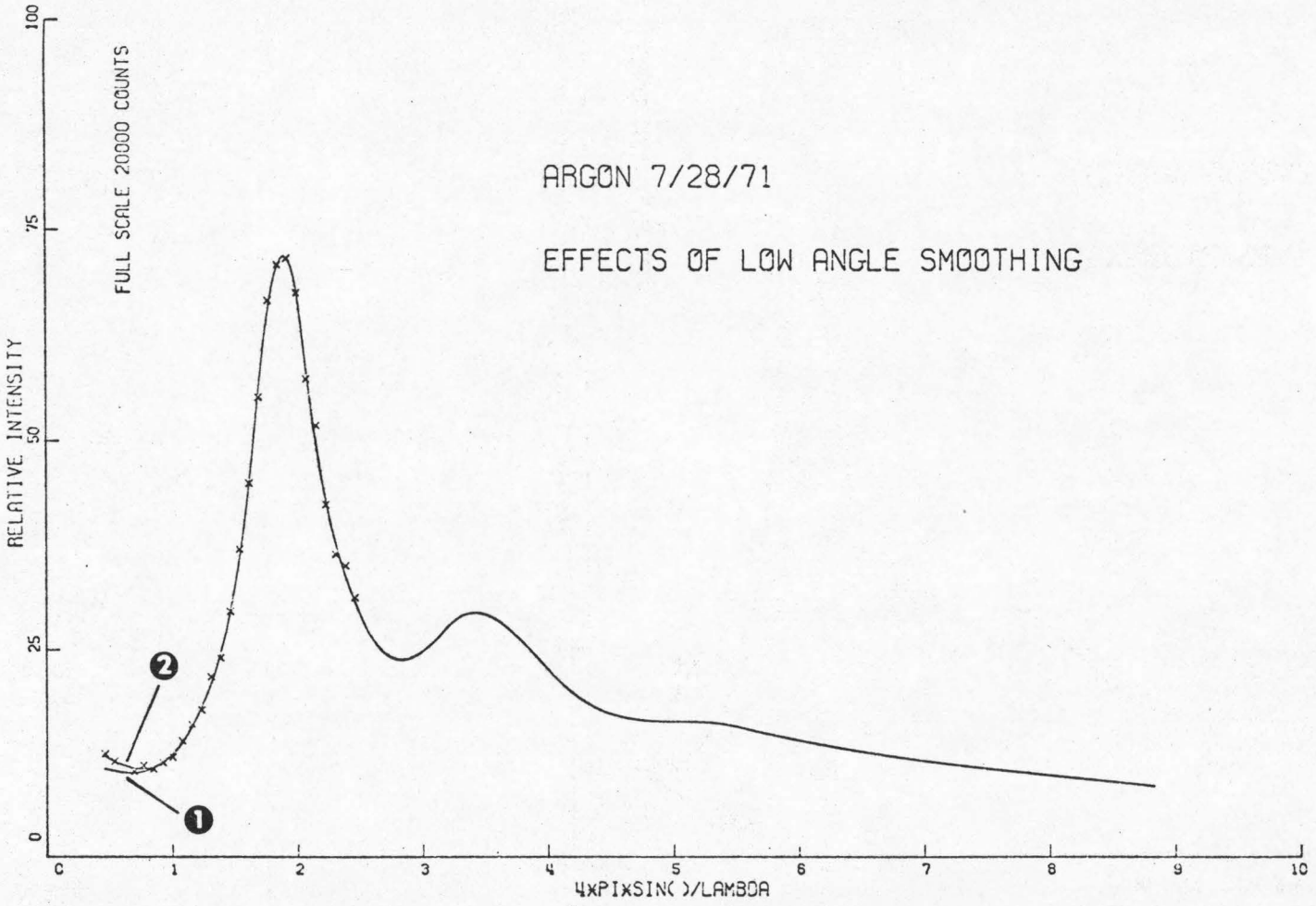

Figure 16.A (through 16.G). Numerical experiment on effect of low angle smoothing, argon spectra, two data points deleted for curve ❶.

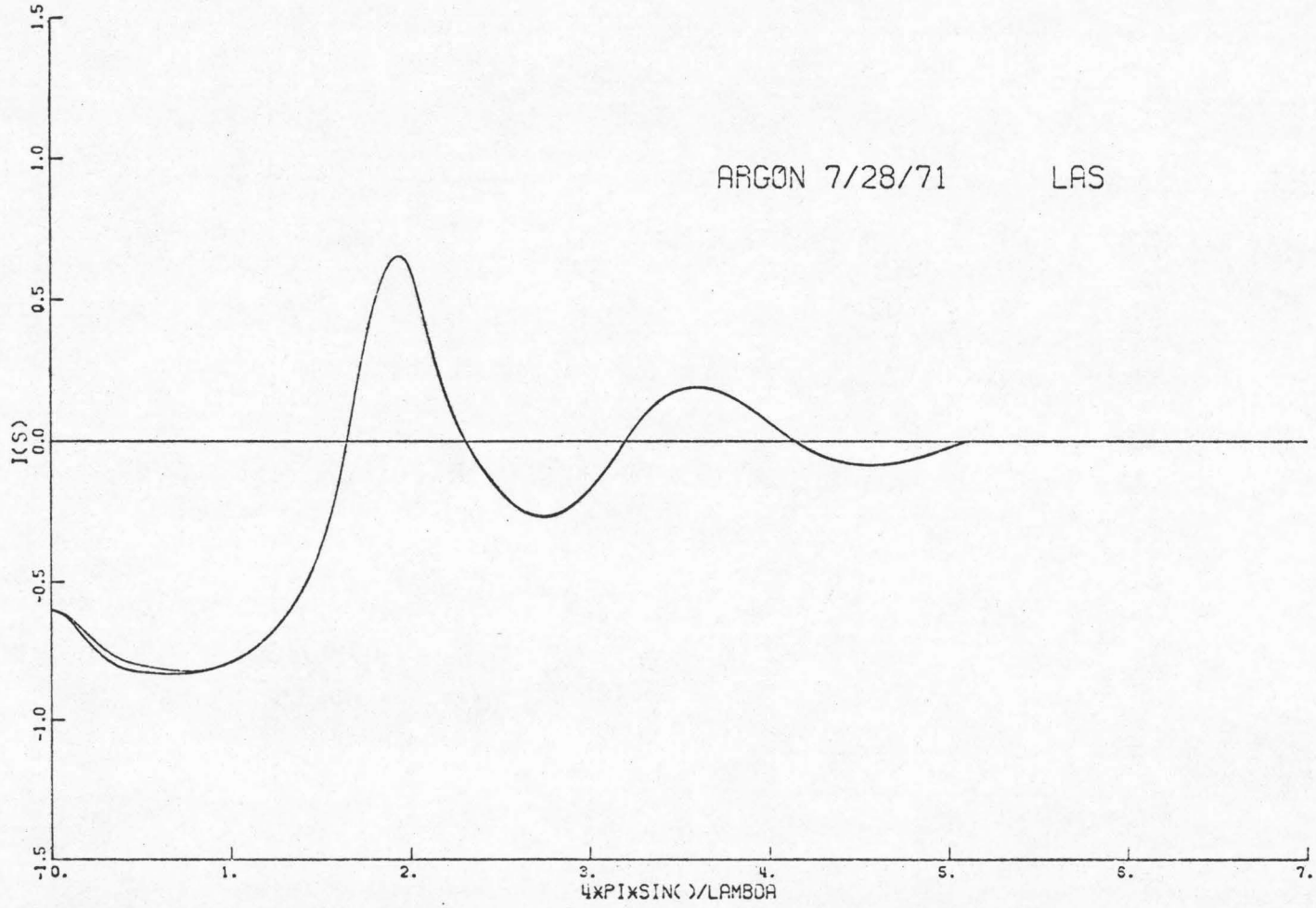

Figure 16.B. Structure factors, i(s), computed from argon spectra in Figure 16.A.

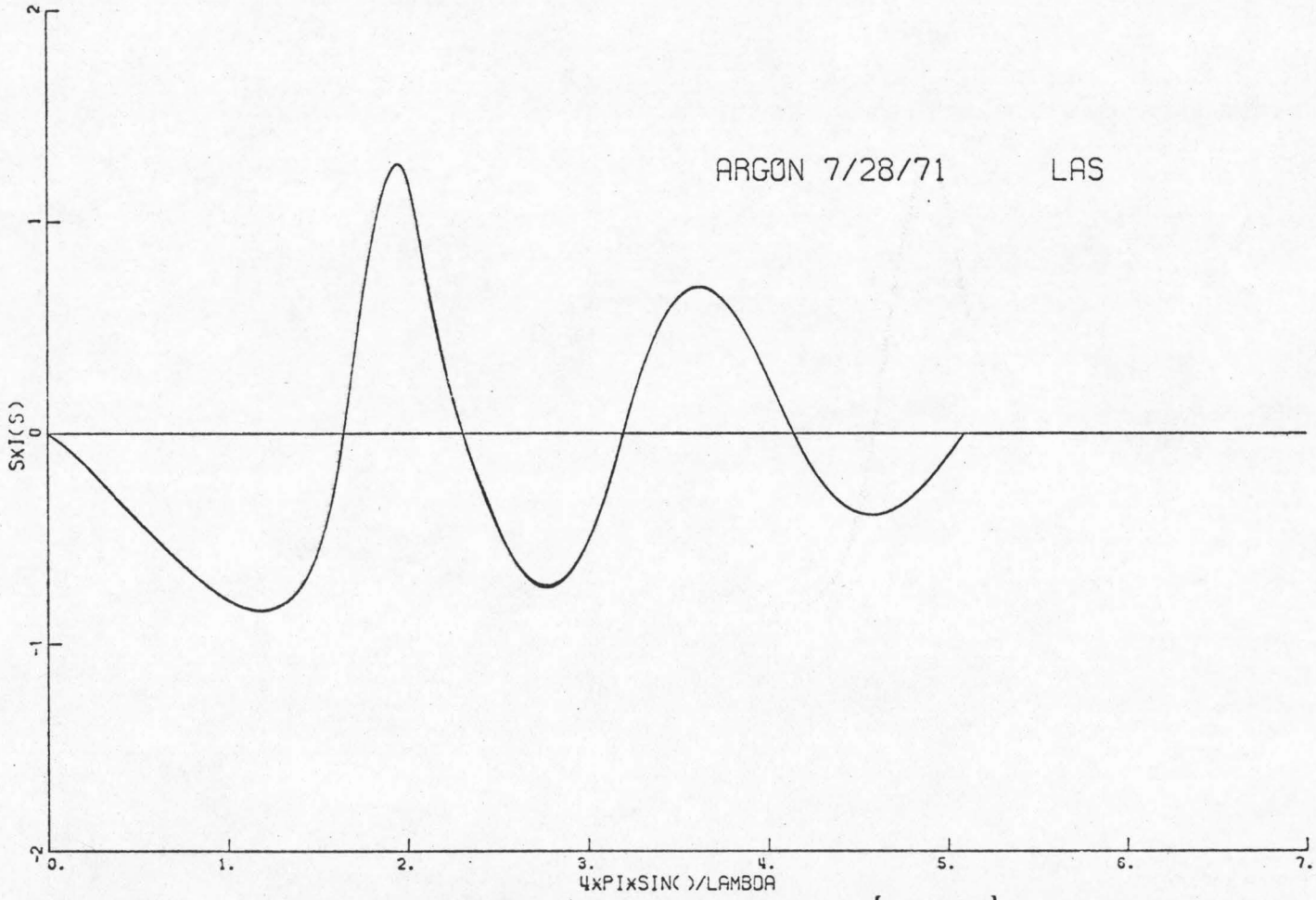

Figure 16.C. Kernels of Fourier transform of $r[g(r)-1]$ computed from structure factors, i(s), in Figure 16.B.

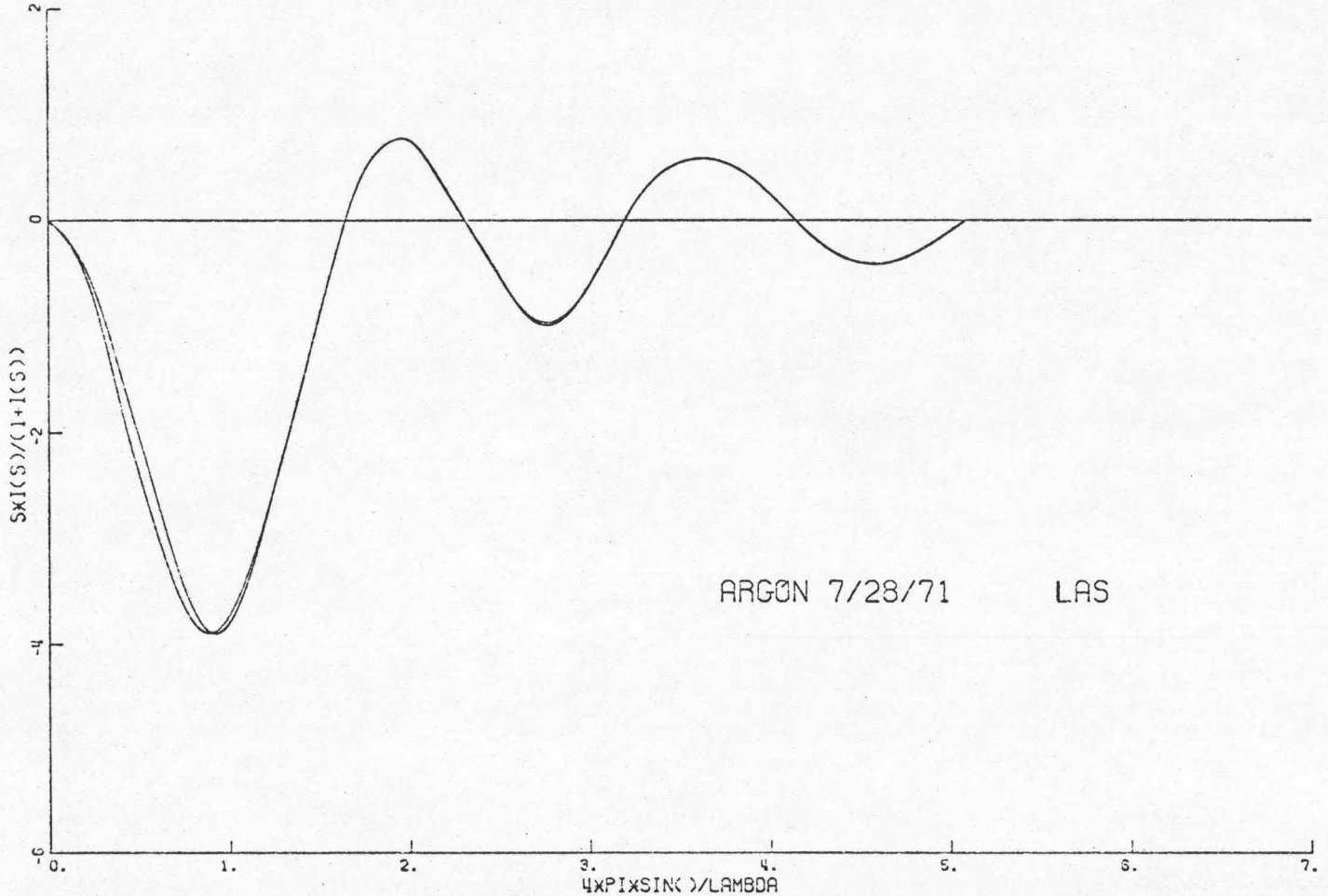

Figure 16.D. Kernels of Fourier transform of rc(r) computed from structure factors, i(s), in Figure 16.B.

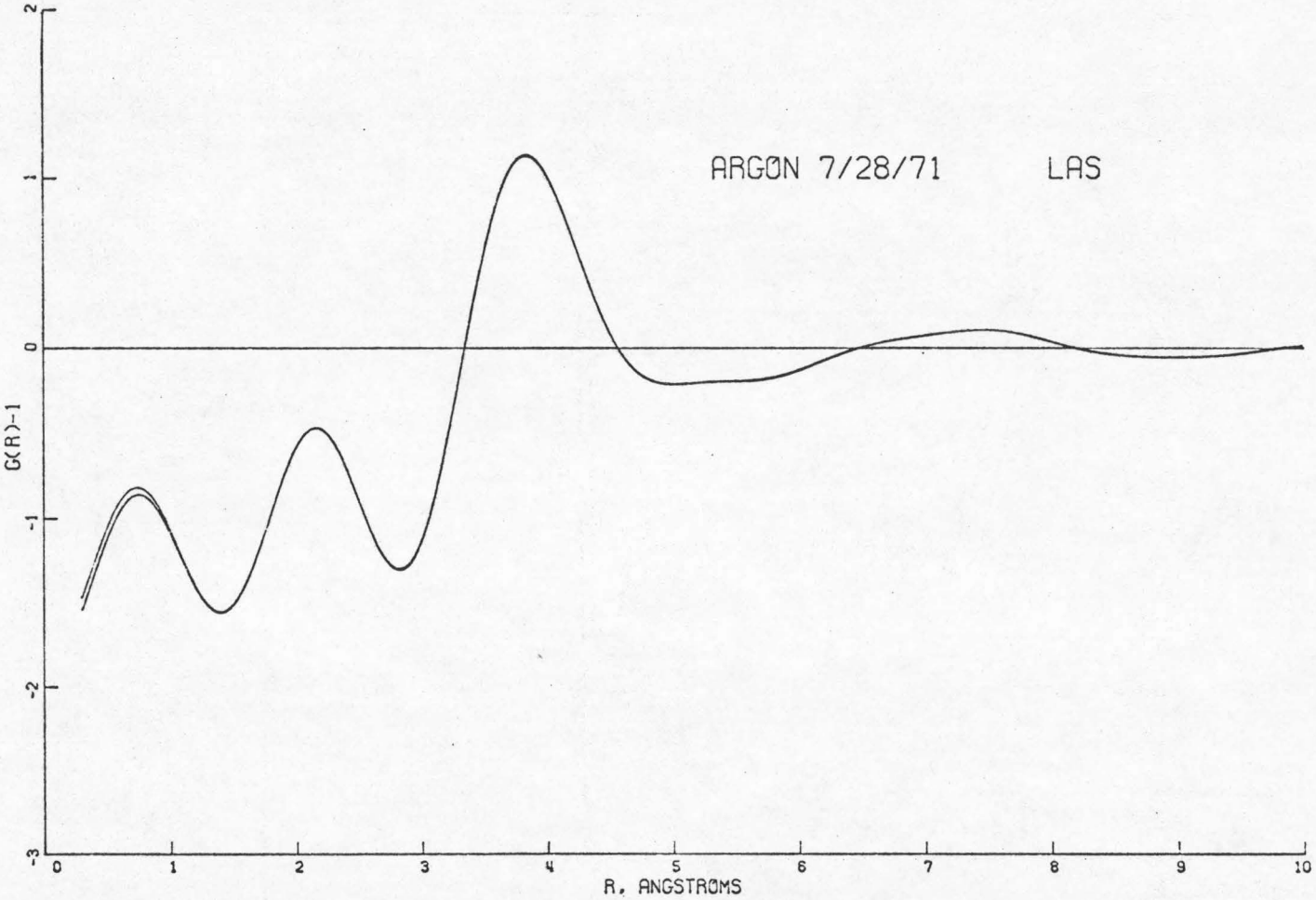

Figure 16.E. Radial distribution functions, g(r), computed from structure factors, i(s), in Figure 16.B.

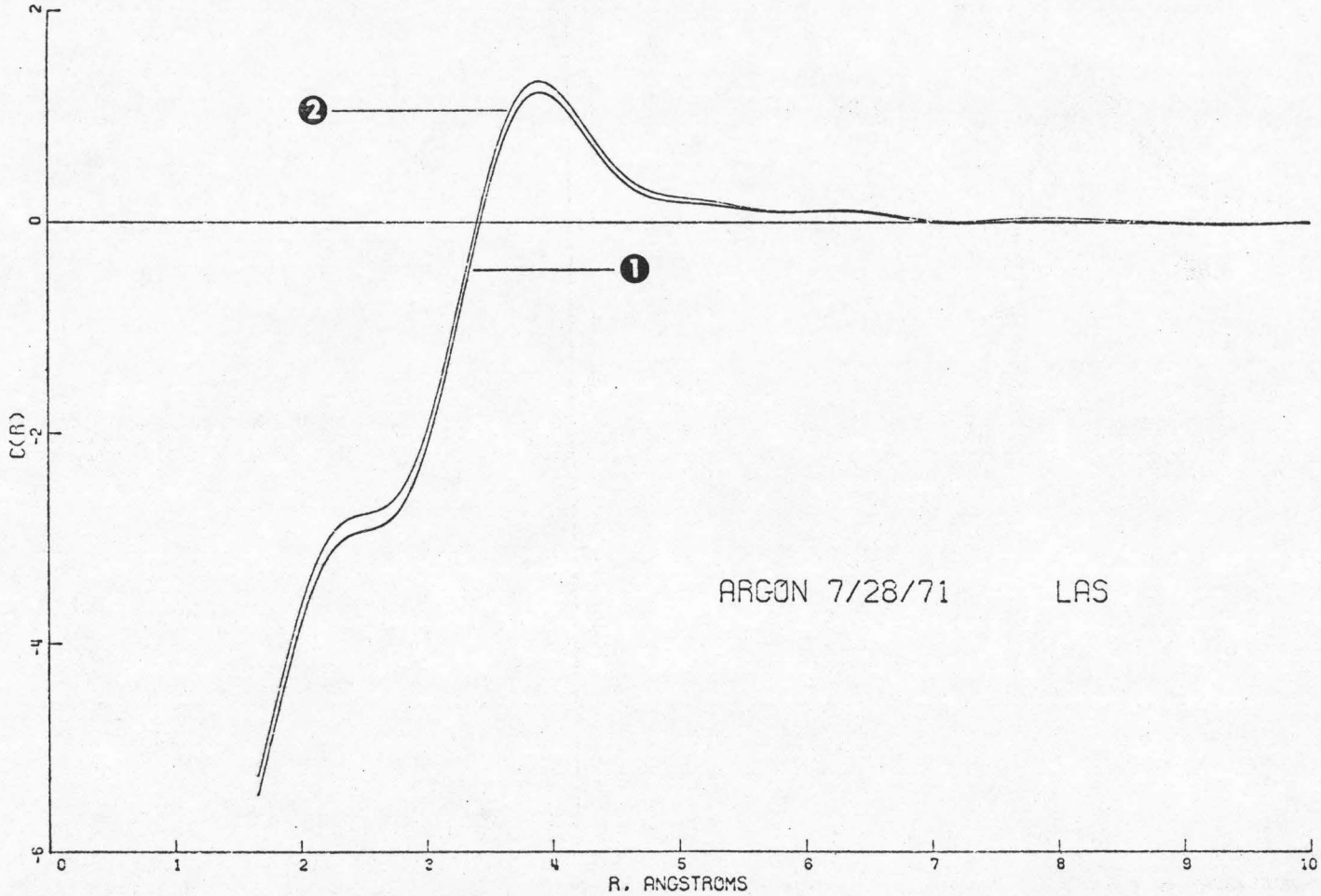

Figure 16.F. Direct correlation functions, c(r), computed from structure factors, i(s), in Figure 16.B, ❶ and ❷ correspond to the same curves in Figure 16.A.

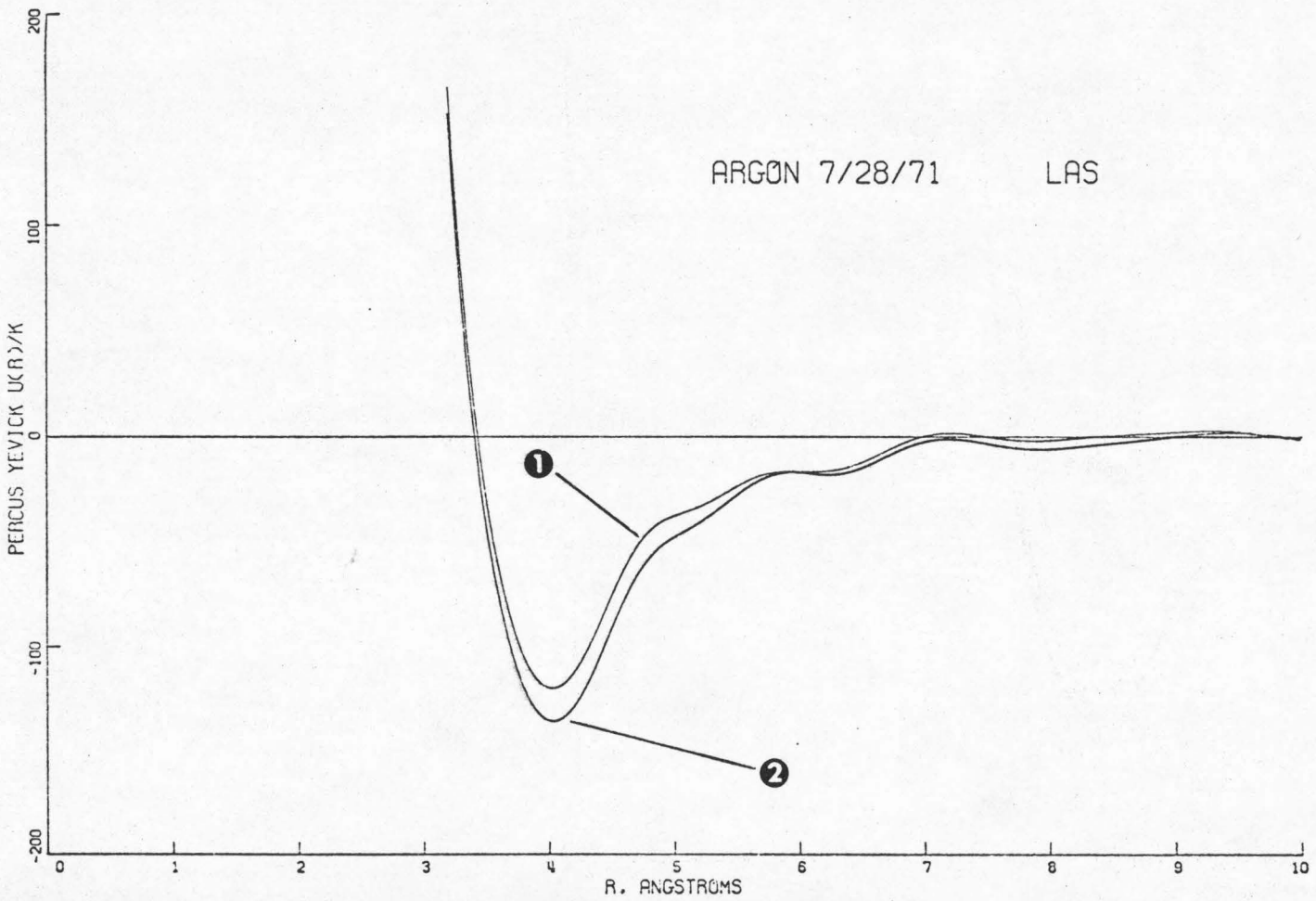

Figure 16.G. Percus-Yevick potentials, u(r)/k (^{o}K), computed from g(r) and c(r) in Figures 16.E and 16.F.

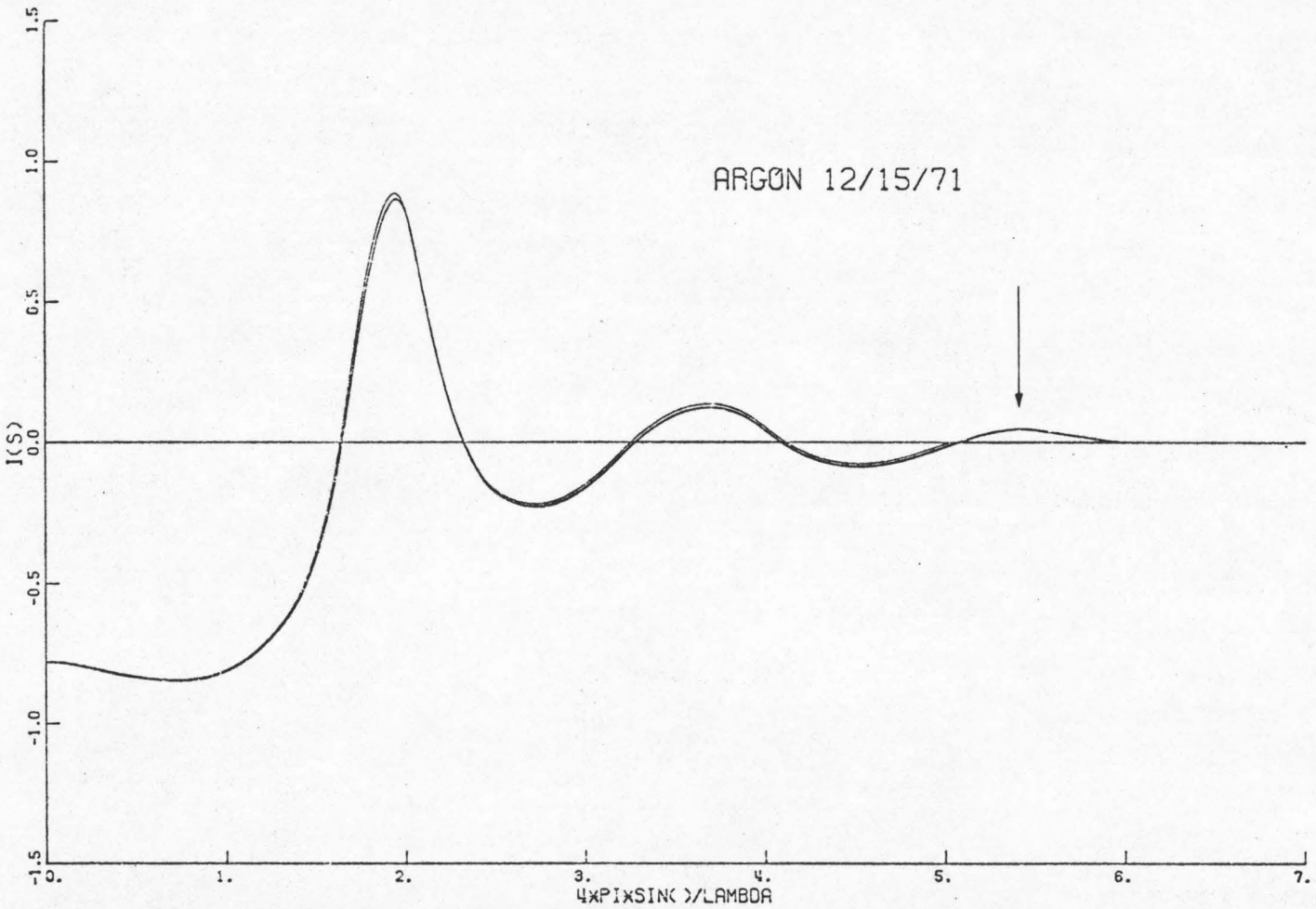

Figure 17.A (through 17.D). Numerical experiment on truncation, one structure factor, i(s), above includes a third peak.

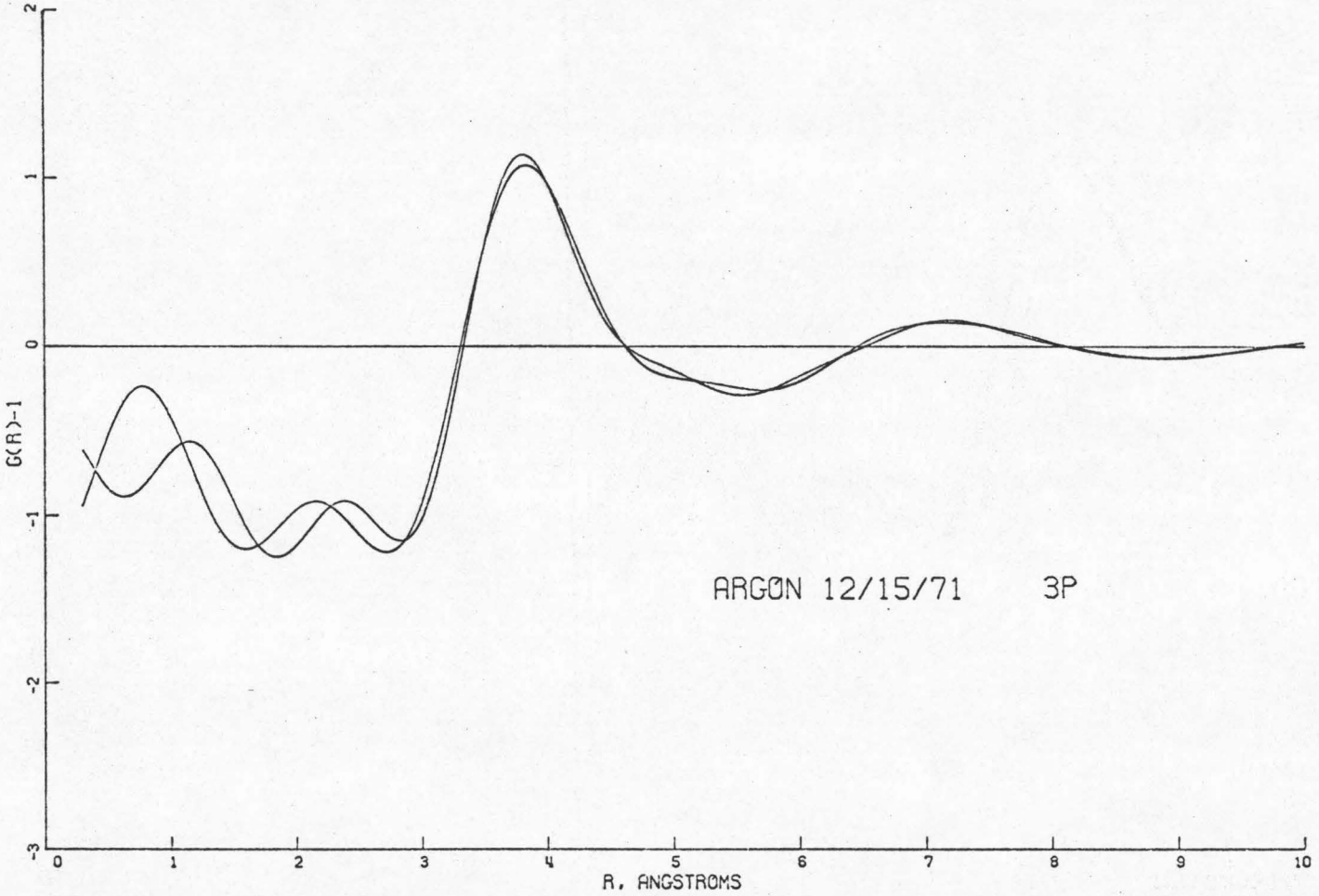

Figure 17.B. Radial distribution functions, g(r), computed from structure factors, i(s), in Figure 17.A.

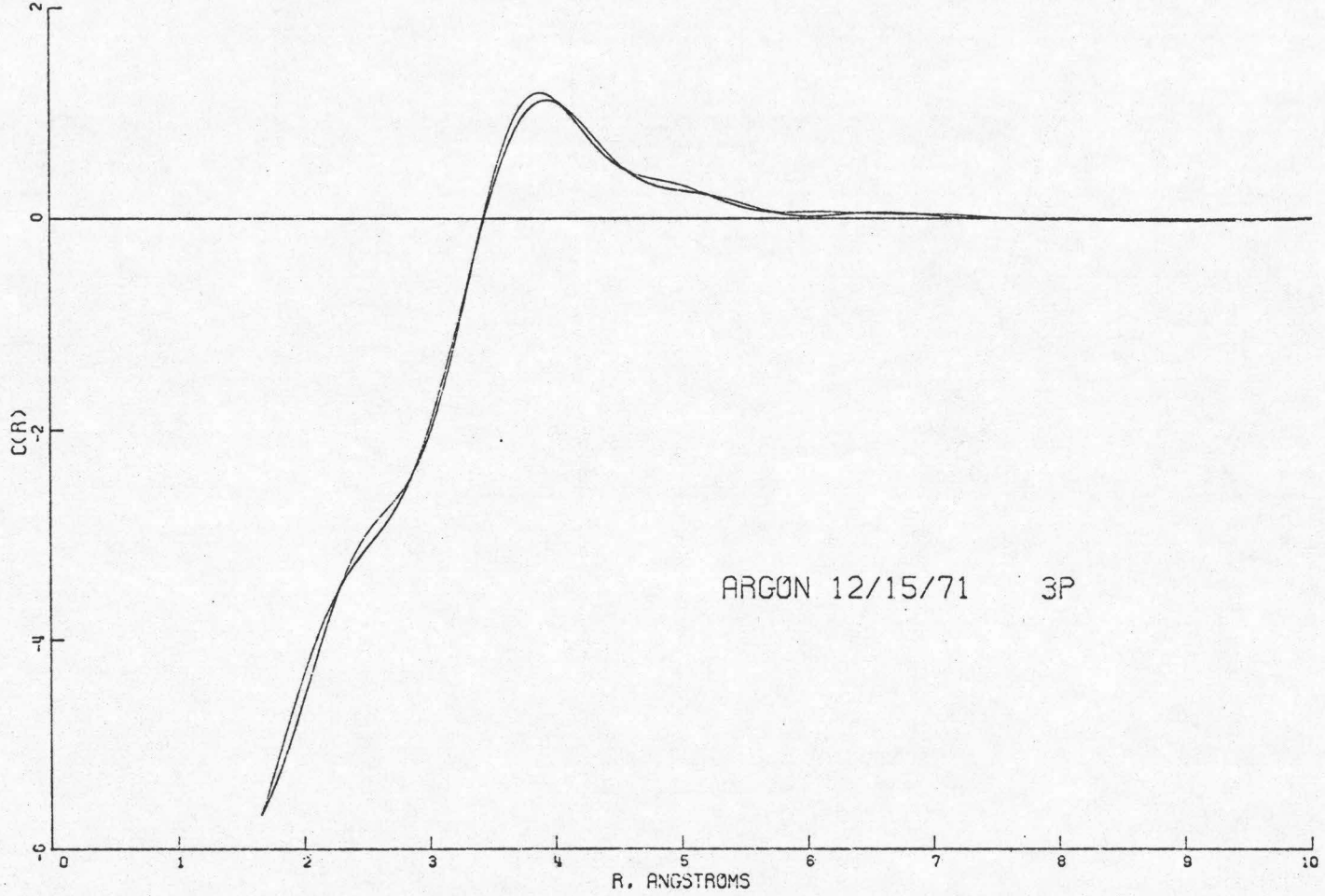

Figure 17.C. Direct correlation functions, c(r), computed from structure factors in Figure 17.A.

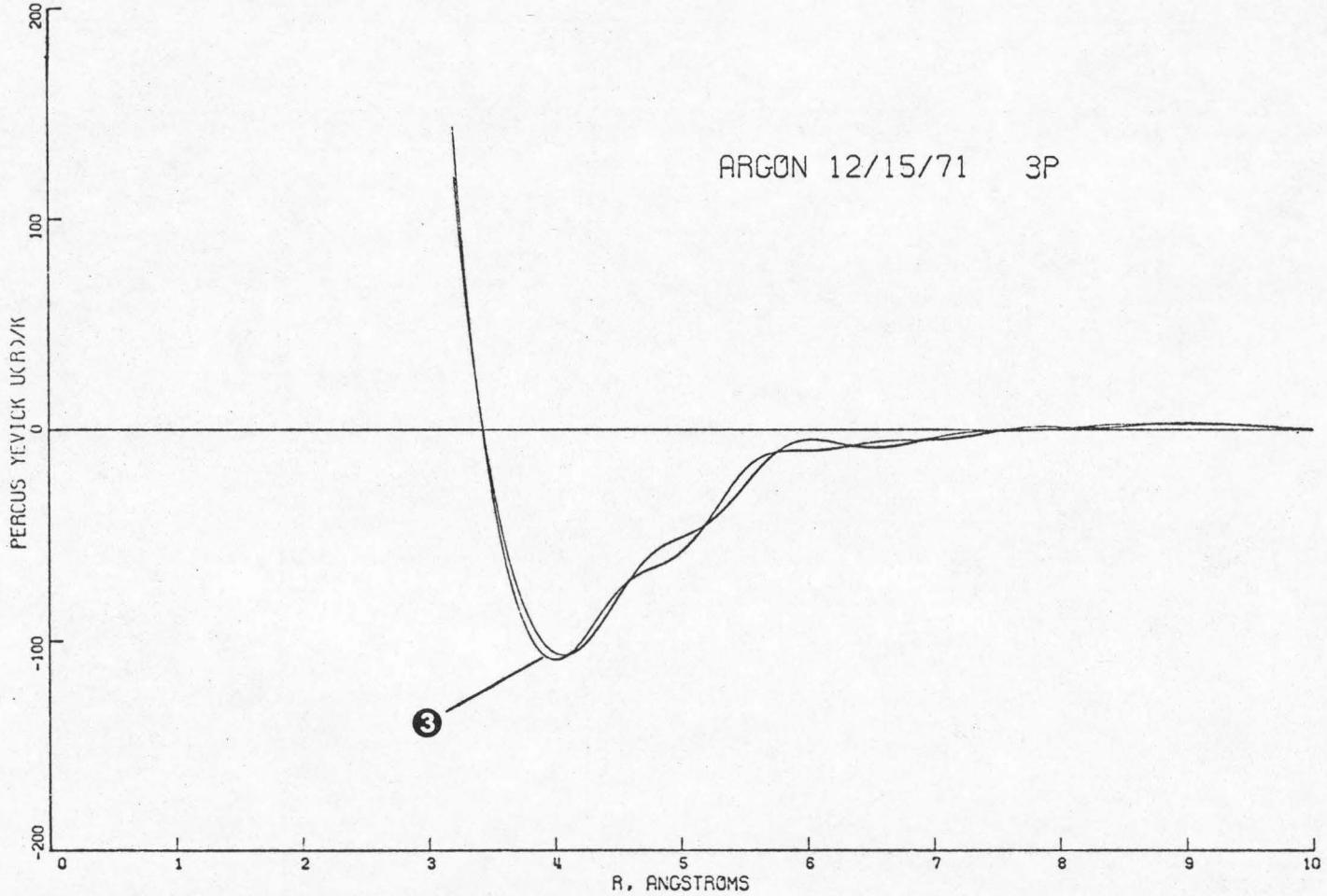

Figure 17.D. Percus-Yevick potentials, u(r)/k (^{o}K), computed from g(r) and c(r) in Figures 17.B and 17.C, ❸ designates u(r)/k that corresponds to i(s) with three peaks.

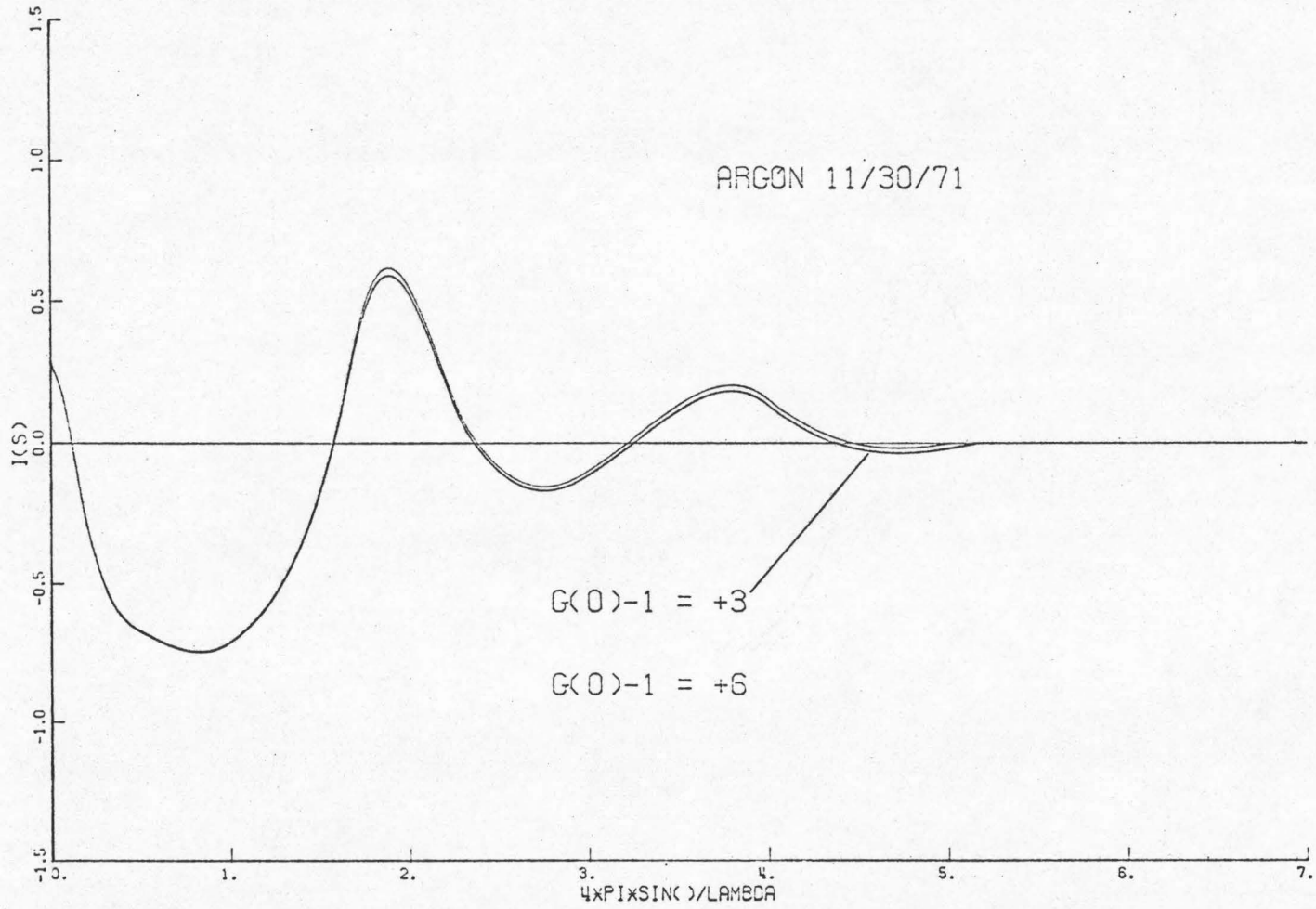

Figure 18.A (through 18.D). Numerical experiment on $g(0) > 0$, structure factors, i(s), above yield $g(0) \approx +3$ and $\approx +6$.

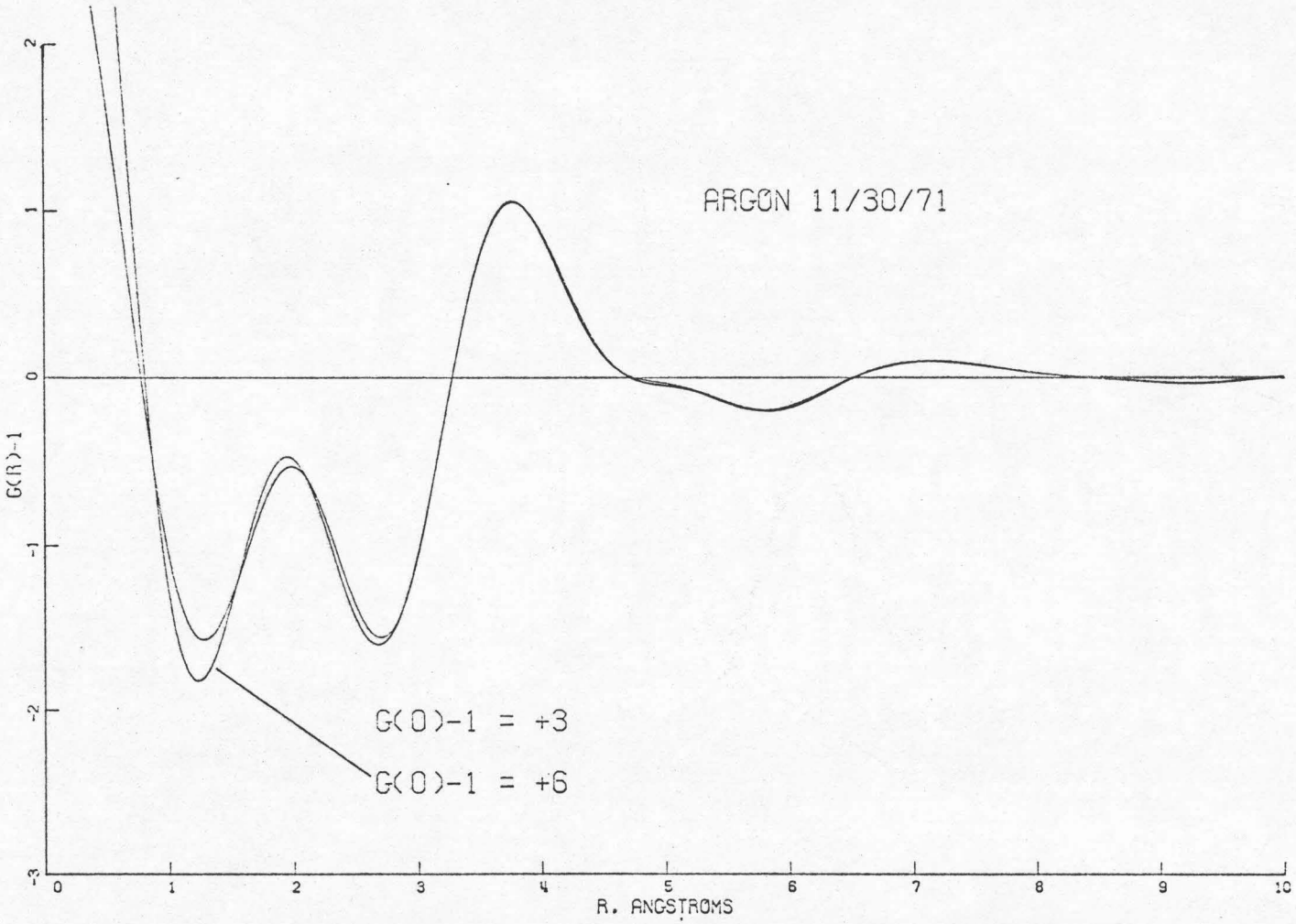

Figure 18.B. Radial distribution functions, g(r), computed from structure factors, i(s), in Figure 18.A.

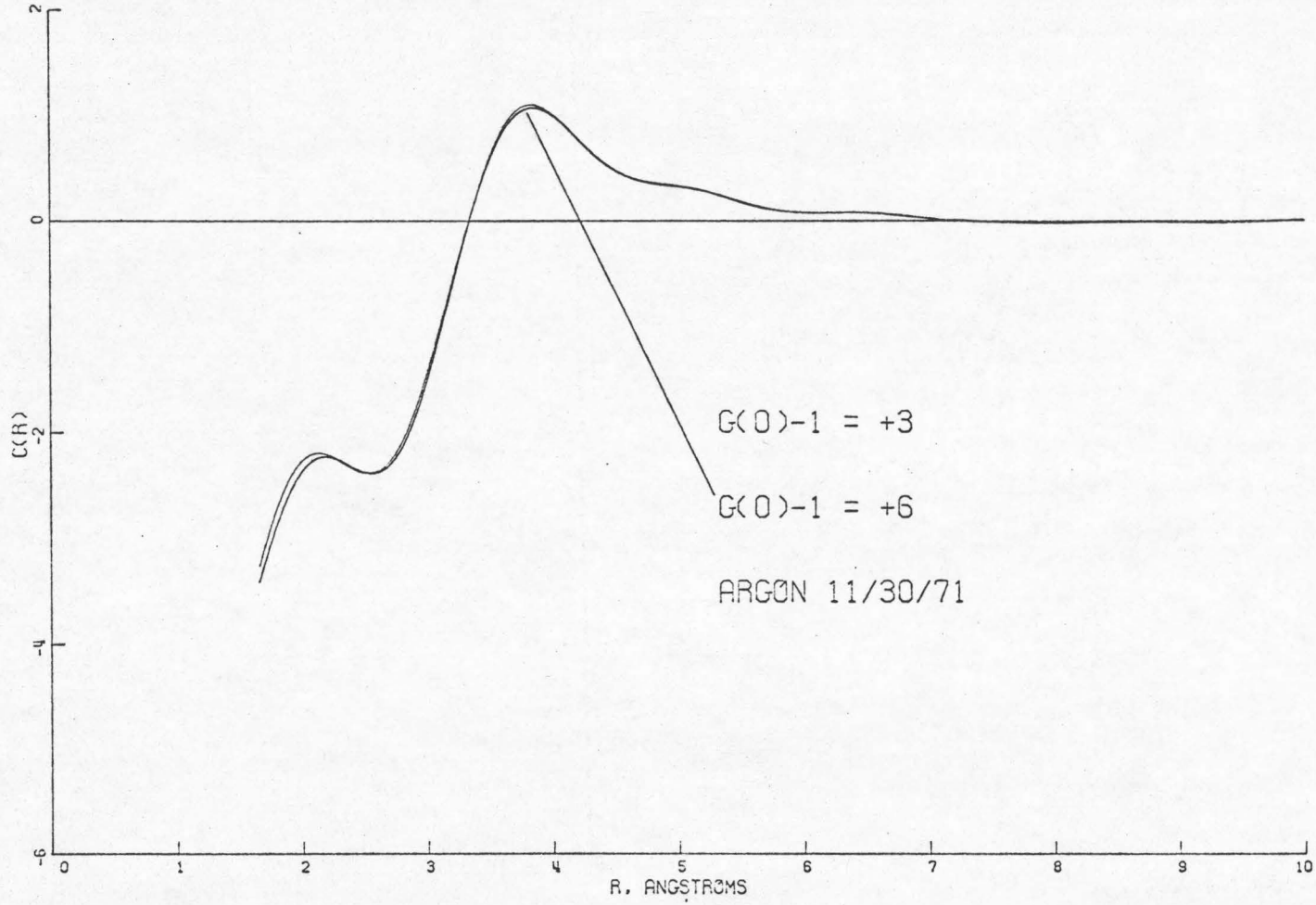

Figure 18.C. Direct correlation functions, c(r), computed from structure factors, i(s), in Figure 18.A.

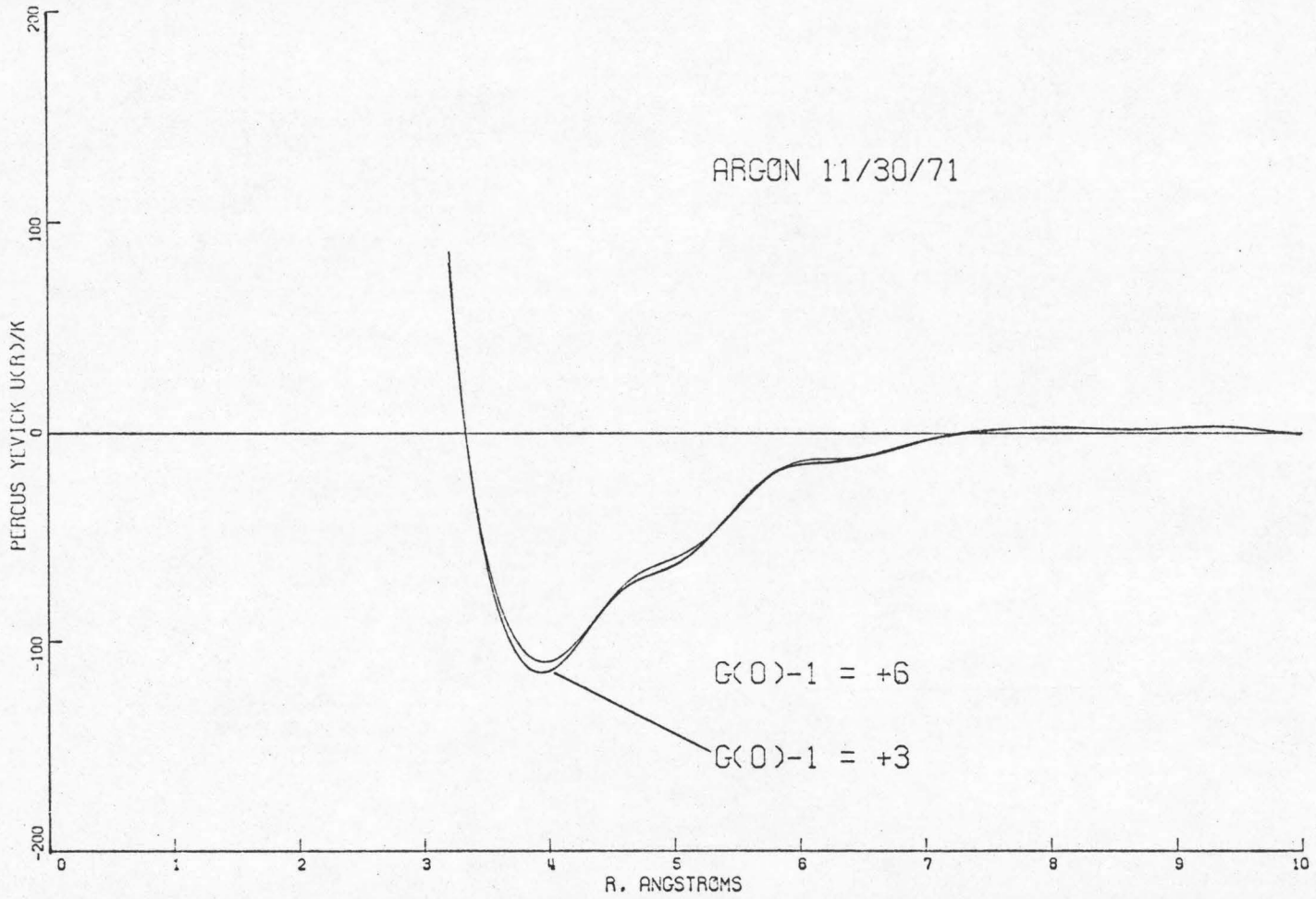

Figure 18.D. Percus-Yevick potentials, u(r)/k (^{o}K), computed from g(r) and c(r) in Figures 18.B and 18.C.

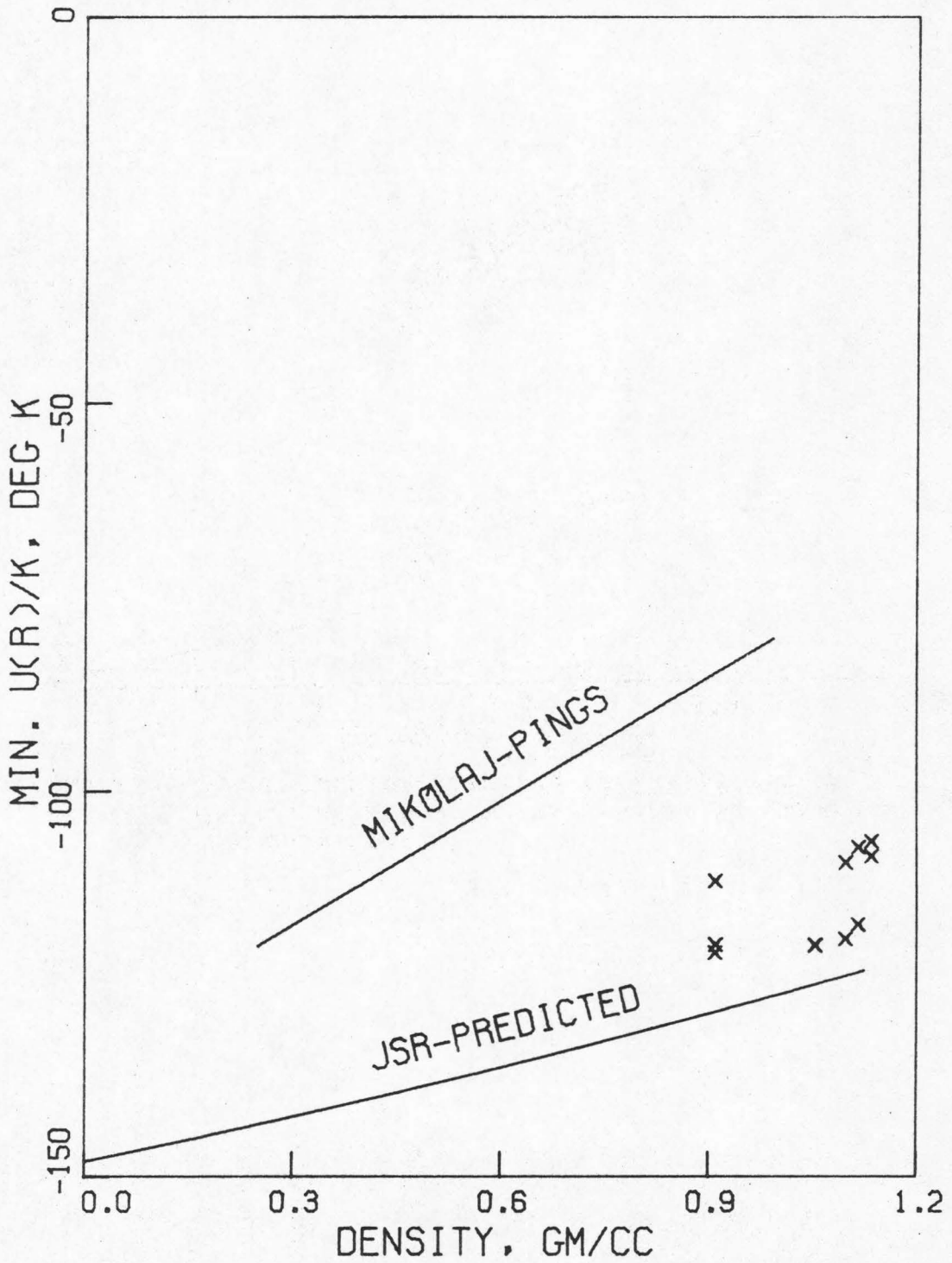

Figure 19. Comparison of computed Percus-Yevick well depths with theoretical result of Rowlinson,[36] X = this work.

TABLE 1.

Cross Reference: Date of Experiment - Thermodynamic State of Argon

Run No.	Date	Temperature	Pressure	Density
1	2/23/71	143°K	39.92 atm	0.91 gm/cc
2	6/16/71	143	39.92	0.91
3	6/23/71	127	36.85	1.116
4	7/28/71	133	36.85	1.054
5	8/4/71	127	36.85	1.116
6	8/24/71	127	18.71	1.098
7	9/28/71	133	36.85	1.054
8	11/30/71	143	39.92	0.91
9	12/8/71	127	18.71	1.098
10	12/15/71	127	54.44	1.135
11	12/21/71	127	54.44	1.135

TABLE 2.

Cell Subtraction Factors, F (see Eq. 15), and Smoothing Input Information*

Run No.	F	Assumed $I_a(s)$ at $s = 0$	Assumed $I_a(s)$ at $s = 8.841$ Å^{-1}	Slope of $I_a(s)$ at $s = 8.841$ Å^{-1}	N_a
1	1.0	3500	1170	-216.2	76.4
2	1.01	4500	1877	-329.5	122.1
3	0.99	2700	1845	-335.1	136.3
4	1.005	2500	1710	-311.0	103.9
5	1.0	3100	1950	-347.9	136.5
6	1.007	3000	1700	-310.0	119.9
7	1.0	3500	1750	-325.0	123.9
8	1.015	6000	1725	-320.2	102.5
9	1.015	3000	1700	-306.0	115.5
10	1.0	2500	1650	-303.9	119.9
11	1.0	2750	1850	-331.0	131.3

*See input description to smoothing computer program in Appendix H for the explicit meaning of all quantities.

TABLE 2. (cont.)

Run No.	Mesh points in s-space	Weighting Information
1	0,1,1.67,2.33,3,4,5.25,8.841	17,18,19 @ 2,4,2
2	0,1,1.67,2.33,3.2,4,5.5,8.841	16,17,18,19,20,38,39,40 @ 2 ea
3	0,1.25,1.67,2.05,2.5,3.2,4,5.5,8.841	18,19 @ 4,4
4	0,1.25,1.67,2.05,2.5,3.2,4.2,5.5,8.841	18,19 @ 4,4
5	0,1.25,1.67,2.05,2.5,3,4,5.4,8.841	19,20 @ 4,4
6	0,1.25,1.67,2.05,2.5,3.2,4.5,6,8.841	17,18,19,20 @ 1,2,2,1
7	0,1.25,1.67,2.05,2.5,3.2,4.2,5.5,8.841	18,19 @ 4,4
8	0,1,1.67,2.33,3,4,5.7,8.841	17,18,19 @ 2,2,2
9	0,1.25,1.67,2.05,2.5,3.2,4,5.5,8.841	17,18,19,20 @ 1,3,3,1
10	0,1.25,1.67,2.05,2.5,3.2,4,5.5,8.841	17,18,19,20 @ 2,4,4,2
11	0,1.25,1.67,2.05,2.5,3.2,4,5.5,8.841	16,17,18,19 @ 2,4,4,2

TABLE 3.

Thermodynamic Data for Argon

Temperature	Pressure	Density	$\rho kT\kappa - 1$
143°K	39.92 atm	0.91 gm/cc	+0.29
133	36.85	1.054	-0.60
127	18.71	1.098	-0.75
127	35.85	1.116	-0.77
127	54.44	1.135	-0.78

TABLE 4.A

Intensity Measurements (total counts)

DATA ANALYSIS
EXPERIMENT OF 2/23/71, T=143 DEG K, RHO=0.91 GM/CC

2θ	S	CELL	CELL+ARGON	ARGON ALONE
3.0	0.4629	506	3072	2809 *
3.5	0.5400	515	2721	2450
4.0	0.6171	550	2575	2284
4.5	0.6942	584	2589	2277
5.0	0.7713	610	2698	2369
5.5	0.8483	817	2779	2335
6.0	0.9254	1076	2963	2373
6.5	1.0024	940	3315	2795
7.0	1.0794	1007	3491	2929
7.5	1.1564	1149	3865	3218
8.0	1.2334	1126	3923	3283
8.5	1.3104	1173	4746	4073
9.0	1.3873	1123	5434	4784
9.5	1.4642	1271	6424	5682
10.0	1.5411	1213	7386	6672
10.5	1.6179	1233	8407	7674
11.0	1.6947	1327	9455	8659
11.5	1.7715	1786	11301	10220
12.0	1.8482	1326	11233	10423
12.5	1.9249	1286	10860	10067
13.0	2.0016	1701	10267	9209
13.5	2.0783	1521	9407	8453
14.0	2.1549	1598	8231	7221
14.5	2.2314	1637	7222	6178
15.0	2.3079	1542	6945	5954
15.5	2.3844	1730	6212	5091
16.0	2.4608	1813	5958	4774
16.5	2.5372	1798	5472	4289
17.0	2.6135	1691	5250	4128 *
17.5	2.6898	2723	6089	4269 *
18.0	2.7660	1911	5571	4284 *
18.5	2.8422	2358	5531	3932
19.0	2.9183	2626	5528	3735
19.5	2.9944	2269	5493	3933
20.0	3.0704	3473	6433	4030
20.5	3.1463	8577	9404	3431 *
21.0	3.2222	2678	6080	4203
21.5	3.2981	2028	5521	4091
22.0	3.3738	2531	5833	4039
22.5	3.4495	5226	7758	4033
23.0	3.5252	15916	16703	5299 *
23.5	3.6007	30011	24072	2458 *

TABLE 4.A (cont.)

Intensity Measurements (total counts)

DATA ANALYSIS
EXPERIMENT OF 2/23/71, T=143 DEG K, RHO=0.91 GM/CC

2θ	S	CELL	CELL+ARGON	ARGON ALONE
24.0	3.6762	5696	8252	4129
24.5	3.7517	2039	5365	3882
25.0	3.8270	2051	5134	3635
25.5	3.9023	2362	4989	3256
26.0	3.9775	2140	4809	3232
26.5	4.0526	2077	4808	3271 *
27.0	4.1277	2156	4450	2849
27.5	4.2027	1944	4350	2901
28.0	4.2776	2027	4328	2812
28.5	4.3524	2039	4313	2783
29.0	4.4271	2211	4432	2767
29.5	4.5018	2159	4338	2707
30.0	4.5764	2171	4284	2640
30.5	4.6508	2994	4517	2243 *
31.0	4.7252	9447	9736	2544
31.5	4.7995	2497	4292	2386
32.0	4.8737	2136	3870	2236
32.5	4.9478	1988	4116	2592
33.0	5.0219	2104	4002	2385
33.5	5.0958	2511	4257	2324
34.0	5.1696	2096	4081	2464
34.5	5.2434	2069	4159	2560
35.0	5.3170	2201	3991	2288
35.5	5.3905	2598	4331	2317
36.0	5.4639	3990	5227	2130
36.5	5.5373	4137	5895	2679 *
37.0	5.6105	2236	3820	2079
37.5	5.6836	2101	3660	2022
38.0	5.7566	2008	3695	2128
38.5	5.8295	2155	3606	1922
39.0	5.9023	2200	3538	1817
39.5	5.9749	2240	3748	1994
40.0	6.0475	2598	3797	1761
40.5	6.1199	9219	8672	1440 *
41.0	6.1923	4952	6058	2170 *
41.5	6.2645	2291	3550	1749
42.0	6.3365	2924	4110	1810
42.5	6.4085	2500	3703	1735
43.0	6.4804	3769	4545	1576
43.5	6.5521	7097	7351	1758
44.0	6.6237	4227	5272	1939
44.5	6.6951	2134	3349	1665

TABLE 4.A (cont.)

Intensity Measurements (total counts)

DATA ANALYSIS
EXPERIMENT OF 2/23/71, T=143 DEG K, RHO=0.91 GM/CC

2θ	S	CELL	CELL+ARGON	ARGON ALONE
45.0	6.7665	1885	3406	1918
45.5	6.8377	2024	3335	1736
46.0	6.9088	2189	3324	1594
46.5	6.9797	2578	3956	1918
47.0	7.0506	2486	3688	1722
47.5	7.1212	1985	3229	1658
48.0	7.1918	1942	3203	1666
48.5	7.2622	2854	3796	1536
49.0	7.3325	1840	3033	1576
49.5	7.4026	1989	3136	1560
50.0	7.4726	1756	2868	1476
50.5	7.5424	1782	3073	1661
51.0	7.6122	1899	2960	1455
51.5	7.6817	3105	3660	1199
52.0	7.7511	2268	3087	1289
52.5	7.8204	1769	2814	1411
53.0	7.8895	1756	3024	1631 *
53.5	7.9585	1851	2750	1282
54.0	8.0273	1806	2697	1265
54.5	8.0960	1942	2781	1241
55.0	8.1645	1930	2760	1230
55.5	8.2328	3451	3932	1196
56.0	8.3010	2501	3322	1340
56.5	8.3691	1912	2729	1214
57.0	8.4370	1948	2961	1417
57.5	8.5047	1700	2594	1247
58.0	8.5722	3580	4073	1238
58.5	8.6396	2470	3216	1260
59.0	8.7069	1728	2507	1139
59.5	8.7739	1779	2513	1104
60.0	8.8408	1711	2660	1306

TABLE 4.B

Intensity Measurements (total counts)

DATA ANALYSIS
EXPERIMENT OF 6/16/71, T=143 DEG K, RHO=0.91 GM/CC

2θ	S	CELL	CELL+ARGON	ARGON ALONE
3.0	0.4629	1725	5678	4722*
3.5	0.5400	984	4309	3759
4.0	0.6171	820	4053	3590
4.5	0.6942	895	4113	3603
5.0	0.7713	1053	4029	3424
5.5	0.8483	1197	4348	3655
6.0	0.9254	1628	4934	3983
6.5	1.0024	1588	5106	4170
7.0	1.0794	1831	5676	4588
7.5	1.1564	1966	6460	5282
8.0	1.2334	1878	6547	5412
8.5	1.3104	1750	7565	6498
9.0	1.3873	1988	8506	7284
9.5	1.4642	2081	9995	8705
10.0	1.5411	1979	11696	10459
10.5	1.6179	2112	13648	12316
11.0	1.6947	2301	15826	14362
11.5	1.7715	3015	17165	15230
12.0	1.8482	2308	17193	15699
12.5	1.9249	2315	16746	15235
13.0	2.0016	2929	16282	14355
13.5	2.0783	2677	14432	12656
14.0	2.1549	2649	13395	11624
14.5	2.2314	2786	12213	10336
15.0	2.3079	2986	11065	9038
15.5	2.3844	2978	10255	8219
16.0	2.4608	3116	9867	7721
16.5	2.5372	3044	9055	6944
17.0	2.6135	3286	8861	6566
17.5	2.6898	4593	9454	6224
18.0	2.7660	3137	8573	6352
18.5	2.8422	4215	9111	6107
19.0	2.9183	4573	9324	6045
19.5	2.9944	4362	8774	5627*
20.0	3.0704	5776	10254	6063
20.5	3.1463	16100	17133	5386*
21.0	3.2222	4802	9848	6325
21.5	3.2981	3458	8990	6440
22.0	3.3738	4121	9873	6819*
22.5	3.4495	10403	13852	6105*
23.0	3.5252	22960	25147	7972*
23.5	3.6007	56372	47142	4788*

TABLE 4.B (cont.)

Intensity Measurements (total counts)

DATA ANALYSIS
EXPERIMENT OF 6/16/71, T=143 DEG K, RHO=0.91 GM/CC

2θ	S	CELL	CELL+ARGON	ARGON ALONE
24.0	3.6762	8044	12727	6658*
24.5	3.7517	3970	8987	5979
25.0	3.8270	3555	8812	6108
25.5	3.9023	3917	8518	5528
26.0	3.9775	3681	8038	5218
26.5	4.0526	3417	7651	5025
27.0	4.1277	3520	7636	4922
27.5	4.2027	3712	7522	4651
28.0	4.2776	3604	7119	4324
28.5	4.3524	3838	7382	4397
29.0	4.4271	3645	7164	4322
29.5	4.5018	3646	7149	4299
30.0	4.5764	3801	6918	3940
30.5	4.6508	5012	7782	3846
31.0	4.7252	15964	16294	3733
31.5	4.7995	3893	7113	4043
32.0	4.8737	3385	6735	4061
32.5	4.9478	3907	6679	3587
33.0	5.0219	3796	6892	3883
33.5	5.0958	4096	7424	4171
34.0	5.1696	3700	6719	3777
34.5	5.2434	3567	6640	3799
35.0	5.3170	3672	6586	3658
35.5	5.3905	4370	7473	3983
36.0	5.4639	7945	9550	3198
36.5	5.5373	6602	8972	3688
37.0	5.6105	3749	6290	3286
37.5	5.6836	3635	6472	3557
38.0	5.7566	3706	5972	2997
38.5	5.8295	3607	6267	3368
39.0	5.9023	3649	6160	3225
39.5	5.9749	4161	6118	2769
40.0	6.0475	4275	6390	2947
40.5	6.1199	18204	16916	2244
41.0	6.1923	7277	9104	3235
41.5	6.2645	4115	6100	2779
42.0	6.3365	4887	6745	2798
42.5	6.4085	4531	6248	2587
43.0	6.4804	7339	8461	2528
43.5	6.5521	12233	12398	2504
44.0	6.6237	6975	8279	2634
44.5	6.6951	3688	5631	2645

TABLE 4.B (cont.)

Intensity Measurements (total counts)

DATA ANALYSIS
EXPERIMENT OF 6/16/71, T=143 DEG K, RHO=0.91 GM/CC

2θ	S	CELL	CELL+ARGON	ARGON ALONE
45.0	6.7665	3561	5684	2800
45.5	6.8377	3639	5683	2735
46.0	6.9088	3645	5627	2673
46.5	6.9797	4850	6739	2808
47.0	7.0506	4263	6342	2885
47.5	7.1212	3368	5297	2565
48.0	7.1918	3454	5390	2588
48.5	7.2622	4654	6368	2592
49.0	7.3325	3439	5176	2385
49.5	7.4026	3375	5180	2440
50.0	7.4726	3401	5184	2423
50.5	7.5424	3516	4925	2070
51.0	7.6122	3364	5107	2376
51.5	7.6817	5202	6731	2507
52.0	7.7511	3480	5240	2414
52.5	7.8204	3254	4927	2284
53.0	7.8895	3202	4856	2256
53.5	7.9585	3096	4828	2314
54.0	8.0273	3146	4820	2266
54.5	8.0960	3244	4681	2048
55.0	8.1645	3379	4909	2167
55.5	8.2328	6245	6945	1879
56.0	8.3010	3864	5335	2201
56.5	8.3691	3677	4863	1882
57.0	8.4370	3534	4856	1991
57.5	8.5047	3392	4414	1665
58.0	8.5722	6268	6994	1915
58.5	8.6396	4134	5322	1973
59.0	8.7069	3047	4514	2046
59.5	8.7739	3174	4337	1767
60.0	8.8408	3074	4451	1962

TABLE 4.C

Intensity Measurements (total counts)

DATA ANALYSIS
EXPERIMENT OF 6/23/71, T=127 DEG K, RHO=1.116 GM/CC

2θ	S	CELL	CELL+ARGON	ARGON ALONE
3.0	0.4629	1458	3514	2745*
3.5	0.5400	772	2640	2229
4.0	0.6171	781	2387	1967
4.5	0.6942	810	2433	1992
5.0	0.7713	818	2569	2120
5.5	0.8483	1179	2812	2158
6.0	0.9254	1606	3145	2246
6.5	1.0024	1512	3468	2613
7.0	1.0794	1689	3722	2758
7.5	1.1564	1776	4406	3382
8.0	1.2334	1761	4517	3493
8.5	1.3104	1698	5712	4715
9.0	1.3873	1743	6648	5615
9.5	1.4642	1932	7636	6480
10.0	1.5411	1948	9188	8012
10.5	1.6179	2041	11646	10402
11.0	1.6947	2209	14379	13020
11.5	1.7715	2914	17547	15737
12.0	1.8482	2191	18864	17490
12.5	1.9249	2119	19020	17679
13.0	2.0016	2555	17435	15804
13.5	2.0783	2463	15354	13769
14.0	2.1549	2295	13018	11528
14.5	2.2314	2434	11810	10217
15.0	2.3079	2475	10410	8778
15.5	2.3844	2658	9081	7315
16.0	2.4608	2662	8610	6827
16.5	2.5372	2908	8123	6161
17.0	2.6135	2967	7772	5756
17.5	2.6898	4234	8297	5400
18.0	2.7660	2865	7601	5627*
18.5	2.8422	4062	7933	5116
19.0	2.9183	3971	8108	5336
19.5	2.9944	3833	8015	5323
20.0	3.0704	5444	9163	5316
20.5	3.1463	14749	15108	4626*
21.0	3.2222	4142	9138	6178
21.5	3.2981	3295	8540	6173
22.0	3.3738	3893	9002	6192
22.5	3.4495	9749	12575	5504*
23.0	3.5252	20692	21947	6871*
23.5	3.6007	52053	39853	1764*

TABLE 4.C (cont.)

Intensity Measurements (total counts)

DATA ANALYSIS
EXPERIMENT OF 6/23/71, T=127 DEG K, RHO=1.116 GM/CC

2θ	S	CELL	CELL+ARGON	ARGON ALONE
24.0	3.6762	7340	11638	6244 *
24.5	3.7517	3467	8353	5795
25.0	3.8270	3364	7716	5225
25.5	3.9023	3501	7853	5251
26.0	3.9775	3351	7403	4904
26.5	4.0526	3385	7321	4788
27.0	4.1277	3271	6913	4458
27.5	4.2027	3305	7033	4545
28.0	4.2776	3398	6518	3953
28.5	4.3524	3467	6566	3942
29.0	4.4271	3220	6375	3932
29.5	4.5018	3603	6386	3646
30.0	4.5764	3503	6464	3794
30.5	4.6508	4809	6948	3276 *
31.0	4.7252	14701	14276	3027 *
31.5	4.7995	3748	6529	3656
32.0	4.8737	3222	6296	3821
32.5	4.9478	3456	6446	3787
33.0	5.0219	3533	6272	3550
33.5	5.0958	3753	6503	3607
34.0	5.1696	3326	6222	3651
34.5	5.2434	3368	6152	3546
35.0	5.3170	3491	6072	3367
35.5	5.3905	4137	6656	3447
36.0	5.4639	7232	8573	2957 *
36.5	5.5373	5949	8308	3683
37.0	5.6105	3524	6092	3349
37.5	5.6836	3167	5852	3385
38.0	5.7566	3272	5863	3312
38.5	5.8295	3378	5704	3068
39.0	5.9023	3197	5652	3155
39.5	5.9749	3544	5735	2966
40.0	6.0475	4123	6007	2783
40.5	6.1199	16658	14728	1696
41.0	6.1923	6473	7959	2892
41.5	6.2645	3664	5651	2780
42.0	6.3365	4701	6336	2651
42.5	6.4085	3845	5659	2644
43.0	6.4804	6711	7370	2105 *
43.5	6.5521	11302	10791	1922 *
44.0	6.6237	6129	7694	2882
44.5	6.6951	3251	5188	2635

TABLE 4.C (cont.)

Intensity Measurements (total counts)

DATA ANALYSIS
EXPERIMENT OF 6/23/71, T=127 DEG K, RHO=1.116 GM/CC

2θ	S	CELL	CELL+ARGON	ARGON ALONE
45.0	6.7665	3221	5154	2623
45.5	6.8377	3429	5004	2310
46.0	6.9088	3446	5048	2340
46.5	6.9797	4697	5890	2198
47.0	7.0506	4005	5511	2362
47.5	7.1212	3104	5051	2610
48.0	7.1918	3225	4831	2295
48.5	7.2622	4299	5962	2580
49.0	7.3325	3039	5070	2680
49.5	7.4026	2993	4662	2308
50.0	7.4726	2900	4798	2517
50.5	7.5424	3042	4675	2282
51.0	7.6122	2891	4734	2460
51.5	7.6817	4554	6018	2436
52.0	7.7511	3572	4954	2144
52.5	7.8204	3022	4394	2017
53.0	7.8895	2827	4375	2152
53.5	7.9585	2857	4531	2284
54.0	8.0273	2983	4326	1981
54.5	8.0960	2865	4193	1941
55.0	8.1645	3032	4241	1859
55.5	8.2328	5313	6216	2044
56.0	8.3010	3590	4742	1924
56.5	8.3691	3229	4372	1838
57.0	8.4370	3208	4515	1999
57.5	8.5047	2871	4263	2012
58.0	8.5722	5618	6294	1891
58.5	8.6396	3604	4768	1944
59.0	8.7069	2836	4297	2075
59.5	8.7739	2901	4059	1787
60.0	8.8408	2995	4063	1719

TABLE 4.D

Intensity Measurements (total counts)

DATA ANALYSIS
EXPERIMENT OF 7/28/71, T=133 DEG K, RHO=1.054 GM/CC

2θ	S	CELL	CELL+ARGON	ARGON ALONE
3.0	0.4629	1290	3174	2491 *
3.5	0.5400	821	2757	2318 *
4.0	0.6171	692	2292	1918 *
4.5	0.6942	848	2532	2069
5.0	0.7713	985	2761	2218
5.5	0.8483	1234	2816	2130
6.0	0.9254	1624	3198	2286
6.5	1.0024	1660	3356	2415
7.0	1.0794	1627	3742	2811
7.5	1.1564	1806	4244	3200
8.0	1.2334	1562	4465	3553
8.5	1.3104	1634	5323	4359
9.0	1.3873	1596	5759	4807
9.5	1.4642	1697	6945	5922
10.0	1.5411	1902	8603	7445
10.5	1.6179	1902	10176	9007
11.0	1.6947	2158	12362	11023
11.5	1.7715	2714	15002	13303
12.0	1.8482	2231	15563	14153
12.5	1.9249	2179	15698	14309
13.0	2.0016	2558	15124	13480
13.5	2.0783	2452	13052	11463
14.0	2.1549	2397	11941	10374
14.5	2.2314	2539	10170	8497
15.0	2.3079	2425	8937	7326
15.5	2.3844	2632	8807	7045
16.0	2.4608	2849	8181	6259
16.5	2.5372	2929	7431	5439
17.0	2.6135	3222	7250	5043
17.5	2.6898	4270	8200	5253 *
18.0	2.7660	3063	7308	5179 *
18.5	2.8422	4012	7786	4978
19.0	2.9183	3988	7735	4925
19.5	2.9944	3549	7601	5085
20.0	3.0704	5592	8882	4893
20.5	3.1463	11119	13216	5239
21.0	3.2222	5281	9563	5753
21.5	3.2981	3578	7677	5082 *
22.0	3.3738	3847	8467	5663
22.5	3.4495	7889	11133	5357 *
23.0	3.5252	27470	28379	8178 *
23.5	3.6007	40322	35471	5696

TABLE 4.D (cont.)

Intensity Measurements (total counts)

DATA ANALYSIS
EXPERIMENT OF 7/28/71, T=133 DEG K, RHO=1.054 GM/CC

2θ	S	CELL	CELL+ARGON	ARGON ALONE
24.0	3.6762	12064	15203	6258 *
24.5	3.7517	3181	8002	5634
25.0	3.8270	3219	7661	5256
25.5	3.9023	3525	7522	4879
26.0	3.9775	3333	6931	4424
26.5	4.0526	3494	6944	4308
27.0	4.1277	3395	6715	4146
27.5	4.2027	3481	6542	3900
28.0	4.2776	3204	6294	3856
28.5	4.3524	3334	6375	3831 *
29.0	4.4271	3392	6005	3411
29.5	4.5018	3432	6124	3493
30.0	4.5764	3652	6144	3338
30.5	4.6508	4500	6814	3349
31.0	4.7252	14991	15866	4303 *
31.5	4.7995	3867	6366	3377
32.0	4.8737	3399	5994	3362
32.5	4.9478	3243	5670	3154
33.0	5.0219	3671	5792	2940 *
33.5	5.0958	3980	6451	3354
34.0	5.1696	3398	5985	3337
34.5	5.2434	3359	6035	3414
35.0	5.3170	3269	5831	3277
35.5	5.3905	4414	6543	3090
36.0	5.4639	5757	7656	3147
36.5	5.5373	7425	9529	3708 *
37.0	5.6105	3647	5738	2876
37.5	5.6836	3399	5627	2957
38.0	5.7566	3213	5298	2772
38.5	5.8295	3217	5460	2929
39.0	5.9023	3339	5554	2925
39.5	5.9749	3617	5548	2697
40.0	6.0475	3957	5791	2671
40.5	6.1199	14259	14175	2925
41.0	6.1923	8467	9946	3261 *
41.5	6.2645	3606	5592	2743
42.0	6.3365	4805	5994	2196 *
42.5	6.4085	3766	5616	2637
43.0	6.4804	5386	6795	2533
43.5	6.5521	10894	11100	2476
44.0	6.6237	7326	8741	2938 *
44.5	6.6951	3320	5297	2666

TABLE 4.D (cont.)

Intensity Measurements (total counts)

DATA ANALYSIS
EXPERIMENT OF 7/28/71, T=133 DEG K, RHO=1.054 GM/CC

2θ	S	CELL	CELL+ARGON	ARGON ALONE
45.0	6.7665	3426	5154	2438
45.5	6.8377	3200	4895	2357
46.0	6.9088	3375	5171	2494
46.5	6.9797	4206	5765	2428
47.0	7.0506	4487	5894	2333
47.5	7.1212	3418	4788	2075
48.0	7.1918	3162	4865	2354
48.5	7.2622	4905	6246	2351
49.0	7.3325	3274	4479	1879
49.5	7.4026	3291	4494	1880
50.0	7.4726	3268	4697	2101
50.5	7.5424	3053	4706	2281
51.0	7.6122	3211	4512	1961
51.5	7.6817	4943	6262	2336
52.0	7.7511	3680	4950	2027
52.5	7.8204	3138	4766	2274
53.0	7.8895	3105	4413	1947
53.5	7.9585	2888	4376	2083
54.0	8.0273	3063	4477	2045
54.5	8.0960	3102	4262	1799
55.0	8.1645	3214	4451	1899
55.5	8.2328	6118	6555	1697
56.0	8.3010	4416	4985	1479
56.5	8.3691	3134	4355	1867
57.0	8.4370	3481	4513	1750
57.5	8.5047	3125	4405	1926
58.0	8.5722	6469	7121	1991
58.5	8.6396	4276	5023	1633
59.0	8.7069	2864	4055	1785
59.5	8.7739	3033	4294	1891
60.0	8.8408	2985	4021	1656

TABLE 4.E

Intensity Measurements (total counts)

DATA ANALYSIS
EXPERIMENT OF 8/4/71, T=127 DEG K, RHO=1.116 GM/CC

2θ	S	CELL	CELL+ARGON	ARGON ALONE
3.0	0.4629	1586	3555	2801*
3.5	0.5400	958	2772	2312
4.0	0.6171	792	2472	2087
4.5	0.6942	907	2555	2110
5.0	0.7713	934	2770	2306
5.5	0.8483	1041	2823	2300
6.0	0.9254	1857	3272	2330
6.5	1.0024	1586	3334	2521
7.0	1.0794	1807	3796	2859
7.5	1.1564	1745	4545	3630
8.0	1.2334	1667	4881	3997
8.5	1.3104	1670	5471	4575
9.0	1.3873	1578	6621	5764
9.5	1.4642	1919	8065	7010
10.0	1.5411	1873	9675	8633
10.5	1.6179	1901	11756	10687
11.0	1.6947	2254	14878	13596
11.5	1.7715	2896	18051	16387
12.0	1.8482	2145	19838	18592
12.5	1.9249	2225	20058	18752
13.0	2.0016	2565	18770	17250
13.5	2.0783	2560	16089	14557
14.0	2.1549	2394	14049	12602
14.5	2.2314	2492	12023	10502
15.0	2.3079	2436	10743	9242
15.5	2.3844	2513	9588	8025
16.0	2.4608	2755	9127	7398
16.5	2.5372	2831	8344	6551
17.0	2.6135	2975	8008	6106
17.5	2.6898	4252	8687	5945*
18.0	2.7660	3150	7875	5826*
18.5	2.8422	3874	8116	5575
19.0	2.9183	4135	8307	5573
19.5	2.9944	3658	8116	5679
20.0	3.0704	5335	9598	6017*
20.5	3.1463	11936	12731	4663*
21.0	3.2222	4966	9431	6051
21.5	3.2981	3521	8621	6209
22.0	3.3738	3643	9235	6724*
22.5	3.4495	8939	11976	5780*
23.0	3.5252	25871	25474	7443*
23.5	3.6007	42653	32803	2916*

TABLE 4.E (cont.)

Intensity Measurements (total counts)

DATA ANALYSIS
EXPERIMENT OF 8/4/71, T=127 DEG K, RHO=1.116 GM/CC

2θ	S	CELL	CELL+ARGON	ARGON ALONE
24.0	3.6762	10466	14115	6745*
24.5	3.7517	3303	8375	6038
25.0	3.8270	3367	8293	5900
25.5	3.9023	3600	8292	5722
26.0	3.9775	3177	7744	5466
26.5	4.0526	3418	7570	5110
27.0	4.1277	3414	7016	4550*
27.5	4.2027	3354	6985	4553
28.0	4.2776	3239	6720	4364
28.5	4.3524	3398	6786	4306
29.0	4.4271	3336	6539	4097
29.5	4.5018	3193	6496	4152
30.0	4.5764	3464	6728	4178
30.5	4.6508	4346	6977	3769
31.0	4.7252	14598	14350	3548
31.5	4.7995	3687	6676	3941
32.0	4.8737	3118	6273	3954
32.5	4.9478	3305	6223	3760*
33.0	5.0219	3295	6470	4009*
33.5	5.0958	3745	6677	3875
34.0	5.1696	3330	6348	3852
34.5	5.2434	3225	6246	3824
35.0	5.3170	3617	6213	3493
35.5	5.3905	3996	6710	3700
36.0	5.4639	6069	8088	3510
36.5	5.5373	6791	8695	3566
37.0	5.6105	3395	6060	3492
37.5	5.6836	3209	5912	3482
38.0	5.7566	3225	5825	3380
38.5	5.8295	3176	5793	3383
39.0	5.9023	3113	5807	3443
39.5	5.9749	3440	5823	3207
40.0	6.0475	3915	6015	3036
40.5	6.1199	14286	13191	2312*
41.0	6.1923	7809	9404	3451*
41.5	6.2645	3458	5762	3124*
42.0	6.3365	4452	5943	2544*
42.5	6.4085	3977	5707	2668*
43.0	6.4804	5410	6655	2518*
43.5	6.5521	11047	11004	2552*
44.0	6.6237	6826	8234	3009
44.5	6.6951	3387	5437	2842

TABLE 4.E (cont.)

Intensity Measurements (total counts)

DATA ANALYSIS
EXPERIMENT OF 8/4/71, T=127 DEG K, RHO=1.116 GM/CC

2θ	S	CELL	CELL+ARGON	ARGON ALONE
45.0	6.7665	3188	5423	2979
45.5	6.8377	3016	5207	2894
46.0	6.9088	3356	5230	2655
46.5	6.9797	4488	6234	2789
47.0	7.0506	4296	5814	2515
47.5	7.1212	3095	5017	2639
48.0	7.1918	3287	5010	2484
48.5	7.2622	4440	5968	2555
49.0	7.3325	3069	5103	2743
49.5	7.4026	3027	5015	2687
50.0	7.4726	2854	4643	2448
50.5	7.5424	3073	4615	2251
51.0	7.6122	3048	4651	2306
51.5	7.6817	4834	6235	2516
52.0	7.7511	3646	5223	2418
52.5	7.8204	3111	4606	2213
53.0	7.8895	3041	4414	2075
53.5	7.9585	2987	4388	2090
54.0	8.0273	2814	4441	2276
54.5	8.0960	3102	4353	1967
55.0	8.1645	2971	4388	2102
55.5	8.2328	5876	6595	2075
56.0	8.3010	3846	5184	2225
56.5	8.3691	3305	4601	2058
57.0	8.4370	3469	4626	1958
57.5	8.5047	3116	4315	1919
58.0	8.5722	6009	6739	2121
58.5	8.6396	4189	5200	1981
59.0	8.7069	2861	4083	1885
59.5	8.7739	3055	4278	1932
60.0	8.8408	2827	4351	2180

TABLE 4.F

Intensity Measurements (total counts)

DATA ANALYSIS
EXPERIMENT OF 8/24/71, T=127 DEG K, RHO=1.098 GM/CC

2θ	S	CELL	CELL+ARGON	ARGON ALONE
3.0	0.4629	1765	3783	2875*
3.5	0.5400	758	2729	2335
4.0	0.6171	663	2456	2108
4.5	0.6942	709	2439	2063
5.0	0.7713	837	2476	2027
5.5	0.8483	1070	2558	1979
6.0	0.9254	1587	3026	2158
6.5	1.0024	1327	3194	2461
7.0	1.0794	1661	3605	2678
7.5	1.1564	1701	4045	3086
8.0	1.2334	1576	4468	3570
8.5	1.3104	1390	4928	4127
9.0	1.3873	1426	5853	5022
9.5	1.4642	1585	6956	6022
10.0	1.5411	1666	8437	7445
10.5	1.6179	1792	10601	9523
11.0	1.6947	1934	13019	11844
11.5	1.7715	2494	15403	13873
12.0	1.8482	2045	16626	15360
12.5	1.9249	1972	16792	15560
13.0	2.0016	2256	15741	14318
13.5	2.0783	1996	14111	12841
14.0	2.1549	2350	12098	10590
14.5	2.2314	2228	10222	8780
15.0	2.3079	2218	9162	7714
15.5	2.3844	2483	8503	6869
16.0	2.4608	2672	8104	6331
16.5	2.5372	2570	7609	5890
17.0	2.6135	2922	7221	5251
17.5	2.6898	3998	7701	4984
18.0	2.7660	2655	6737	4919
18.5	2.8422	3462	7126	4739
19.0	2.9183	3617	7540	5028
19.5	2.9944	3290	7099	4798
20.0	3.0704	4911	8396	4940
20.5	3.1463	10307	11357	4060*
21.0	3.2222	4602	8834	5556
21.5	3.2981	3133	7649	5405
22.0	3.3738	3303	8055	5677
22.5	3.4495	6618	10424	5636
23.0	3.5252	24570	24964	7107*
23.5	3.6007	35285	28825	3067*

TABLE 4.F (cont.)

Intensity Measurements (total counts)

DATA ANALYSIS
EXPERIMENT OF 8/24/71, T=127 DEG K, RHO=1.098 GM/CC

2θ	S	CELL	CELL+ARGON	ARGON ALONE
24.0	3.6762	10821	13685	5751*
24.5	3.7517	2941	7942	5776*
25.0	3.8270	3076	7502	5228
25.5	3.9023	2937	7323	5144
26.0	3.9775	2909	6662	4497
26.5	4.0526	2827	6725	4613
27.0	4.1277	3266	6384	3937
27.5	4.2027	2928	6290	4089
28.0	4.2776	3031	5946	3662
28.5	4.3524	3082	6254	3925
29.0	4.4271	3075	5959	3629
29.5	4.5018	2750	5542	3453
30.0	4.5764	3109	5745	3378
30.5	4.6508	3988	6211	3168
31.0	4.7252	13464	13441	3148
31.5	4.7995	3626	5915	3137
32.0	4.8737	2844	5558	3375
32.5	4.9478	2850	5564	3372
33.0	5.0219	3176	5774	3327
33.5	5.0958	3558	5732	2986*
34.0	5.1696	2825	5952	3769*
34.5	5.2434	3024	5884	3543*
35.0	5.3170	2891	5748	3507*
35.5	5.3905	3642	6127	3301
36.0	5.4639	4956	6633	2782*
36.5	5.5373	6645	8273	3105
37.0	5.6105	3076	5658	3263
37.5	5.6836	2877	5375	3133
38.0	5.7566	2951	5524	3222
38.5	5.8295	2810	5278	3084
39.0	5.9023	2875	5222	2976
39.5	5.9749	3077	5463	3057
40.0	6.0475	3513	5210	2461*
40.5	6.1199	12148	11742	2231*
41.0	6.1923	7631	8721	2742
41.5	6.2645	3322	5244	2639
42.0	6.3365	4006	5748	2605
42.5	6.4085	3440	5087	2386
43.0	6.4804	4616	5880	2255
43.5	6.5521	9550	9922	2418
44.0	6.6237	6542	7800	2657
44.5	6.6951	2944	4776	2460

TABLE 4.F (cont.)

Intensity Measurements (total counts)

DATA ANALYSIS
EXPERIMENT OF 8/24/71, T=127 DEG K, RHO=1.098 GM/CC

2θ	S	CELL	CELL+ARGON	ARGON ALONE
45.0	6.7665	2937	4917	2606
45.5	6.8377	3060	4781	2372
46.0	6.9088	2929	4659	2352
46.5	6.9797	3729	5305	2368
47.0	7.0506	3885	5412	2351
47.5	7.1212	2760	4634	2459
48.0	7.1918	2892	4517	2237
48.5	7.2622	4012	5352	2189
49.0	7.3325	2889	4564	2286
49.5	7.4026	2702	4425	2294
50.0	7.4726	2729	4127	1975
50.5	7.5424	2756	4249	2075
51.0	7.6122	2761	4221	2043
51.5	7.6817	4449	5517	2008
52.0	7.7511	3378	4778	2114
52.5	7.8204	2793	4060	1857
53.0	7.8895	2852	3912	1662
53.5	7.9585	2728	4126	1974
54.0	8.0273	2855	3918	1666
54.5	8.0960	2616	4049	1986
55.0	8.1645	2696	3913	1787
55.5	8.2328	5305	6273	2091
56.0	8.3010	3694	4777	1865
56.5	8.3691	2911	3960	1665
57.0	8.4370	3038	4344	1950
57.5	8.5047	2891	3996	1719
58.0	8.5722	5755	6381	1850
58.5	8.6396	3807	4999	2002
59.0	8.7069	2757	3731	1561
59.5	8.7739	2633	3706	1634
60.0	8.8408	2448	3660	1734

TABLE 4.G

Intensity Measurements (total counts)

DATA ANALYSIS
EXPERIMENT OF 9/28/71(I), T=133 DEG K, RHO=1.054 GM/CC

2θ	S	CELL	CELL+ARGON	ARGON ALONE
3.0	0.4629	1648	3937	3007*
3.5	0.5400	916	3081	2559
4.0	0.6171	569	2797	2469
4.5	0.6942	948	2834	2283
5.0	0.7713	871	2673	2162
5.5	0.8483	1009	3114	2517
6.0	0.9254	1630	3178	2205
6.5	1.0024	1429	3623	2762
7.0	1.0794	1556	3961	3015
7.5	1.1564	1763	4577	3496
8.0	1.2334	1721	5167	4101
8.5	1.3104	1574	5742	4758
9.0	1.3873	1509	6863	5910
9.5	1.4642	1770	8079	6951
10.0	1.5411	1793	9456	8302
10.5	1.6179	1934	11655	10399
11.0	1.6947	2085	13967	12602
11.5	1.7715	2878	16600	14700
12.0	1.8482	2230	17139	15655
12.5	1.9249	2297	17827	16286
13.0	2.0016	2547	16221	14499
13.5	2.0783	2385	14561	12936
14.0	2.1549	2533	12706	10968
14.5	2.2314	2714	11515	9639
15.0	2.3079	2623	10179	8354
15.5	2.3844	2514	9168	7406
16.0	2.4608	2694	8437	6536
16.5	2.5372	2817	8396	6395
17.0	2.6135	2822	8104	6086
17.5	2.6898	4379	8916	5766
18.0	2.7660	3063	7255	5038
18.5	2.8422	3666	8013	5344
19.0	2.9183	4297	8363	5217
19.5	2.9944	3712	8142	5409
20.0	3.0704	5547	9394	5289
20.5	3.1463	11287	13271	4878*
21.0	3.2222	5203	9816	5930
21.5	3.2981	3266	7893	5443
22.0	3.3738	3712	8839	6043
22.5	3.4495	7754	11437	5574
23.0	3.5252	27688	28286	7278*
23.5	3.6007	38266	32193	3059*

TABLE 4.G (cont.)

Intensity Measurements (total counts)

DATA ANALYSIS
EXPERIMENT OF 9/28/71(I), T=133 DEG K, RHO=1.054 GM/CC

2θ	S	CELL	CELL+ARGON	ARGON ALONE
24.0	3.6762	12058	15244	6033
24.5	3.7517	3310	7940	5404
25.0	3.8270	3495	8067	5381
25.5	3.9023	3511	7697	4991
26.0	3.9775	3549	7561	4819
26.5	4.0526	3381	7092	4473
27.0	4.1277	3301	6821	4258
27.5	4.2027	3146	7087	4639 *
28.0	4.2776	3485	6675	3958
28.5	4.3524	3418	6502	3831
29.0	4.4271	3286	6485	3913
29.5	4.5018	3222	6279	3752
30.0	4.5764	3548	6195	3407
30.5	4.6508	4564	7104	3513
31.0	4.7252	15062	15495	3625
31.5	4.7995	3915	6418	3328
32.0	4.8737	3216	6295	3753
32.5	4.9478	3291	6274	3669
33.0	5.0219	3548	6397	3585
33.5	5.0958	4078	6632	3396
34.0	5.1696	3369	6267	3590
34.5	5.2434	3222	5958	3396
35.0	5.3170	3513	6165	3368
35.5	5.3905	4343	6457	2997
36.0	5.4639	5765	7770	3173
36.5	5.5373	7382	9222	3331
37.0	5.6105	3424	6076	3341
37.5	5.6836	3311	5791	3145
38.0	5.7566	3209	5662	3096
38.5	5.8295	3331	5749	3083
39.0	5.9023	3256	5826	3219
39.5	5.9749	3594	5806	2927
40.0	6.0475	4092	6078	2798
40.5	6.1199	13481	12883	2075 *
41.0	6.1923	8657	10099	3155
41.5	6.2645	3686	5685	2727
42.0	6.3365	4626	6314	2600
42.5	6.4085	4005	5771	2554
43.0	6.4804	5323	6492	2215
43.5	6.5521	10829	11344	2641
44.0	6.6237	7457	8509	2515
44.5	6.6951	3539	5090	2244

TABLE 4.G (cont.)

Intensity Measurements (total counts)

DATA ANALYSIS
EXPERIMENT OF 9/28/71(I), T=133 DEG K, RHO=1.054 GM/CC

2θ	S	CELL	CELL+ARGON	ARGON ALONE
45.0	6.7665	3167	5234	2687
45.5	6.8377	3279	5350	2712
46.0	6.9088	3270	5437	2806
46.5	6.9797	3912	5842	2694
47.0	7.0506	4282	6023	2577
47.5	7.1212	3207	5121	2539
48.0	7.1918	3143	4951	2421
48.5	7.2622	4710	6031	2239
49.0	7.3325	3226	4845	2248
49.5	7.4026	3273	4991	2356
50.0	7.4726	3185	4869	2305
50.5	7.5424	3126	4654	2138
51.0	7.6122	3147	4622	2089
51.5	7.6817	4799	5919	2057
52.0	7.7511	3774	5268	2231
52.5	7.8204	2933	4452	2091
53.0	7.8895	2890	4287	1962
53.5	7.9585	2933	4595	2235
54.0	8.0273	3088	4556	2072
54.5	8.0960	3313	4291	1627
55.0	8.1645	3053	4529	2074
55.5	8.2328	6093	6352	1454
56.0	8.3010	4121	5270	1958
56.5	8.3691	3290	4438	1795
57.0	8.4370	3484	4416	1617
57.5	8.5047	3110	4227	1730
58.0	8.5722	6312	7177	2111
58.5	8.6396	4320	5186	1720
59.0	8.7069	2915	4237	1898
59.5	8.7739	3015	4066	1648
60.0	8.8408	2771	4193	1971

TABLE 4.H

Intensity Measurements (total counts)

DATA ANALYSIS
EXPERIMENT OF 11/30/71, T=143 DEG K, RHO=0.91 GM/CC

2θ	S	CELL	CELL+ARGON	ARGON ALONE
3.0	0.4629	2156	5982	4878*
3.5	0.5400	1250	4624	3978
4.0	0.6171	805	3924	3504
4.5	0.6942	766	3656	3253
5.0	0.7713	971	3844	3328
5.5	0.8483	1117	4051	3452
6.0	0.9254	1703	4357	3436
6.5	1.0024	1582	4959	4095
7.0	1.0794	1644	5015	4109
7.5	1.1564	1677	5540	4607
8.0	1.2334	1691	6267	5317
8.5	1.3104	1523	7081	6216
9.0	1.3873	1596	7945	7029
9.5	1.4642	1705	9523	8534
10.0	1.5411	1835	11267	10192
10.5	1.6179	1756	12843	11804
11.0	1.6947	2028	15032	13820
11.5	1.7715	2801	16603	14913
12.0	1.8482	2146	16414	15107
12.5	1.9249	2378	16217	14755
13.0	2.0016	2488	15693	14149
13.5	2.0783	2335	13801	12339
14.0	2.1549	2168	12673	11303
14.5	2.2314	2444	11243	9685
15.0	2.3079	2489	10060	8460
15.5	2.3844	2471	9236	7633
16.0	2.4608	2631	9105	7384
16.5	2.5372	2743	8501	6691
17.0	2.6135	2933	8179	6227
17.5	2.6898	4307	8670	5780
18.0	2.7660	2917	8078	6105*
18.5	2.8422	3698	8572	6051*
19.0	2.9183	4062	8484	5694
19.5	2.9944	3606	8205	5710
20.0	3.0704	5216	9263	5628
20.5	3.1463	12320	13900	5258*
21.0	3.2222	4426	9193	6068*
21.5	3.2981	3335	8171	5802
22.0	3.3738	3740	8716	6043
22.5	3.4495	9454	12532	5739
23.0	3.5252	24205	25348	7866*
23.5	3.6007	44255	35760	3635*

TABLE 4.H (cont.)

Intensity Measurements (total counts)

DATA ANALYSIS
EXPERIMENT OF 11/30/71, T=143 DEG K, RHO=0.91 GM/CC

2θ	S	CELL	CELL+ARGON	ARGON ALONE
24.0	3.6762	9535	12928	5972
24.5	3.7517	3322	8037	5602
25.0	3.8270	3390	7973	5477
25.5	3.9023	3191	7713	5354
26.0	3.9775	3202	7843	5466
26.5	4.0526	3360	7102	4599*
27.0	4.1277	3202	6551	4157*
27.5	4.2027	3072	7022	4717
28.0	4.2776	2945	6450	4233
28.5	4.3524	3087	6474	4143
29.0	4.4271	3331	6535	4012
29.5	4.5018	3578	6526	3808
30.0	4.5764	3445	6234	3610
30.5	4.6508	4541	7097	3629
31.0	4.7252	14971	14834	3373
31.5	4.7995	3695	6549	3714
32.0	4.8737	3355	6233	3653
32.5	4.9478	3356	5911	3324
33.0	5.0219	3470	6169	3489
33.5	5.0958	3648	6412	3589
34.0	5.1696	3498	6137	3425
34.5	5.2434	3120	6014	3591
35.0	5.3170	3499	6060	3338
35.5	5.3905	4203	6708	3434
36.0	5.4639	6812	8048	2735*
36.5	5.5373	6670	9109	3899*
37.0	5.6105	3564	5848	3060
37.5	5.6836	3344	5802	3183
38.0	5.7566	3494	5581	2842
38.5	5.8295	3291	5615	3032
39.0	5.9023	3133	5500	3039
39.5	5.9749	3572	5906	3097
40.0	6.0475	3831	5873	2858
40.5	6.1199	14376	13783	2460
41.0	6.1923	7591	9021	3036
41.5	6.2645	3692	5717	2803
42.0	6.3365	4835	6131	2313
42.5	6.4085	4031	5876	2690
43.0	6.4804	5787	7066	2490
43.5	6.5521	11447	11211	2154
44.0	6.6237	7111	8093	2462
44.5	6.6951	3219	5429	2878

TABLE 4.H (cont.)

Intensity Measurements (total counts)

DATA ANALYSIS
EXPERIMENT OF 11/30/71, T=143 DEG K, RHO=0.91 GM/CC

2θ	S	CELL	CELL+ARGON	ARGON ALONE
45.0	6.7665	3125	4964	2486
45.5	6.8377	3204	4927	2385
46.0	6.9088	3207	5219	2674
46.5	6.9797	4228	5783	2426
47.0	7.0506	4245	5894	2522
47.5	7.1212	3177	4715	2190
48.0	7.1918	3193	4874	2336
48.5	7.2622	4334	5740	2294
49.0	7.3325	3113	4941	2465
49.5	7.4026	3162	4835	2319
50.0	7.4726	2946	4464	2119
50.5	7.5424	3259	4471	1877
51.0	7.6122	3112	4617	2139
51.5	7.6817	4895	5885	1987
52.0	7.7511	3823	5075	2030
52.5	7.8204	2899	4276	1967
53.0	7.8895	3054	4533	2100
53.5	7.9585	2979	4486	2113
54.0	8.0273	2994	4404	2019
54.5	8.0960	2980	4302	1928
55.0	8.1645	3176	4439	1909
55.5	8.2328	5820	6473	1837
56.0	8.3010	4032	5138	1926
56.5	8.3691	3354	4499	1827
57.0	8.4370	3567	4566	1725
57.5	8.5047	3042	4028	1605
58.0	8.5722	6105	6938	2076 *
58.5	8.6396	4105	4880	1611
59.0	8.7069	2958	3943	1588
59.5	8.7739	2938	4072	1733
60.0	8.8408	2899	4078	1770

TABLE 4.I

Intensity Measurements (total counts)

DATA ANALYSIS
EXPERIMENT OF 12/8/71, T=127 DEG K, RHO=1.098 GM/CC

2θ	S	CELL	CELL+ARGON	ARGON ALONE
3.0	0.4629	1367	3225	2584*
3.5	0.5400	705	2542	2208
4.0	0.6171	661	2398	2081
4.5	0.6942	711	2451	2106
5.0	0.7713	861	2521	2099
5.5	0.8483	1055	2863	2340
6.0	0.9254	1438	2877	2156
6.5	1.0024	1371	3138	2443
7.0	1.0794	1468	3668	2916
7.5	1.1564	1606	4266	3433
8.0	1.2334	1511	4478	3685
8.5	1.3104	1571	5011	4176
9.0	1.3873	1662	6009	5115
9.5	1.4642	1680	7317	6402
10.0	1.5411	1742	8564	7604
10.5	1.6179	1820	10870	9855
11.0	1.6947	1998	13242	12115
11.5	1.7715	2731	16222	14664
12.0	1.8482	1996	17618	16467
12.5	1.9249	2060	17635	16434
13.0	2.0016	2386	16615	15209
13.5	2.0783	2381	14159	12742
14.0	2.1549	2278	12320	10950
14.5	2.2314	2394	11190	9736
15.0	2.3079	2446	9561	8060
15.5	2.3844	2365	8655	7190
16.0	2.4608	2739	8487	6773
16.5	2.5372	2697	7648	5944
17.0	2.6135	2647	7479	5790
17.5	2.6898	4171	8116	5431
18.0	2.7660	2701	6972	5217
18.5	2.8422	3370	7193	4984
19.0	2.9183	3847	7558	5015
19.5	2.9944	3276	7698	5514*
20.0	3.0704	4896	8425	5136
20.5	3.1463	11307	12054	4402*
21.0	3.2222	4383	8465	5477
21.5	3.2981	2917	7779	5777
22.0	3.3738	3469	8289	5893
22.5	3.4495	7601	11039	5756
23.0	3.5252	24865	25506	8125*
23.5	3.6007	38210	30006	3150*

TABLE 4.I (cont.)

Intensity Measurements (total counts)

DATA ANALYSIS
EXPERIMENT OF 12/8/71, T=127 DEG K, RHO=1.098 GM/CC

2θ	S	CELL	CELL+ARGON	ARGON ALONE
24.0	3.6762	9302	12764	6191 *
24.5	3.7517	3077	7763	5578
25.0	3.8270	3338	7413	5031
25.5	3.9023	3366	7330	4917
26.0	3.9775	3196	6991	4690
26.5	4.0526	3293	6732	4351
27.0	4.1277	3127	6856	4586 *
27.5	4.2027	2893	6104	3996
28.0	4.2776	2849	5995	3912
28.5	4.3524	3025	5843	3623
29.0	4.4271	2999	5744	3536
29.5	4.5018	3168	6117	3778
30.0	4.5764	3256	5922	3510
30.5	4.6508	3951	6394	3460
31.0	4.7252	14000	14103	3678 *
31.5	4.7995	3465	5968	3381
32.0	4.8737	3184	5774	3391
32.5	4.9478	2895	5648	3476
33.0	5.0219	2895	5469	3292
33.5	5.0958	3677	6127	3357
34.0	5.1696	3107	5754	3409
34.5	5.2434	3149	5698	3317
35.0	5.3170	3437	5724	3120
35.5	5.3905	3837	6219	3308
36.0	5.4639	5750	7422	3052
36.5	5.5373	6617	8413	3378 *
37.0	5.6105	3213	5385	2937
37.5	5.6836	3078	5264	2915
38.0	5.7566	3187	5308	2873
38.5	5.8295	3114	5298	2916
39.0	5.9023	3149	5293	2882
39.5	5.9749	3277	5306	2794
40.0	6.0475	3721	5606	2751
40.5	6.1199	12907	11780	1869 *
41.0	6.1923	8186	9164	2872
41.5	6.2645	3320	5190	2636
42.0	6.3365	4056	5506	2383
42.5	6.4085	3526	5259	2542
43.0	6.4804	5227	6227	2197
43.5	6.5521	10282	10417	2484
44.0	6.6237	6778	7676	2443
44.5	6.6951	3249	4960	2449

TABLE 4.I (cont.)

Intensity Measurements (total counts)

DATA ANALYSIS
EXPERIMENT OF 12/8/71, T=127 DEG K, RHO=1.098 GM/CC

2θ	S	CELL	CELL+ARGON	ARGON ALONE
45.0	6.7665	2957	4790	2504
45.5	6.8377	2932	4843	2575
46.0	6.9088	3233	5079	2577
46.5	6.9797	3896	5419	2403
47.0	7.0506	3887	5443	2432
47.5	7.1212	2946	4848	2565
48.0	7.1918	2821	4537	2350
48.5	7.2622	4438	5700	2259
49.0	7.3325	2934	4588	2312
49.5	7.4026	3108	4360	1948
50.0	7.4726	2912	4533	2273
50.5	7.5424	2791	4405	2238
51.0	7.6122	2940	4293	2011
51.5	7.6817	4710	5683	2026
52.0	7.7511	3182	4799	2328 *
52.5	7.8204	2868	4166	1939
53.0	7.8895	2840	4055	1849
53.5	7.9585	2780	3992	1833
54.0	8.0273	2742	3964	1834
54.5	8.0960	2906	4007	1750
55.0	8.1645	2867	4194	1967
55.5	8.2328	5490	6052	1789
56.0	8.3010	3793	4925	1980
56.5	8.3691	3111	4099	1683
57.0	8.4370	3254	4274	1748
57.5	8.5047	2813	4070	1887
58.0	8.5722	5856	6273	1729
58.5	8.6396	3998	4877	1775
59.0	8.7069	2770	3785	1636
59.5	8.7739	2746	3792	1663
60.0	8.8408	2974	3755	1449

TABLE 4.J

Intensity Measurements (total counts)

DATA ANALYSIS
EXPERIMENT OF 12/15/71, T=127 DEG K, RHO=1.135 GM/CC

2θ	S	CELL	CELL+ARGON	ARGON ALONE
3.0	0.4629	1373	3099	2464*
3.5	0.5400	555	2142	1882
4.0	0.6171	624	1996	1701
4.5	0.6942	727	2191	1843
5.0	0.7713	916	2500	2057
5.5	0.8483	924	2576	2124
6.0	0.9254	1353	2830	2161
6.5	1.0024	1365	2825	2143
7.0	1.0794	1558	3449	2661
7.5	1.1564	1740	3792	2902
8.0	1.2334	1668	4115	3251
8.5	1.3104	1540	4797	3990
9.0	1.3873	1505	5580	4781
9.5	1.4642	1663	6564	5670
10.0	1.5411	1580	8357	7497
10.5	1.6179	1712	10230	9287
11.0	1.6947	2020	12941	11816
11.5	1.7715	2459	15829	14444
12.0	1.8482	2100	17064	15868
12.5	1.9249	1904	17445	16349
13.0	2.0016	2350	16563	15196
13.5	2.0783	2250	14377	13055
14.0	2.1549	2199	12162	10856
14.5	2.2314	2237	10530	9188
15.0	2.3079	2464	9358	7865
15.5	2.3844	2347	8253	6817
16.0	2.4608	2497	7577	6034
16.5	2.5372	2699	7490	5806
17.0	2.6135	2609	7002	5359
17.5	2.6898	3901	7755	5275
18.0	2.7660	2692	6996	5269
18.5	2.8422	3433	7156	4934
19.0	2.9183	3718	7418	4992
19.5	2.9944	3116	7056	5006
20.0	3.0704	4864	8468	5243
20.5	3.1463	10947	12134	4823*
21.0	3.2222	4510	8560	5526
21.5	3.2981	2974	7309	5295
22.0	3.3738	3293	7935	5691
22.5	3.4495	7550	10619	5443
23.0	3.5252	23976	24687	8157*
23.5	3.6007	36897	29059	3482*

TABLE 4.J (cont.)

Intensity Measurements (total counts)

DATA ANALYSIS
EXPERIMENT OF 12/15/71, T=127 DEG K, RHO=1.135 GM/CC

2θ	S	CELL	CELL+ARGON	ARGON ALONE
24.0	3.6762	9191	12444	6040*
24.5	3.7517	3069	7456	5306
25.0	3.8270	3174	7235	5001
25.5	3.9023	3267	7240	4931
26.0	3.9775	2978	6770	4656
26.5	4.0526	3111	6454	4236
27.0	4.1277	3162	6153	3890
27.5	4.2027	3142	6204	3947
28.0	4.2776	2708	6071	4119*
28.5	4.3524	3154	5660	3379*
29.0	4.4271	3183	5804	3494
29.5	4.5018	2962	5707	3551
30.0	4.5764	2930	5784	3645
30.5	4.6508	4147	6549	3513
31.0	4.7252	13803	13841	3712*
31.5	4.7995	3437	5825	3296
32.0	4.8737	2926	5418	3260
32.5	4.9478	3015	5511	3282
33.0	5.0219	3236	5551	3154
33.5	5.0958	3515	6027	3418
34.0	5.1696	2673	5633	3645
34.5	5.2434	3057	5543	3265
35.0	5.3170	2946	5570	3371
35.5	5.3905	3937	6056	3113
36.0	5.4639	5429	6936	2871
36.5	5.5373	6469	8480	3631*
37.0	5.6105	3241	5614	3181
37.5	5.6836	2777	5295	3207
38.0	5.7566	2985	5388	3141
38.5	5.8295	3143	5292	2924
39.0	5.9023	3045	5134	2837
39.5	5.9749	3209	5318	2895
40.0	6.0475	3621	5189	2452
40.5	6.1199	12421	11048	1653*
41.0	6.1923	8014	9031	2964
41.5	6.2645	3427	4909	2312
42.0	6.3365	4266	5325	2090
42.5	6.4085	3806	5290	2401
43.0	6.4804	4906	5730	2004
43.5	6.5521	10161	9810	2088
44.0	6.6237	6539	7664	2691
44.5	6.6951	3121	4581	2205

TABLE 4.J (cont.)

Intensity Measurements (total counts)

DATA ANALYSIS
EXPERIMENT OF 12/15/71, T=127 DEG K, RHO=1.135 GM/CC

2θ	S	CELL	CELL+ARGON	ARGON ALONE
45.0	6.7665	2985	4891	2618
45.5	6.8377	2791	4706	2579
46.0	6.9088	3109	4587	2217
46.5	6.9797	3662	5208	2415
47.0	7.0506	3635	5539	2766 *
47.5	7.1212	2869	4556	2366
48.0	7.1918	2952	4401	2147
48.5	7.2622	4097	5523	2395
49.0	7.3325	2845	4430	2257
49.5	7.4026	2884	4377	2173
50.0	7.4726	2927	4152	1915
50.5	7.5424	2890	4322	2113
51.0	7.6122	3002	4168	1873
51.5	7.6817	4327	5363	2055
52.0	7.7511	3413	4794	2184
52.5	7.8204	2760	4056	1946
53.0	7.8895	2902	3885	1666
53.5	7.9585	2838	3989	1819
54.0	8.0273	2887	4185	1977
54.5	8.0960	2643	3943	1922
55.0	8.1645	2769	3870	1753
55.5	8.2328	5426	6079	1931
56.0	8.3010	3872	4616	1656
56.5	8.3691	3023	4015	1704
57.0	8.4370	3009	4126	1826
57.5	8.5047	2721	3751	1672
58.0	8.5722	5756	5870	1473
58.5	8.6396	4083	4871	1752
59.0	8.7069	2685	3861	1811
59.5	8.7739	2738	3640	1550
60.0	8.8408	2520	3669	1745